



---

# Evaluation of Asphalt Binder Performance with Laboratory and Field Test Sections

Technical Report 0-6674-01-R1

---

Cooperative Research Program

TEXAS A&M TRANSPORTATION INSTITUTE  
COLLEGE STATION, TEXAS

in cooperation with the  
Federal Highway Administration and the  
Texas Department of Transportation  
<http://tti.tamu.edu/documents/0-6674-01-R1.pdf>



1. Report No. FHWA/TX-18/0-6674-01-R1		2. Government Accession No.		3. Recipient's Catalog No.	
4. Title and Subtitle EVALUATION OF ASPHALT BINDER PERFORMANCE WITH LABORATORY AND FIELD TEST SECTIONS				5. Report Date Published: November 2018	
				6. Performing Organization Code	
7. Author(s) Pravat Karki and Fujie Zhou				8. Performing Organization Report No. Report 0-6674-01-R1	
9. Performing Organization Name and Address Texas A&M Transportation Institute The Texas A&M University System College Station, Texas 77843-3135				10. Work Unit No. (TRAIS)	
				11. Contract or Grant No. Project 0-6674-01	
12. Sponsoring Agency Name and Address Texas Department of Transportation Research and Technology Implementation Office 125 E. 11 <sup>th</sup> Street Austin, Texas 78701-2483				13. Type of Report and Period Covered Technical Report: December 2014–August 2018	
				14. Sponsoring Agency Code	
15. Supplementary Notes Project performed in cooperation with the Texas Department of Transportation and the Federal Highway Administration. Project Title: Improving Fracture Resistance Measurements in Asphalt Binder Specifications with Verification on Asphalt Mixture Cracking Performance URL: <a href="http://tti.tamu.edu/documents/0-6674-01-R1.pdf">http://tti.tamu.edu/documents/0-6674-01-R1.pdf</a>					
16. Abstract The current performance-grade (PG) specification for asphalt binders was developed 25 years ago. Over the years, many changes have occurred, including crude oil sources, improved refinery technologies to extract more saturates from crude oil before producing asphalt binders, new additives (such as re-refined engine oil bottoms [REOB], polyphosphoric acid [PPA], bio-rejuvenators), and increased use of reclaimed materials. Consequently, asphalt binders with the same PG may perform completely differently, especially in cracking resistance. Researchers evaluated the performance of asphalt binders engineered with various modification techniques including REOB, PPA, aromatic extracts, bio-rejuvenators, and fatty acids. Both rheological and chemical properties of the engineered binders were characterized in the laboratory. It was found that binders produced with same target PG but with different modification techniques can have quite different rheological and embrittlement properties. Specifically, the parameter $\Delta T_c$ from bending beam rheolometer is a good parameter for asphalt binder quality or embrittlement. The current binder selection catalog should be expanded for different applications, specifically for asphalt overlay mixes. Researchers also surveyed 11 existing field test sections constructed with soft and polymer modified binders and constructed 6 more new test sections around Texas. The plant mixes from these test sections were collected during the construction and then tested in the laboratory for their dynamic modulus, rutting resistance, and cracking resistance. Based on the laboratory test results and field performance data, researchers recommended a new statewide binder selection catalog. The implementation of the recommendation will make pavements last longer as intended.					
17. Key Words Asphalt, Binder, Performance, Cracking, Fatigue, Selection, Rutting, Durability			18. Distribution Statement No restrictions. This document is available to the public through NTIS: National Technical Information Service Alexandria, Virginia <a href="http://www.ntis.gov">http://www.ntis.gov</a>		
19. Security Classif. (of this report) Unclassified		20. Security Classif. (of this page) Unclassified		21. No. of Pages 100	22. Price



# **EVALUATION OF ASPHALT BINDER PERFORMANCE WITH LABORATORY AND FIELD TEST SECTIONS**

Pravat Karki  
Assistant Transportation Researcher  
Texas A&M Transportation Institute

and

Fujie Zhou  
Research Engineer  
Texas A&M Transportation Institute

Report 0-6674-01-R1

Project 0-6674-01

Project Title: Improving Fracture Resistance Measurements in Asphalt Binder Specifications  
with Verification on Asphalt Mixture Cracking Performance

Performed in cooperation with the  
Texas Department of Transportation  
and the  
Federal Highway Administration

Published: November 2018

TEXAS A&M TRANSPORTATION INSTITUTE  
College Station, Texas 77843-3135



## **DISCLAIMER**

This research was performed in cooperation with the Texas Department of Transportation (TxDOT) and the Federal Highway Administration (FHWA). The contents of this report reflect the views of the authors, who are responsible for the facts and the accuracy of the data presented herein. The contents do not necessarily reflect the official view or policies of the FHWA or TxDOT. This report does not constitute a standard, specification, or regulation and it is not intended for construction, bidding, or permit purposes. The engineer in charge was Dr. Fujie Zhou, P.E. (Texas, # 95969).

There is no invention or discovery conceived or first actually reduced to practice in the course of or under this contract, including any art, method, process, machine, manufacture, design or composition of matter, or any new useful improvement thereof, or any variety of plant, which is or may be patentable under the patent laws of the United States of America or any foreign country.

The United States Government and the State of Texas do not endorse products or manufacturers. Trade or manufacturers' names appear herein solely because they are considered essential to the object of this report.

## **ACKNOWLEDGMENTS**

This project was made possible by the Texas Department of Transportation in cooperation with the Federal Highway Administration. The authors thank the many personnel who contributed to the coordination and accomplishment of the work presented here. Special thanks are extended to Darrin Jensen for serving as the project manager. Many people volunteered their time to serve as project advisors, including:

- Jerry Peterson.
- Gisel Carrasco.
- Dar-Hao Chen (retired).



# TABLE OF CONTENTS

	<b>Page</b>
<b>List of Figures</b> .....	<b>ix</b>
<b>List of Tables</b> .....	<b>x</b>
<b>Chapter 1: Introduction</b> .....	<b>1</b>
Background .....	1
Objectives .....	2
Literature Review .....	2
Rheological Properties of Asphalt Binders .....	2
Durability of Asphalt Binders .....	3
Rutting Resistance of Asphalt Binders.....	3
Fatigue Cracking Resistance of Asphalt Binders .....	4
Report Organization .....	5
<b>Chapter 2: Monitoring of Eleven Previous Field Test Sections</b> .....	<b>7</b>
Introduction .....	7
SH15 Test Sections .....	7
General Description.....	7
Material Sampling, Laboratory Testing, and Results .....	8
Field Survey.....	9
US62 Test Sections .....	15
General Description.....	15
Material Sampling, Laboratory Testing, and Results .....	17
Field Survey.....	18
Loop 820 Test Sections .....	22
General Description.....	22
Material Sampling, Laboratory Testing, and Results .....	24
Field Survey.....	25
<b>Chapter 3: Construction and Monitoring of Six New Test Sections</b> .....	<b>27</b>
Introduction .....	27
Fairground Road Test Sections .....	27
General Description.....	27
Material Sampling, Laboratory Testing, and Results .....	28
Field Survey.....	30
FM31 Test Sections.....	31
General Description.....	31
Material Sampling, Laboratory Testing, and Results .....	32
Field Survey.....	33
FM468 Test Sections.....	34
General Description.....	34
Material Sampling, Laboratory Testing and Results .....	35
Field Survey.....	37
<b>Chapter 4: Characterization of Engineered Asphalt Binders</b> .....	<b>41</b>
Introduction .....	41
Rheological Properties: Frequency Sweep Tests .....	43
Effect of Binder Sources and PGs .....	45

Effect of Reclaimed Binders .....	46
Effect of Engineering Agents .....	46
Effect of Aging .....	47
Rutting Resistance: MSCR Tests .....	48
Effect of Binder Sources and PGs .....	49
Effect of Reclaimed Binders .....	49
Effect of Engineering Agents .....	49
Durability: $\Delta T_c$ Tests .....	52
Effect of Binder Source and PG .....	52
Effect of Reclaimed Binders .....	53
Effect of Engineering Agents .....	54
Effect of Aging .....	57
Fatigue Cracking Resistance: LAS Tests and Limitations .....	58
Effect of Binder Sources and PGs .....	60
Effect of Aging .....	60
Effect of Engineering Agents .....	61
Fatigue Cracking Resistance: Pure LAS Tests .....	62
Effect of Binder Sources and PGs .....	65
Effect of Aging .....	66
Effect of Engineering Agents .....	67
Correlation with Laboratory Mixture Cracking Tests .....	67
Correlation with Full-Scale Accelerated Pavement Tests .....	68
<b>Chapter 5: Updated Statewide Asphalt Binder Selection Catalog .....</b>	<b>71</b>
Introduction .....	71
Statewide PG Binder Selection Catalog Currently Used in Texas .....	71
Statewide Asphalt Binder Selection Catalog Developed Under 0-6674 .....	73
New Statewide Asphalt Binder Selection Catalog .....	74
<b>Chapter 6: Summary, Conclusions, and Recommendations .....</b>	<b>83</b>
Summary .....	83
Conclusions .....	83
Previously Constructed Field Test Sections .....	83
Newly Constructed Field Test Sections .....	83
Statewide Asphalt Binder Selection Catalog Update .....	83
Characterization of Engineered Asphalt Binders .....	84
Recommendations .....	85
<b>References .....</b>	<b>87</b>

## LIST OF FIGURES

Figure 1. SH15 Test Sections: Location Map via Google. ....	8
Figure 2. SH15 Test Sections: Survey Pictures. ....	14
Figure 3. SH15 Test Sections: Survey Results. ....	15
Figure 4. US62 Test Sections: Location Map via Google. ....	16
Figure 5. US62 Test Sections: Survey Pictures. ....	21
Figure 6. US62 Test Sections: Survey Results. ....	22
Figure 7. Loop 820 Test Sections: Location Map via Google. ....	23
Figure 8. Loop 820 Test Sections: Survey Pictures. ....	25
Figure 9. Loop 820 Test Sections: Cracking Conditions. ....	26
Figure 10. North Fairground Road Test Sections: Location Map via Google. ....	28
Figure 11. North Fairground Road Test Sections: Survey Pictures. ....	30
Figure 12. FM31 Test Sections: Location Map via Google. ....	31
Figure 13. FM31 Test Sections: Survey Pictures. ....	34
Figure 14. FM468 Test Sections: Location Map via Google. ....	35
Figure 15. FM468 Test Sections: Survey Pictures. ....	39
Figure 16. Frequency Sweep Tests and Analyses: An Illustration. ....	45
Figure 17. Frequency Sweep Test Results: Original Binders. ....	45
Figure 18. Frequency Sweep Test Results: Effect of Reclaimed Binders. ....	46
Figure 19. Frequency Sweep Test Results: Effect of Engineering Agents. ....	47
Figure 20. Frequency Sweep Test Results: Effect of Chemical Aging. ....	48
Figure 21. MSCR Test Results: Original Binders. ....	50
Figure 22. MSCR Test Results: Effect of Reclaimed Binders. ....	51
Figure 23. MSCR Test Results: Effect of Engineering Agents. ....	52
Figure 24. $\Delta T_c$ Results: Original Binders. ....	53
Figure 25. $\Delta T_c$ Results: Effect of Reclaimed Binders. ....	54
Figure 26. $\Delta T_c$ Results: Effect of Engineering Agents. ....	57
Figure 27. $\Delta T_c$ Results: Effect of Chemical Aging. ....	58
Figure 28. LAS Test and Analysis: An Illustration. ....	59
Figure 29. LAS Test Results: Original Binders. ....	60
Figure 30. LAS Test Results: Effect of Chemical Aging. ....	61
Figure 31. LAS Test Results: Effect of Engineering Agents. ....	62
Figure 32. PLAS Test and Analysis: An Illustration. ....	65
Figure 33. PLAS Test Results: Original Binders. ....	66
Figure 34. PLAS Test Results: Effect of Chemical Aging. ....	66
Figure 35. PLAS Test Results: Effect of Engineered Binders. ....	67
Figure 36. PLAS Test Results: Correlation with Mixture Cracking Results. ....	68
Figure 37. Three-Dimensional Layout of the FHWA-ALF Test Section (Gibson et al. 2012). ....	69
Figure 38. PLAS Test Results: Correlation with FHWA-ALF Cracking Test Results. ....	70
Figure 39. Asphalt Binder Grade Recommendation: TxDOT Method. ....	72
Figure 40. Asphalt Binder Grade Adjustment: TxDOT Method. ....	73
Figure 41. PG Recommendation for New Construction. ....	79
Figure 42. PG Recommendation for Asphalt Overlay over Existing AC. ....	80
Figure 43. PG Recommendation for Asphalt Overlay over JPCP. ....	81
Figure 44. Asphalt Binder PG Recommendation and Adjustment: New Method. ....	82

## LIST OF TABLES

Table 1. SH15 Test Sections: GPS Coordinates.....	8
Table 2. SH15 Test Sections: Stiffness Properties.....	9
Table 3. SH15 Test Sections: Rutting Properties.....	9
Table 4. SH15 Test Sections: Cracking Properties.....	9
Table 5. US62 Test Sections: GPS Coordinates.....	17
Table 6. US62 Test Sections: Stiffness Properties.....	17
Table 7. US62 Test Sections: Rutting Properties.....	17
Table 8. US62 Test Sections: Cracking Properties.....	18
Table 9. Loop 820 Test Sections: GPS Coordinates.....	24
Table 10. Loop 820 Test Sections: Stiffness Properties.....	24
Table 11. Loop 820 Test Sections: Rutting Properties.....	24
Table 12. Loop 820 Test Sections: Cracking Properties.....	25
Table 13. North Fairground Road Test Sections: GPS Coordinates.....	28
Table 14. North Fairground Road Test Sections: Stiffness Properties.....	29
Table 15. North Fairground Road Test Sections: Rutting Properties.....	29
Table 16. North Fairground Road Test Sections: Cracking Properties.....	29
Table 17. FM31 Test Sections: GPS Coordinates.....	32
Table 18. FM 31 Test Sections: Stiffness Properties.....	32
Table 19. FM31 Test Sections: Rutting Properties.....	32
Table 20. FM31 Test Sections: Cracking Properties.....	33
Table 21. FM468 Test Sections: GPS Coordinates.....	35
Table 22. FM468 Test Sections: Stiffness Properties.....	36
Table 23. FM468 Test Sections: Rutting Properties.....	36
Table 24. FM468 Test Sections: Cracking Properties.....	36
Table 25. List of Materials Used to Produce Engineered Asphalt Binders.....	42
Table 26. Overlay Performance Simulation Factorial: 0-6674.....	75
Table 27. Asphalt Binder Grade Recommendation: 0-6674.....	76
Table 28. Asphalt Binder Grade Recommendation: New Catalog.....	77

# CHAPTER 1: INTRODUCTION

## BACKGROUND

The current performance-grade (PG) specification for asphalt binders was developed 25 years ago during the Strategic Highway Research Program (SHRP). One of the limitations of the PG specification was that it was established based primarily upon the study of unmodified binders. Since the completion of the SHRP in 1993, many state departments of transportation (DOTs) have adopted the PG specification. Over the years, experience has proven that the PG system, while good for ensuring overall quality, fails in some cases to guarantee good rutting and cracking performance. Although asphalt binders produced still meet the requirements of the PG specification, many highway agencies in the United States are increasingly experiencing premature failures of pavements. These failures can be associated with any of the following changes:

- Availability of a much wider range of crude oil sources.
- Development of new techniques to extract more saturates from crude oil sources before producing asphalt binders.
- Development of new techniques to engineer asphalt binders such as the use of re-refined engine oil bottoms (REOB) and polyphosphoric acid (PPA).
- Increased use of reclaimed materials such as ground tire rubber, reclaimed asphalt pavements (RAP), and recycled roof shingles (RAS) in asphalt pavement construction.

The advancement of any of these techniques is not necessarily at fault by itself. For example, recent studies have shown that mixes with soft but highly polymer-modified binders have actually improved cold weather cracking properties over mixes, while rutting resistance of the mixes is maintained. It is therefore crucial to use these techniques and engineer the binders that meet the required PG and satisfy mix performance criteria set by the state agencies.

Under project 0-6674 (Zhou et al. 2014), Texas A&M Transportation Institute (TTI) researchers studied which asphalt binder tests could capture the representative properties of softer, highly modified asphalt binders (PGxx-28, PGxx-34, or lower grades). Researchers also investigated the performance of different field test sections constructed with these binders in the northern districts of Texas (Hu et al. 2014). Researchers also conducted parametric analyses of overlay performance by varying traffic, environment, structure, and overlay mixes using computer simulations, and then recommended updating the statewide binder selection catalog used by the Texas Department of Transportation (TxDOT).

As the continuation of project 0-6674, project 0-6674-01 involves validating the use of softer, highly modified binders in different areas of Texas, exploring different techniques to engineer asphalt binders, and expanding asphalt binder selection catalog for different applications, which were not included in the scope of the previous project.

## OBJECTIVES

The main objectives of this study were to:

- Continue monitoring the field test sections constructed under project 0-6674 for the duration of 0-6674-01 and use the collected performance data to validate the benefits of softer binders in the colder areas of Texas.
- Validate statewide binder selection catalog building test sections in west, south, and east Texas districts.
- Evaluate 10 often used asphalt binders recently engineered with various modification techniques using the asphalt binder test recommended under project 0-6674 (Zhou et al. 2014).
- Update the statewide binder selection catalog developed under project 0-6674 (Hu et al. 2014).

## LITERATURE REVIEW

Asphalt binder performance is influenced by many factors. To perform well, asphalt binder must meet a series of criteria for different properties. The following properties were identified as crucial to discriminate asphalt binder performance.

### Rheological Properties of Asphalt Binders

Asphalt binder rheology has been studied in terms for various parameters, most notably crossover frequency,  $\omega_c$ , and rheological index,  $R$ . The Christensen-Anderson model (Christensen and Anderson 1992) can be used to fit the master curves constructed by conjoining frequency sweep data using the principle of time-temperature superposition of viscoelastic materials and determining the values of  $\omega_c$  and  $R$  parameters for each asphalt binder.

Crossover frequency,  $\omega_c$ , is an indicator of general consistency or hardness at a selected temperature, and is defined as the frequency at a given temperature where storage and loss moduli are equal (i.e., where phase angle is  $45^\circ$ ) (Anderson et al. 2011).  $R$  is a shape factor of master curve and is defined as the difference between the logarithmic values of the glassy modulus and the shear complex modulus at the crossover frequency. This index primarily describes how efficiently binders transfer from elastic state to viscous (steady) state (Anderson et al. 2011). Higher  $R$  value refers to a flatter master curve and a slower elastic-to-steady state transition and vice versa. Therefore, a binder with lower  $R$  (i.e., faster transition) and higher  $\omega_c$  (i.e., softer) is more resistant to cracking. With aging or with the use of RAP/RAS, the  $\omega_c$  value increases while the  $R$  value decreases. This trend reverses itself when bio-rejuvenators are used (Karki and Zhou 2016). The black-space diagram of  $\omega_c$  and  $R$  can be used to study the effect of engineering agents such REOB, bio-rejuvenators, and aging on overall hardness and elastic-to-

steady-state transition properties of base binders (Karki and Zhou 2016; Mogawer et al. 2017; Karki et al. 2018).

Recognizing the potential of differentiating the impact of engineering agents and aging on binder properties, TTI researchers conducted frequency sweep tests to determine these parameters and evaluated rheological properties engineered binders for this study as well.

### **Durability of Asphalt Binders**

In last several years, the difference in critical low temperature obtained from creep stiffness and creep slope ( $\Delta T_c$ ) has been identified as an effective indicator of asphalt binder durability. The low temperature PG, also known as critical low temperature, is defined as the maximum value of the temperature at which the creep stiffness ( $T_{cs}$ ) and the creep slope ( $T_{cm}$ ) of asphalt binders at 60 seconds after loading are equal to 300 MPa and 0.300, respectively (AASHTO M320 2010).  $\Delta T_c$  is defined as the difference between these two temperatures,  $\Delta T_c = T_{cs} - T_{cm}$  (Bennert et al. 2016; Li et al. 2016). Researchers (Bennert et al. 2016; Li et al. 2017) have suggested limiting  $\Delta T_c$  at  $-5^\circ\text{C}$  to avoid cracking due to lower quality of asphalt binders.

Under project 0-6881 (Karki et al. 2018), TTI researchers determined that  $\Delta T_c$  could be used to evaluate impact of engineering agents (REOB, PPA, aromatic extract, bio-rejuvenator) on durability of asphalt binders. Researchers found that REOB or PPA degrades asphalt binder durability by making  $\Delta T_c$  more negative irrespective of the sources of asphalt binders, REOB, and PPA. On contrary, researchers found that the trend reverses when binders are modified with aromatic extract and bio-rejuvenator (Karki et al. 2018). Recognizing this potential, TTI researchers have extensively used this parameter to evaluate durability of engineered binders in this project as well.

### **Rutting Resistance of Asphalt Binders**

Conventionally, the temperatures at which  $G^*/\text{Sin}\delta$  at 10 rad/sec is equal to 1.0 kPa for unaged or 2.2 kPa for rolling thin film oven (RTFO)-aged asphalt binders (AASHTO T315 2012) or the minimum of these two temperatures, referred to as the high temperature PG of asphalt binders (AASHTO M320 2010), are used to discriminate rutting potential of asphalt binders. This approach assumes rutting is more prevalent in binders that are softer and more viscous (lower  $G^*$ , higher  $\delta$ ) than in binders that are stiffer and are more elastic (higher  $G^*$ , lower  $\delta$ ). However,  $G^*/\text{Sin}\delta$  does not fulfill this purpose always, for example in the case of asphalt binders that have been modified with polymers (Bahia et al. 2001; D'Angelo and Dongre 2002; Dongre and D'Angelo 2003, 2006; Stuart et al. 2000). To address this deficiency of  $G^*/\text{sin}\delta$ , researchers have used parameters measured using repeated creep and recovery tests (Bahia et al. 2001; Bouldin et al. 2001), zero shear viscosity tests (Anderson 2002; D'Angelo et al. 2007; Desmazes et al. 2000; Phillips and Robertus 1996; Sybilski 1996), and elastic recovery measured from ductility tests of asphalt binders following (AASHTO T51 2013). The unrecoverable strain and

percent recovery parameters measured from the multiple stress creep and recovery (MSCR) tests of asphalt binders (AASHTO T350 2014) have shown good correlations with asphalt mixture rutting potential (Zhou et al. 2014; Zhang et al. 2015).

Under project 0-6674 (Zhou et al. 2014), TTI researchers coordinated with five different laboratories, conducted MSCR Round Robin tests, and found that MSCR test parameters better differentiate rutting potential of asphalt binders than the current PG test parameter ( $G^*/\sin \delta$ ), especially for those highly modified asphalt binders (such as PG64-34). Researchers recommended implementing the MSCR test for discriminating binders for rutting.

### **Fatigue Cracking Resistance of Asphalt Binders**

PG binder specification uses the  $G^* \cdot \sin(\delta)$  parameter to characterize fatigue resistance of asphalt binders. Many researchers have questioned the correlation between  $G^* \cdot \sin(\delta)$  parameter and fatigue property of asphalt binders (Anderson et al. 2001; Andriescu et al. 2004; Bahia et al. 2001, 2002; Deacon et al. 1997; Tsai and Monismith 2005). The general consensus is that the current Superpave binder specification does not adequately predict the contribution of binder fatigue property to mixture fatigue performance.

Bahia and his associates used time sweep tests to differentiate fatigue damage of asphalt binders based on associated fatigue lives (2001, 2002). They repeatedly applied strain-controlled cyclic loading at a fixed amplitude on an asphalt binder sample (8 mm in diameter and 2 mm in thickness) with dynamic shear rheometer (DSR) for these tests. However, these tests often take a long time to reach fatigue condition. Andriescu et al. (2004) employed a double edge notched tension test to calculate the critical tip opening displacement for binder fatigue cracking. Most recently, the accelerated version of the time sweep test, namely linear amplitude sweep (LAS) test, was developed to address the long testing time issue with the time sweep test (Hintz et al. 2011a; b; Johnson 2010). The LAS test has also been incorporated in a provisional standard: AASHTO TP 101-12 *Standard Method of Test for Estimating Fatigue Resistance of Asphalt Binders Using the Linear Amplitude Sweep* (2014).

Under project 0-6674, TTI researchers recommended using this test for evaluating asphalt binder fatigue resistance (Zhou et al. 2014). However, as discussed later in Chapter 4, researchers have recently found that some LAS test results are counterintuitive (Zhou et al. 2017). Therefore, this report first discusses this deficiency of the LAS test, and then presents the development of the new binder fatigue cracking including deriving the fatigue energy index based on fracture mechanics. The report also discusses the sensitivity of the new binder fatigue to different methods and levels of engineering and aging.



## **REPORT ORGANIZATION**

This report is organized in six chapters. Chapter 1 provides a brief introduction of the project and the problem statement. Chapter 2 describes survey results of the field test sections that were previously constructed under project 0-6674 and continually monitored for this project. Chapter 3 presents survey results of six new field test sections that were specially constructed in different environmental zones of Texas under this project. Chapter 4 discusses different ways of engineering asphalt binders and their characteristics of these engineered binders determined using test methods identified in project 0-6674. Chapter 5 presents a new method to select and adjust asphalt binder PG and catalog. Finally, Chapter 6 offers the conclusions drawn from this study based on field test surveys, characterization of engineered asphalt binders, and recommendations on the use of softer asphalt binders in Texas.



## **CHAPTER 2: MONITORING OF ELEVEN PREVIOUS FIELD TEST SECTIONS**

### **INTRODUCTION**

This project surveyed the performance of 11 field test sections constructed under project 0-6674 to confirm the benefits of soft, highly modified binders in the colder areas of Texas. TTI researchers have been surveying cracking and rutting distresses of these sections periodically since their initial construction. This chapter describes the test sections, the materials sampled from these sections, the properties measured using these mixtures, and the results of the survey conducted on each of these field test sections for the duration of this project 0-6674-01.

### **SH15 TEST SECTIONS**

#### **General Description**

Four test sections were constructed on SH15 near Perryton, Texas, under project 0-6674 (Hu et al. 2014). The starting point of the first section is about 4.3 miles away from the intersection of SH15 and US83 (see point A in Figure 1) and is right across the milepost number 368. Each of these sections is bound northeast and measures 1000 ft in length. Table 1 presents the GPS coordinates for each test section as recorded from a mobile device.

The sections were constructed by replacing 1 in. of existing pavement with 1.5 in. of Type D and 1 in. of Type F mix. The Type D overlay was prepared with different percentages or grades of asphalt binder as shown below:

- Section 1: 5.5 percent PG 58-28 (control mix).
- Section 2: 5.8 percent PG 58-28.
- Section 3: 5.8 percent PG 64-34.
- Section 4: 5.5 percent PG 64-34.

As seen, Section 1 used the control mix prepared with PG58-28 asphalt binder while Section 2 used the mix with the same asphalt binder but higher asphalt binder content. Section 3 and Section 4 use the softer but highly modified PG64-34 asphalt binder but slightly different asphalt binder contents. The mix designs followed the TxDOT specification.

The sections were constructed on October 7, 2013. The average paving temperature was measured as 245°F. The temperature measurement was taken directly from the material behind the paver.

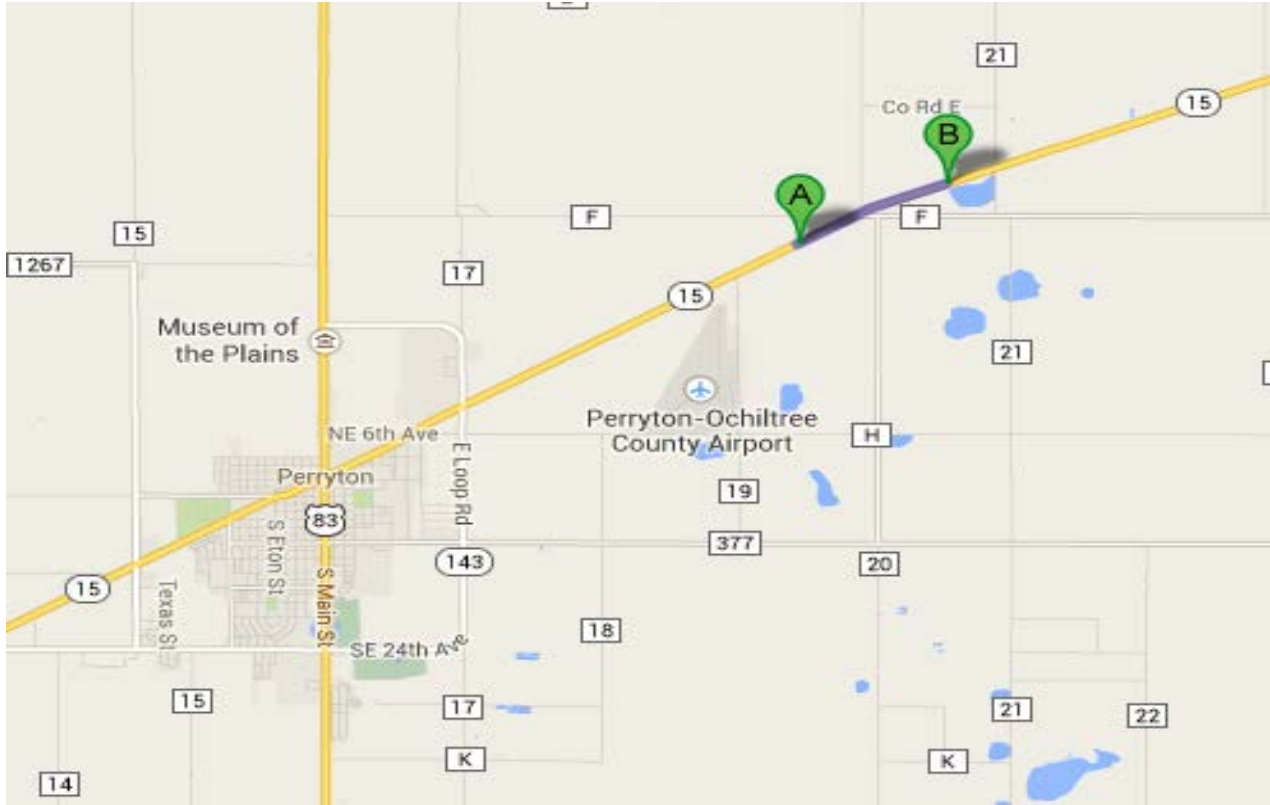


**Figure 1. SH15 Test Sections: Location Map via Google.**

**Table 1. SH15 Test Sections: GPS Coordinates.**

Section	Start		End		Length (ft)
	Latitude	Longitude	Latitude	Longitude	
1	36°25.887'	-100°44.277'	36°26.006'	-100°44.033'	1390
2	36°26.040'	-100°43.966'	36°26.154'	-100°43.705'	1450
3	36°26.201'	-100°43.560'	36°26.293'	-100°43.268'	1530
4	36°26.328'	-100°43.155'	36°26.395'	-100°42.956'	1050

### **Material Sampling, Laboratory Testing, and Results**

For each test section, TTI researchers sampled seven buckets of plant mixes per section for mixture tests, namely dynamic modulus test, repeated load permanent deformation test, and Overlay test (OT). Test results are shown in Table 2, Table 3, and Table 4, respectively.

**Table 2. SH15 Test Sections: Stiffness Properties.**

Temp. (°C)	Freq. (Hz)	Dynamic Modulus (ksi)			
		Section 1 5.5% PG58-28	Section 2 5.8% PG58-28	Section 3 5.8% PG64-34	Section 4 5.5% PG64-34
4	25	1799.6	1903.0	1728.4	1894.3
	10	1567.7	1668.2	1480.7	1638.6
	5	1394.9	1495.4	1301.5	1453.9
	1	1023.8	1116.9	925.8	1059.4
	0.5	882.9	970.7	786.4	910.1
	0.1	602.2	673.2	511.4	611.0
20	25	806.3	845.4	685.6	784.7
	10	631.3	665.3	520.6	605.5
	5	521.2	551.0	418.5	494.0
	1	309.8	333.4	230.1	282.1
	0.5	246.5	267.1	177.9	221.1
	0.1	132.3	147.3	90.7	116.3
40	25	176.3	184.3	142.3	165.7
	10	117.1	124.2	91.7	109.5
	5	83.1	89.5	65.6	78.8
	1	35.0	38.8	29.6	34.9
	0.5	25.4	28.5	23.5	27.1
	0.1	12.7	14.5	14.0	15.3
	0.01	6.3	7.2	8.5	7.5

**Table 3. SH15 Test Sections: Rutting Properties.**

Rutting Properties	Section 1 5.5% PG58-28	Section 2 5.8% PG58-28	Section 3 5.8% PG64-34	Section 4 5.5% PG64-34
$\alpha$	0.6437	0.6697	0.7685	0.7694
$\mu$	0.634	0.7035	0.539	0.44

**Table 4. SH15 Test Sections: Cracking Properties.**

Cracking Properties	Section 1 5.5% PG58-28	Section 2 5.8% PG58-28	Section 3 5.8% PG64-34	Section 4 5.5% PG64-34
OT cycles	912	1590	9001	6549
A	$9.7044 \times 10^{-9}$	$3.3559 \times 10^{-9}$	$1.2234 \times 10^{-10}$	$2.2459 \times 10^{-10}$
n	5.6184	5.9097	6.8181	6.6514

### Field Survey

The last survey of these sections under project 0-6674 was conducted on June 7, 2014. At the time, no cracking or rutting issues were observed. Since then, the sections have been surveyed six more times, in March 2015, September 2015, March 2016, September 2016, March 2017, and January 2018. Figure 2 presents the conditions of sections as observed in recent surveys.

### *Rutting*

Researchers detected rutting in each of these sections for the first time in January 2018. The detected rut was only about 1/16 in. in depth, as shown in Figure 2. They had not observed any rutting prior to this survey.

### *Cracking*

**Section 1:** Researchers spotted cracking in this section for the first time in March 2016 (see Figure 3). At the time, there were 14 transverse cracks that totaled 213 ft/mile and 8 different stretches of alligator cracking that totaled 20.5 percent of total lane area. In September 2017, researchers found that almost all cracks healed, most likely due to heat in the summer. In March 2017, cracks reappeared with much higher severity, a total of 22 transverse cracks that totaled 3052 ft/mile and 13 different stretches of alligator cracking that totaled 25.5 percent of total lane area. The most recent survey conducted on January 10, 2018, showed that cracks have interconnected with each other throughout the section covering both wheel paths, as shown in Figure 2.

**Section 2:** Researchers observed cracking in this section for the first time in March 2016 (see Figure 3). At the time, there were only 2 transverse cracks that totaled 26 ft/mile and 1 longitudinal crack that totaled 29 ft/mile. In March 2017, researchers detected more cracks: 10 transverse cracks that totaled 179 ft/mile, 7 longitudinal cracks that totaled 183 ft/mile, and 2 stretches of alligator cracking that totaled 3.3 percent of total lane area. Healing was not observed in this section. In January 2018, researchers found that the transverse cracks covered the full width of the sections, and that cracks have interconnected with each other, more noticeably in the inner wheel path throughout the section, as shown in Figure 2.

**Section 3:** Researchers observed cracking in this section for the first time in September 2016 (see Figure 3). At the time, there was only 1 stretch of alligator cracking that totaled 1.8 percent of total area. In March 2017, researchers detected 3 new transverse cracks that totaled 53 ft/mile and 7 new stretches of alligator cracking that totaled 18.4 percent of total lane area. The recent survey in March 2018 showed that all these cracks have interconnected, as shown in Figure 2.

**Section 4:** Researchers observed cracking in this section for the first time in March 2017 (see Figure 3). At the time, they detected 3 transverse cracks that totaled 54 ft/mile, and 6 stretches of alligator cracks that totaled to 21.3 percent of total lane area. The survey in January 2018 showed that transverse cracks have extended full-width, and alligator cracks have interconnected with each other, as shown in Figure 2.



Alligator Cracking: 03/07/2017



Transverse Cracking: 03/07/2017



Overall Cracking: 01/10/2018



Rutting (1/16 in.): 01/10/2018

**SH15 Section 1**





Alligator Cracking: 03/07/2017



Transverse Cracking: 03/07/2017



Longitudinal Cracking: 03/07/2017



Cracking: 01/10/2018



Rutting (1/16 in.): 01/10/2018

**SH15 Section 2**





Alligator Cracking: 03/07/2017



Transverse Cracking: 03/07/2017



Overall Cracking: 01/10/2018



Rutting (1/16 in.): 01/10/2018

**SH15 Section 3**



Alligator Cracking: 03/07/2017



Transverse Cracking: 03/07/2017



Overall Cracking: 01/10/2018



Rutting (1/16 in.): 01/10/2018

**SH15 Section 4**

**Figure 2. SH15 Test Sections: Survey Pictures.**

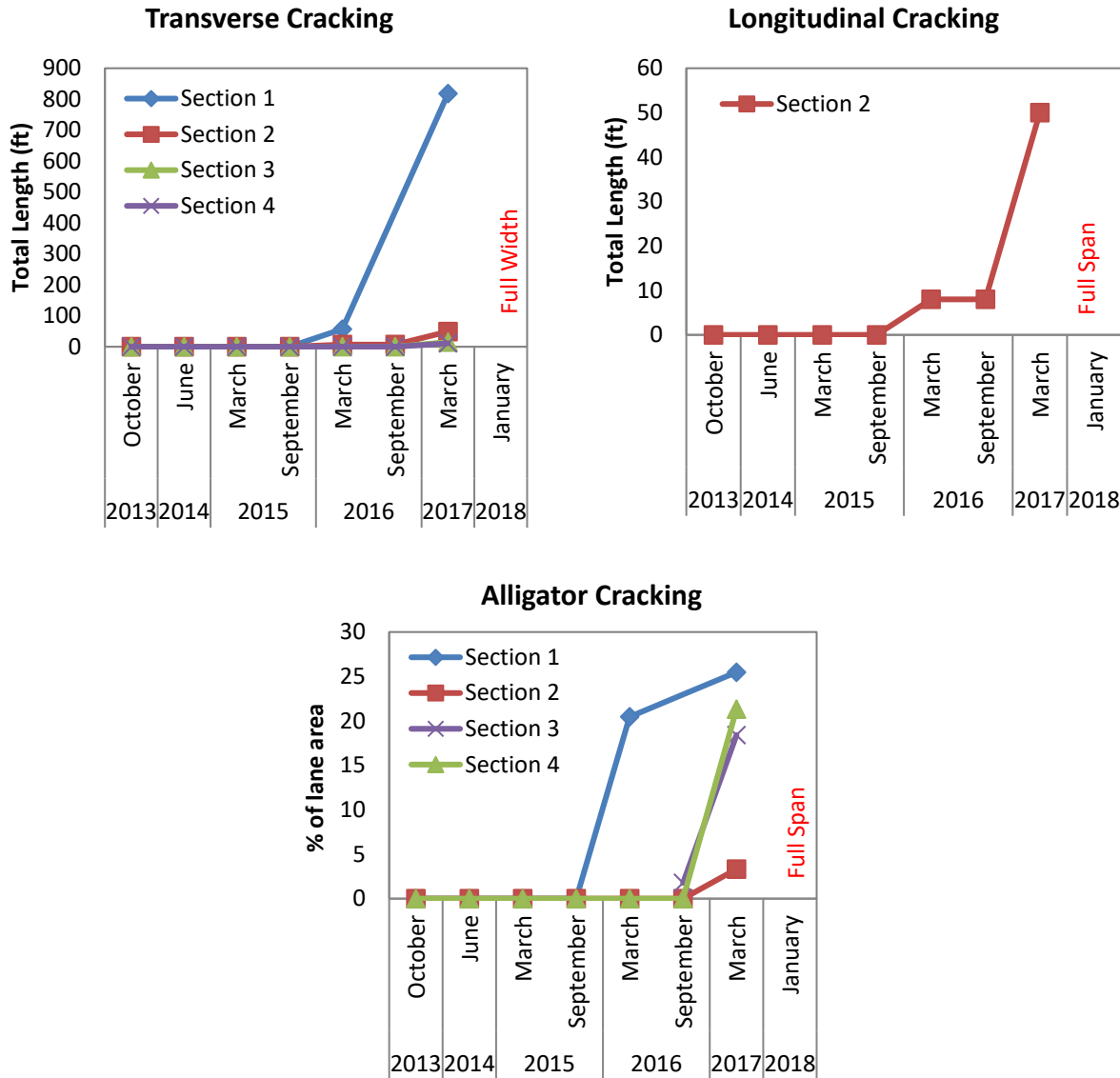


**Figure 3. SH15 Test Sections: Survey Results.**

The fact that alligator cracking, longitudinal, and transverse cracks appear later and with smaller severity values in Sections 3 and 4 than in Sections 1 and 2 suggest that PG64-34 was able to delay the initiation and the propagation of cracking as expected.

## US62 TEST SECTIONS

### General Description

Three sections were constructed on the eastbound side of US62 close to Childress, Texas, under project 0-6674 (Hu et al. 2014). Figure 4 shows the starting point of Section 1 (Point A) and the end point of Section 3 (Point B). Each of these sections is bound northeast and measures about

1500 ft in length. Milepost number 442 lies just next to the starting point of Section 3. Table 5 presents the GPS coordinates for each test section as recorded from a mobile device.

The sections were constructed by replacing 8 in. of existing pavement with 2 in. of Type D mix and 3 in. of Type B mix. Note that the 3 in. of Type B mix was used throughout the whole project, and the only difference is the surface Type D mix. The Type D mix in these three sections differed either in asphalt binder grade or in the use of reclaimed materials as follows:

- Section 1: PG 64-34 + RAP/RAS.
- Section 2: PG 70-28 → *Control Mix*.
- Section 3: PG 70-28 + RAP/RAS.

As seen, Section 1 uses the mix prepared with PG64-34 asphalt binder together with reclaimed materials, Section 2 uses the mix prepared with virgin mix and a PG70-28 asphalt binder (without RAP/RAS), and Section 3 uses the mix prepared with PG70-28 asphalt binder together with reclaimed materials. The only difference between Sections 1 and 3 is the asphalt binder type: PG64-34 in Section 1 versus PG70-28 in Section 3.

The construction of overlay was conducted on October 3, 2013. The average paving temperature was measured behind the paver as 320°F.

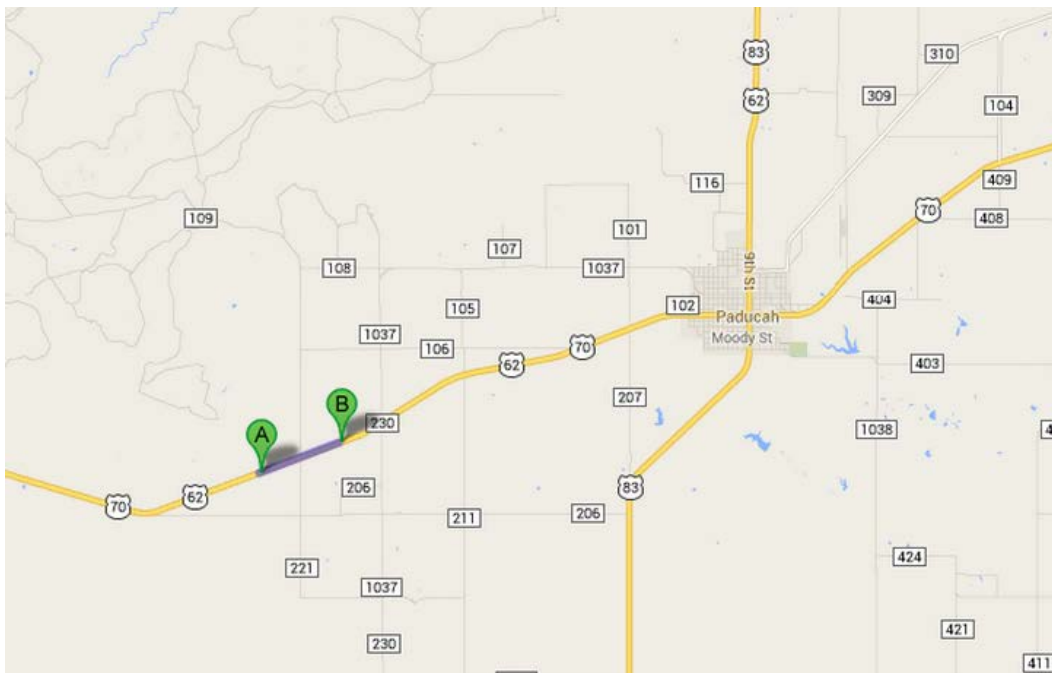


**Figure 4. US62 Test Sections: Location Map via Google.**

**Table 5. US62 Test Sections: GPS Coordinates.**

Section	Start		End		Length (ft)
	Latitude	Longitude	Latitude	Longitude	
1	36°25.887'	-100°44.277'	36°26.006'	-100°44.033'	1390
2	36°26.040'	-100°43.966'	36°26.154'	-100°43.705'	1450
3	36°26.201'	-100°43.560'	36°26.293'	-100°43.268'	1530

**Material Sampling, Laboratory Testing, and Results**

For each test section, TTI researchers sampled seven buckets of mixes for laboratory testing, namely dynamic modulus test, repeated load permanent deformation test, and OT. The test results are shown in Table 6, Table 7, and Table 8, respectively.

**Table 6. US62 Test Sections: Stiffness Properties.**

Temp. (°C)	Freq. (Hz)	Dynamic Modulus (ksi)		
		Section 1 PG64-34 + RAP + RAS	Section 2 PG70-28	Section 3 PG70-28 + RAP + RAS
4	25	1479.8	1488.6	1826.0
	10	1265.2	1283.2	1608.1
	5	1108.0	1135.1	1453.8
	1	782.5	821.7	1120.8
	0.5	665.0	702.8	989.5
	0.1	432.9	470.8	718.9
20	25	631.4	599.0	850.3
	10	481.5	459.7	685.0
	5	390.2	377.2	578.7
	1	220.2	219.7	375.0
	0.5	174.2	175.6	309.4
	0.1	93.4	96.9	189.0
40	25	128.5	130.7	215.7
	10	86.1	88.3	156.2
	5	63.4	65.4	122.0
	1	29.6	31.0	64.7
	0.5	24.0	24.8	52.4
	0.1	14.1	14.4	30.1
	0.01	8.5	8.4	15.8

**Table 7. US62 Test Sections: Rutting Properties.**

Rutting Properties	Section 1 PG64-34 + RAP + RAS	Section 2 PG70-28	Section 3 PG70-28 + RAP + RAS
$\alpha$	0.7285	0.7581	0.7424
$\mu$	0.5345	0.629	0.4905

**Table 8. US62 Test Sections: Cracking Properties.**

Cracking Properties	Section 1 PG64-34 + RAP + RAS	Section 2 PG70-28	Section 3 PG70-28 + RAP + RAS
OT cycles	5426	33192	417
A	$3.2171 \times 10^{-10}$	$1.0113 \times 10^{-11}$	$4.3272 \times 10^{-8}$
n	6.5529	7.5019	5.2083

### **Field Survey**

The last survey of these sections under project 0-6674 was conducted on June 6, 2014. At the time, neither cracking nor rutting was detected in any of these sections. Since then, the sections have been surveyed six more times: March 2015, September 2015, March 2016, September 2016, March 2017, and January 2018. Figure 5 presents the conditions of sections as observed in recent surveys.

#### *Rutting*

None of these sections has exhibited any noticeable rutting as of January 10, 2018 (see Figure 5).

#### *Cracking*

**Section 1:** Researchers observed cracks in this section first in March 2017 (see Figure 6). At the time, there were 10 longitudinal cracks that totaled 1181 ft/mile and only 2 transverse cracks that totaled 76 ft/mile. In January 2018, 20 longitudinal cracks that totaled 2192 ft/mile were observed. The total number and length of transverse cracks remained intact.

**Section 2:** Researchers observed transverse cracks in this section first in March 2015 (see Figure 6). The total number of these cracks increased from 44 cracks that totaled 239 ft/mile in March 2015 to 163 cracks that totaled 886 ft/mile in January 2018. Similarly, researchers observed longitudinal cracks in this section first in January 2018. There were 3 longitudinal cracks that totaled 134 ft/mile.

**Section 3:** Researchers observed transverse cracks in this section first in March 2015 (see Figure 6). The total number of these cracks remained almost the same from 19 cracks that totaled 588 ft/mile in March 2015 to 20 cracks that totaled 1170 ft/mile in January 2018. Similarly, researchers observed longitudinal cracks in this section first in January 2018. There were 10 longitudinal cracks that totaled 3917 ft/mile.





Longitudinal Cracking: 01/10/2018



Transverse Cracking: 01/10/2018

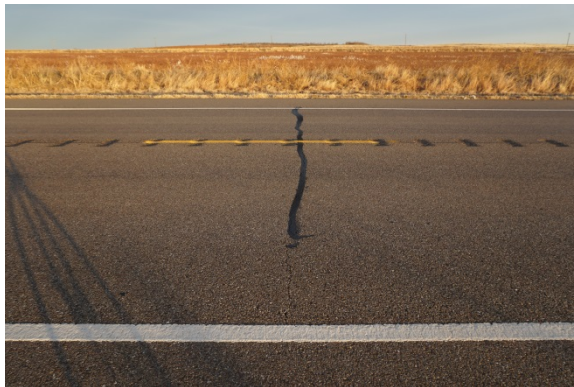


Rutting (None): 01/10/2018

**US62 Section 1**



Longitudinal Cracking: 01/10/2018



Transverse Cracking: 01/10/2018



Rutting (None): 01/10/2018

**US62 Section 2**





Longitudinal: 01/10/2018



Transverse Cracking: 01/10/2018



Rutting: 01/10/2018 (None)

**US62 Section 3**

**Figure 5. US62 Test Sections: Survey Pictures.**

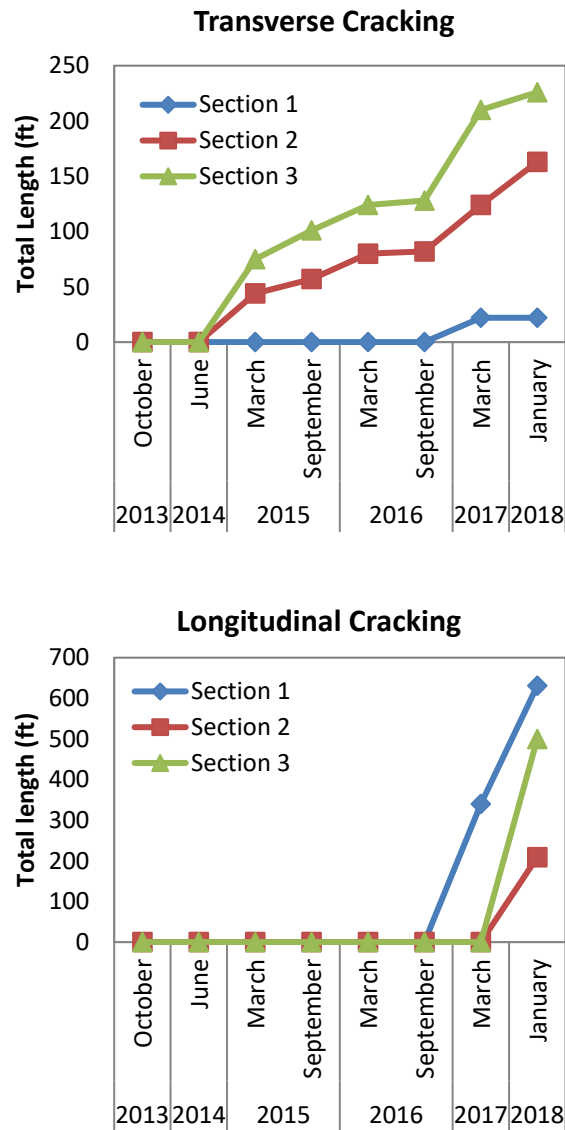


**Figure 6. US62 Test Sections: Survey Results.**

Considering both transverse and longitudinal cracking, it is clear that Section 1 has less total cracking length than Sections 2 and 3. Such observation indicated that PG64-34 was able to impede the initiation and the propagation of such cracks in this case.

## LOOP 820 TEST SECTIONS

### General Description

Four sections located on the westbound side of Loop 820 in the Fort Worth, Texas, were built in July 2012 under project 0-6674 (Hu et al. 2014). These sections were side by side on four lanes on Loop 820. The lanes start 61 ft away from the first pole after the Quebec Bridge (point A in

Figure 7) and end very close to Milepost 9 (point B in Figure 7), measuring 992 ft in length. Table 9 presents the GPS coordinates for each test section as recorded from a mobile device.

Each of these lanes/sections was constructed with 2-in. thick Type D mix containing different combinations of asphalt binder, reclaimed materials, and warm mix additive from Advera as shown below:

- Section 0: PG64-22 + 13%RAP + 5%RAS + Advera → *Control Mix*.
- Section 1: PG64-22 + 13%RAP + 5%RAS pre-blended with Advera.
- Section 2: PG64-28 + 13%RAP + 5%RAS + Advera.
- Section 3: PG64-22 (0.4 percent more) + 13%RAP + 5%RAS + Advera.

As seen, Section 0 uses the control mix prepared with PG64-22 asphalt binder, 13 percent RAP, 5 percent RAS, and the warm mix additive of Advera. Section 1 uses the mix prepared with the same materials as the control mix except that RAS was pre-blended with Advera additive before mixing with other components of the mix. Section 2 uses the mix that is similar to the control mix except that PG64-22 asphalt binder is replaced with PG64-28. Section 3 uses the mix that is very similar to the control mix except that it contains 0.4 percent more asphalt binder than the control mix. Section 0 (innermost lane) is next to the left shoulder or central median while Section 3 is (slowest lane) is next to the right shoulder.

Sections 1–3 were constructed in the night of July 19, 2012. The average paving temperatures measured behind the paver were 262°F, 268°F, and 272°F for Sections 1, 2, and 3, respectively.

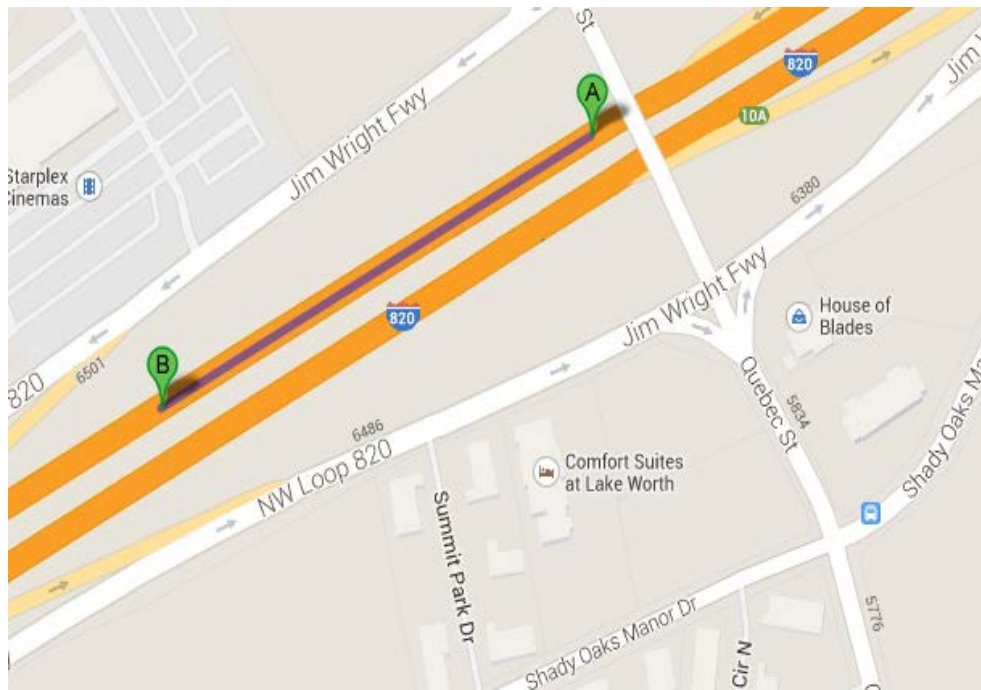


**Figure 7. Loop 820 Test Sections: Location Map via Google.**

**Table 9. Loop 820 Test Sections: GPS Coordinates.**

Section	Start		End		Length (ft)
	Latitude	Longitude	Latitude	Longitude	
0,1, 2, 3	32°48.239'	-97°25.887'	32°48.162'	-97°25.761'	992

**Material Sampling, Laboratory Testing, and Results**

From each test section, TTI researchers obtained 10 buckets of plant mixes during the construction for laboratory testing. The stiffness, rutting, and cracking properties obtained from the laboratory mixture tests are shown in Table 10, Table 11, and Table 12, respectively.

**Table 10. Loop 820 Test Sections: Stiffness Properties.**

Temp. (°C)	Freq. (Hz)	Dynamic Modulus (ksi)			
		Section 0 PG64-22 + RAP + RAS + Advera	Section 1 PG64-22 + RAP + RAS blended with Advera	Section 2 PG64-28 + RAP + RAS + Advera	Section 3 0.4% more PG64-22 + RAP + RAS + Advera
4	25	2393.7	2033.0	2011.2	2309.5
	10	2220.5	1845.6	1826.3	2117.5
	5	2088.4	1700.5	1685.5	1971.6
	1	1781.6	1381.1	1362.6	1639.8
	0.5	1647.0	1243.6	1226.0	1494.0
	0.1	1341.7	935.6	928.7	1178.2
20	25	1458.7	1119.8	1046.6	1242.6
	10	1264.9	940.9	866.0	1052.0
	5	1120.6	820.1	747.5	922.5
	1	825.7	570.5	511.5	658.3
	0.5	713.8	485.4	432.8	566.8
	0.1	489.6	314.8	280.3	381.5
40	25	468.2	384.5	333.8	398.8
	10	358.9	288.2	249.6	305.9
	5	292.2	230.4	200.1	246.0
	1	162.7	127.2	110.1	134.7
	0.5	129.9	100.8	88.4	109.1
	0.1	72.8	56.0	49.6	65.1
	0.01	34.2	27	24.5	37.6

**Table 11. Loop 820 Test Sections: Rutting Properties.**

Rutting Properties	Section 0 PG64-22 + RAP + RAS + Advera	Section 1 PG64-22 + RAP + RAS blended with Advera	Section 2 PG64-28 + RAP + RAS + Advera	Section 3 0.4% more PG64-22 + RAP + RAS + Advera
$\alpha$	0.6921	0.7311	0.6674	0.7102
$\mu$	0.312	0.671	0.4915	0.548

**Table 12. Loop 820 Test Sections: Cracking Properties.**

<b>Cracking Properties</b>	<b>Section 0 PG64-22 + RAP + RAS + Advera</b>	<b>Section 1 PG64-22 + RAP + RAS blended with Advera</b>	<b>Section 2 PG64-28 + RAP + RAS + Advera</b>	<b>Section 3 0.4% more PG64-22 + RAP + RAS + Advera</b>
OT cycles	8	12	22	24
A	$8.2469 \times 10^{-5}$	$3.8011 \times 10^{-5}$	$1.1941 \times 10^{-5}$	$1.0112 \times 10^{-5}$
n	3.1366	3.3491	3.6667	3.7123

**Field Survey**

The last survey of these sections for project 0-6674 was conducted on June 12, 2014. The survey found no cracking or rutting issues in any of these sections, except some segregation issues in Section 4. Since then, the sections have been surveyed four more times: March 2016, November 2016, July 2017, and March 2018. Figure 8 presents the conditions of these sections as observed in recent surveys.

*Rutting*

None of these sections has exhibited any noticeable rutting as of March 26, 2018 (see Figure 8).



Sections 0 to 3: View from Quebec Bridge on 03/26/2018

**Figure 8. Loop 820 Test Sections: Survey Pictures.**



## Cracking

Loop 820 is a very busy road and four test sections were paved side by side, which results in a survey problem. It is okay to clearly determine the cracking conditions of Sections 0 and 3, but the conditions of Sections 1 and 2 could not be well observed. Many efforts were made, but no fruitful result was obtained. Thus, TTI researchers had to turn to Google Maps for an overall comparison. Figure 9 shows an overall pavement conditions. Section 1 has the most reflective cracking, followed by Section 0; that Section 2 has the least reflective cracking and Section 3 has the second least reflective cracking. Such observation clearly indicated that the use of soft but modified asphalt binder can improve cracking resistance; meanwhile, adding more virgin asphalt binder into the mix can also increase cracking resistance of asphalt binder mixes with RAP/RAS.



Satellite View Accessed on 06/25/2018 via Google Map  
**Figure 9. Loop 820 Test Sections: Cracking Conditions.**

## **CHAPTER 3: CONSTRUCTION AND MONITORING OF SIX NEW TEST SECTIONS**

### **INTRODUCTION**

This project constructed a total of six new field test sections in west, east, and south Texas districts, surveyed their performance for the duration of this project 0-6674-01, and used the collected performance data to validate the updated binder selection catalog.

To accomplish this objective, TTI researchers selected three districts in east, south, and west Texas and constructed two new field sections in each of these locations—one section with PG64-22 control binder and the other section with soft PG64-28 asphalt binder. Researchers conducted tests for measuring stiffness, rutting resistance, and cracking resistance of mixes collected during the construction. Researchers monitored the performance of these test sections twice a year since construction. This chapter describes the test sections, the materials sampled from these sections, the properties measured using these mixtures, and the results of survey conducted on each of these field test sections for the duration of this project 0-6674-01.

### **FAIRGROUND ROAD TEST SECTIONS**

#### **General Description**

Two test sections were constructed on North Fairground Road in in the City of Midland, Texas, on October 2016 for this part of the project. Section 1 was northbound while Section 2 was southbound (see Figure 10). Table 13 presents the GPS coordinates for each test section as recorded from a mobile device. A different asphalt binder grade was used in each of these test sections while keeping the mix design the same as shown below:

- Section 1: 5.7% PG 64-22 + 14%RAP → *Control Mix*.
- Section 2: 5.7% PG 64-28 + 14%RAP.

As seen, Section 1 used the control mix prepared with PG64-22 asphalt binder (unmodified) by weight of total mix, while Section 2 used the mix prepared with PG64-28 asphalt binder (softer, modified). In both sections, 5.7 percent asphalt binder and 14.0 percent RAP content were used. The mix designs follow the TxDOT specification. The sections were constructed on October 26, 2016. The average paving temperature was measured as 300°F. The temperature measurement was taken directly from the material behind the paver. TTI researchers used several permanent reference objects to locate the test sections for performance monitoring.

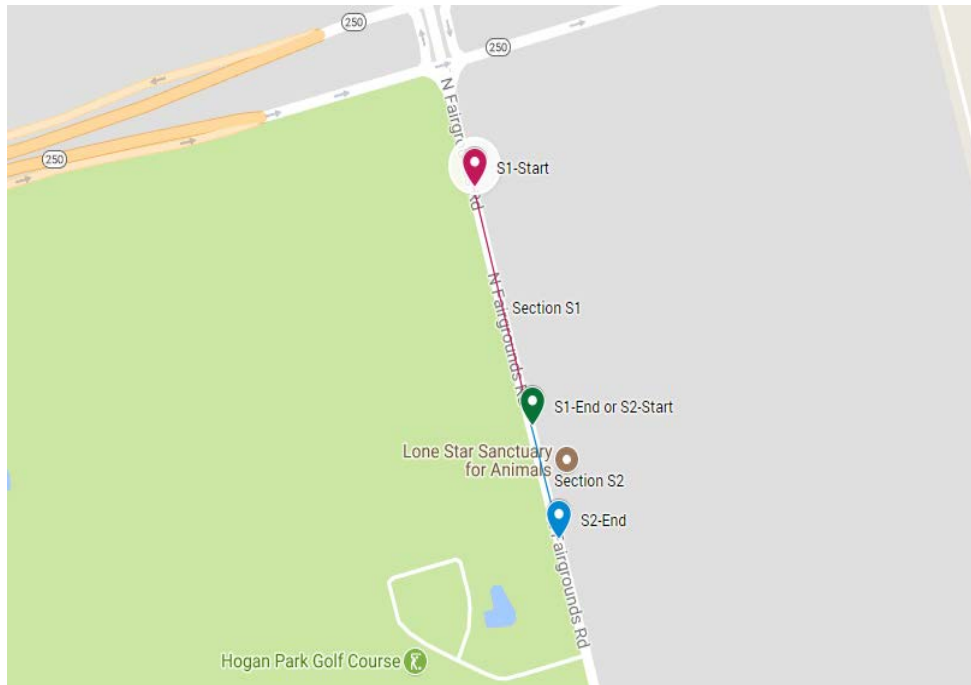


**Figure 10. North Fairground Road Test Sections: Location Map via Google.**

**Table 13. North Fairground Road Test Sections: GPS Coordinates.**

Section	Start		End		Length (ft)
	Latitude	Longitude	Latitude	Longitude	
1	32°02'50"	-102°03'47"	32°02'36"	-102°03'33"	1088
2	32°02'33"	-102°03'32"	32°02'35"	-102°03'32"	1224

### **Material Sampling, Laboratory Testing, and Results**

For each test section, TTI researchers sampled 10 buckets of mixes for asphalt binder and mixture tests, including dynamic modulus, repeated load, and OT tests. Test results are shown in Table 14, Table 15, and Table 16, respectively.



**Table 14. North Fairground Road Test Sections: Stiffness Properties.**

Temp. (°C)	Freq. (Hz)	Dynamic Modulus (ksi)	
		Section 1 5.7% PG 64-22 14%RAP	Section 2 5.7% PG 64-28 14%RAP
4	25	22491.0	17290.5
	10	21304.0	16079.0
	5	20385.5	15104.0
	1	18037.5	12717.0
	0.5	16965.5	11617.0
	0.1	14351.0	9191.5
20	25	13664.5	9601.5
	10	12098.0	8185.5
	5	10938.5	7162.5
	1	8239.5	4961.0
	0.5	7170.5	4163.5
	0.1	4798.5	2540.5
40	25	5148.5	2701.0
	10	3794.5	1828.5
	5	2912.5	1377.5
	1	1389.5	683.0
	0.5	983.0	532.1
	0.1	450.9	301.0
	0.01	191.7	172.1

**Table 15. North Fairground Road Test Sections: Rutting Properties.**

Rutting Properties	Section 1 5.7% PG 64-22 14%RAP	Section 2 5.7% PG 64-28 14%RAP
$\alpha$	0.7505	0.7978
$\mu$	0.4404	0.3592

**Table 16. North Fairground Road Test Sections: Cracking Properties.**

Cracking Properties	Section 1 5.7% PG 64-22 14%RAP	Section 2 5.7% PG 64-28 14%RAP
OT cycles	19	60
A	$1.59 \times 10^{-5}$	$1.77 \times 10^{-6}$
n	3.5899	4.1924

## Field Survey

Since the construction, the sections have been surveyed two times, that is, in July 3, 2017, and March 27, 2018. Figure 11 presents the conditions of sections as observed in these two surveys. Overall, both these sections have shown no sign of distresses till date except one pull-up in Section 1.

### *Rutting*

Both these sections have exhibited no sign of rutting as of March 27, 2018 (Figure 11).

### *Cracking*

Both these sections have exhibited no sign of any type of cracking as of March 27, 2018 (Figure 11).



Rutting/Cracking: None; Pull-Up: One  
07/03/2017



Rutting/Cracking: None, Pull-Up: One  
03/27/2018

### **North Fairground Road Section 1**



Rutting/Cracking/Pull-Up: None  
03/07/2017



Rutting/Cracking/Pull-Up: None  
03/27/2018

### **North Fairground Road Section 2**

**Figure 11. North Fairground Road Test Sections: Survey Pictures.**

## FM31 TEST SECTIONS

### General Description

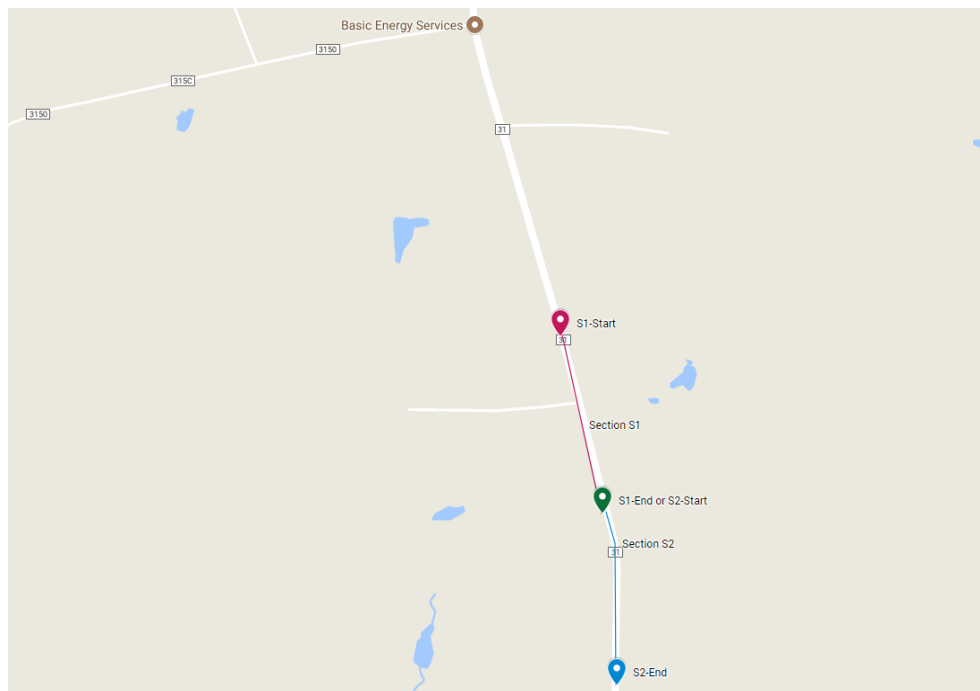
Two test sections were constructed on FM31 near the City of De Berry, Texas, for this project. Section 1 was northbound while Section 2 was southbound (see Figure 12). The starting point of Section 2 was only 52 ft at the end point of Section 1.

Table 17 presents the GPS coordinates for each test section as recorded from a cell phone. A different asphalt binder grade was used in each of these test sections while keeping the mix design the same as shown below:

- Section 1: 5.2 percent PG 64-22 + 17%RAP → *Control Mix*.
- Section 2: 5.2 percent PG 64-28 + 17%RAP.

As seen, Section 1 used the control mix prepared with PG64-22 asphalt binder (unmodified) by weight of total mix, while Section 2 used the mix prepared with PG64-28 asphalt binder (softer, modified). In both sections, 5.2 percent asphalt binder and 17.0 percent RAP content were used. The mix designs follow the TxDOT specification.

The sections were constructed on November 9, 2016. The average paving temperature was measured as 300°F. The temperature measurement was taken directly from the material behind the paver. TTI researchers used several reference objects to locate the test sections for future performance monitoring.



**Figure 12. FM31 Test Sections: Location Map via Google.**

**Table 17. FM31 Test Sections: GPS Coordinates.**

Section ID	Start		End		Length (ft)
	Latitude	Longitude	Latitude	Longitude	
1	32°16'55"	-94°09'47"	32°16'42"	-94°09'45"	1208
2	32°16'42"	-94°09'45"	32°16'23"	-94°10'02"	1389

**Material Sampling, Laboratory Testing, and Results**

For each test section, TTI researchers sampled seven buckets of mixes for laboratory testing, namely dynamic modulus tests, repeated load permanent deformation tests, and Texas OT. The test results are shown in Table 18, Table 19, and Table 20, respectively.

**Table 18. FM 31 Test Sections: Stiffness Properties.**

Temp. (°C)	Freq. (Hz)	Dynamic Modulus (ksi)	
		Section 1 5.2% PG 64-22 17%RAP	Section 1 5.2% PG 64-28 17%RAP
4	25	16660.0	10802.0
	10	14947.0	9265.0
	5	13668.0	8130.0
	1	10870.0	5790.5
	0.5	9646.0	4933.5
	0.1	7151.5	3254.5
20	25	8095.5	4235.5
	10	6605.0	3232.0
	5	5610.0	2616.5
	1	3691.0	1487.5
	0.5	3056.0	1173.0
	0.1	1835.0	640.9
40	25	1979.0	842.2
	10	1393.0	553.7
	5	1039.0	410.5
	1	497.1	207.3
	0.5	366.0	167.8
	0.1	189.1	103.7
	0.01	90.2	64.4

**Table 19. FM31 Test Sections: Rutting Properties.**

Rutting Properties	Section 1 5.2% PG 64-22 17%RAP	Section 1 5.2% PG 64-28 17%RAP
$\alpha$	0.7405	0.7998
$\mu$	0.4812	0.3788

**Table 20. FM31 Test Sections: Cracking Properties.**

<b>Cracking Properties</b>	<b>Section 1 5.2% PG 64-22 17%RAP</b>	<b>Section 1 5.2% PG 64-28 17%RAP</b>
OT cycles	19	60
A	$1.35 \times 10^{-6}$	$8.19 \times 10^{-9}$
n	4.2657	5.6667

### **Field Survey**

Since the construction, the sections have been surveyed twice, on May 5, 2017, and on January 9, 2018. Figure 13 presents the conditions of sections as observed in these two surveys. Overall, both sections have performed well.

#### *Rutting*

As of January 9, 2018, Section 1 has shown no sign of rutting while Section 2 has shown about 1/16 in. of rut depth (Figure 13).

#### *Cracking*

Both these sections have exhibited no sign of any type of cracking as of January 9, 2018 (Figure 13).



Cracking: None  
01/09/2018



Rutting: None  
01/09/2018

**FM31 Section 1**



Cracking: None  
01/09/2018



Rutting: 1/16 in.  
01/09/2018

**FM31 Section 2**

**Figure 13. FM31 Test Sections: Survey Pictures.**

**FM468 TEST SECTIONS**

**General Description**

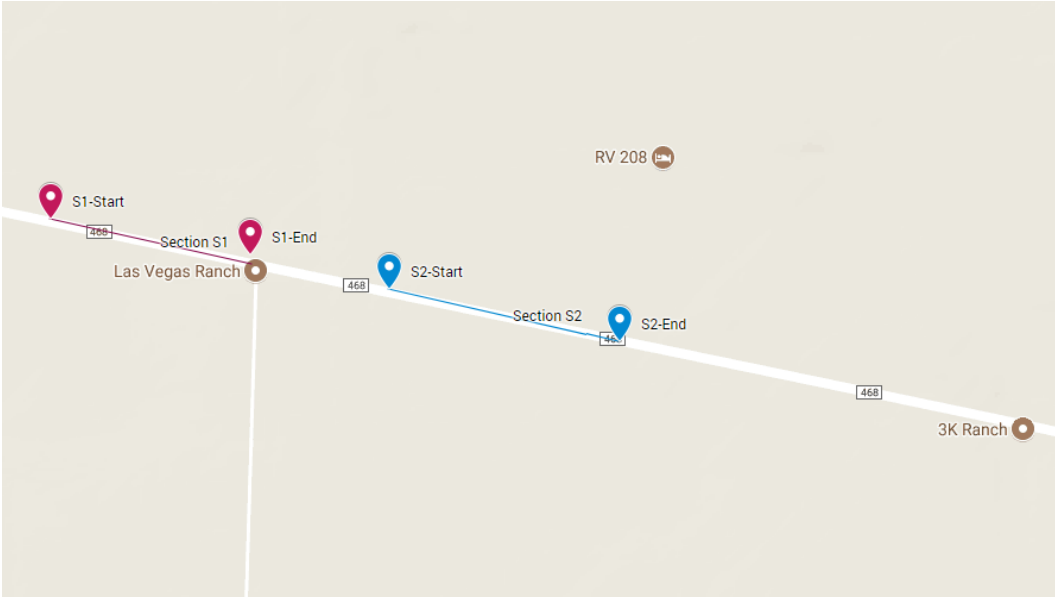
Two test sections were constructed on FM 468 near Cotulla, Texas, for this project. Section 1 was westbound while Section 2 was eastbound (see Figure 14).

Table 21 presents the GPS coordinates for each test section as recorded from a cell phone. A different asphalt binder grade was used in each of these test sections while keeping the mix design the same as shown below:

- Section 1: 5.8 percent PG 64-22 + 17%RAP → *Control Mix.*
- Section 2: 5.8 percent PG 64-28 + 17%RAP.

As seen, Section 1 used the control mix prepared with PG64-22 asphalt binder (unmodified) by weight of total mix, while Section 2 used the mix prepared with PG64-28 asphalt binder (softer, modified). Both mixes contain 5.8 percent asphalt binder and 17.0 percent RAP content by total weight of mix. The mix designs follow the TxDOT specification.

The sections were constructed on December 9, 2015. The average paving temperature was measured as 275°F. The temperature measurement was taken directly from the material behind the paver. TTI researchers used several reference objects to locate the test sections for distress survey.



**Figure 14. FM468 Test Sections: Location Map via Google.**

**Table 21. FM468 Test Sections: GPS Coordinates.**

Section ID	Start		End		Length (ft)
	Latitude	Longitude	Latitude	Longitude	
1	28°32'57"	-99°29'47"	28°32'55"	-99°29'34"	1190
2	28°32'53"	-99°29'25"	28°32'50"	-99°29'10"	1200

**Material Sampling, Laboratory Testing and Results**

From each test section, TTI researchers obtained 10 buckets of plant mixes during the construction for laboratory testing. The stiffness, rutting, and cracking properties obtained from the laboratory mixture tests are shown in Table 22, Table 23, and Table 24, respectively.

**Table 22. FM468 Test Sections: Stiffness Properties.**

Temp. (°C)	Freq. (Hz)	Dynamic Modulus (ksi)	
		Section 1 5.8% PG 64-22, 17%RAP	Section 2 5.8% PG 64-28, 17%RAP
	25	18837.0	16421.0
	10	17568.5	14792.5
	5	16526.5	13554.0
	1	13874.5	10657.0
	0.5	12770.0	9427.5
	0.1	10065.0	6811.5
	20	25	10111.0
10		8541.5	6187.5
5		7408.0	5226.5
1		4974.5	3231.0
0.5		4113.0	2584.5
0.1		2391.0	1362.5
40		25	2817.5
	10	1982.0	1174.5
	5	1478.5	848.1
	1	688.1	384.9
	0.5	502.1	284.6
	0.1	244.2	148.4
	0.01	110.7	78.9

**Table 23. FM468 Test Sections: Rutting Properties.**

Rutting Properties	Section 1 5.8% PG 64-22, 17%RAP	Section 2 5.8% PG 64-28, 17%RAP
$\alpha$	0.7405	0.7998
$\mu$	0.4812	0.3788

**Table 24. FM468 Test Sections: Cracking Properties.**

Cracking Properties	Section 1 5.8% PG 64-22, 17%RAP	Section 2 5.8% PG 64-28, 17%RAP
OT cycles	19	60
A	$1.77 \times 10^{-6}$	$1.15 \times 10^{-6}$
n	4.1924	4.3094



## **Field Survey**

Since the construction, the sections have been surveyed thrice, on April 8, 2016, October 9, 2017, and March 29, 2018. Figure 15 presents the conditions of these two sections observed in these surveys.

In the first survey, researchers did not observe any sign of rutting or cracking in either of these sections on that date. In the second survey, researchers found that Section 2 had been accidentally removed. Therefore, survey was conducted on Section 1 thereafter.

### *Rutting*

Both sections did not show any sign of rutting in the first survey that was conducted on April 8, 2016. When the sections were surveyed on October 9, 2017, both sections showed some rutting. Section 1 showed 1/16 to 8/16 in. of rut depth in outer wheel paths while 1/16 to 5/16 in. of rut depth in the inner wheel paths (see Figure 15). Similarly, Section 2 showed 1/16 to 2/16 in. in depth in outer wheel paths while 1/16 in. in the inner wheel paths. When these sections were surveyed on March 29, 2018, they showed that rut depths barely increased in both these sections, possibly due to lower temperatures that are prevalent from October to March.

Noteworthy here are two important facts: first, the rutting was more severe in outer wheel paths than in inner wheel paths, and second, rut depth rutting was more severe in the section with modified PG64-28 asphalt binder than the section with unmodified PG64-22 asphalt binder.

### *Cracking*

As of March 29, 2018, both these sections have exhibited no sign of cracking (see Figure 15).



No Cracking: 03/29/2017



Rutting in Outer Wheel Path: 1/16-8/16 in.  
10/09/2017



Rutting in Inner Wheel Path: 1/16-8/16 in.  
10/09/2017



Rutting in Outer Wheel Path: 1/16-8/16 in.  
03/29/2018



Rutting in Inner Wheel Path: 1/16-8/16 in.  
03/29/2018

**FM468 Section 1**



03/29/2017  
(Cracking: None)



Rutting in Outer Wheel Path: 1/16-2/16 in.  
10/09/2017



Rutting in Inner Wheel Path: 1/16 in.  
10/09/2017



Rutting in Outer Wheel Path: 2/16-3/16 in.  
03/29/2018



Rutting in Inner Wheel Path: 1/16 in.  
03/29/2018

**FM468 Section 2**

**Figure 15. FM468 Test Sections: Survey Pictures.**





## **CHAPTER 4: CHARACTERIZATION OF ENGINEERED ASPHALT BINDERS**

### **INTRODUCTION**

Most recently, various asphalt binder modification techniques have been used to engineer the asphalt binders to meet the asphalt binder specification. These techniques include the use of PPA, REOB, to name a few. PPA and REOB are mainly added to asphalt binders with the purpose of modifying the original asphalt binder to meet PG specification. Several state DOTs have placed bans on using some of the new asphalt binder modification techniques. Therefore, it is important to evaluate the performance of engineered asphalt binders.

This project evaluated the performance of the 10 most often used asphalt binders engineered with various modification techniques with the asphalt binder test recommended under project 0-6674 (Zhou et al. 2014). Under project 0-6674 (Zhou et al. 2014), TTI researchers recommended a series of asphalt binder tests to characterize rutting and cracking resistance of asphalt binder. The tests primarily include MSCR tests and LAS tests for characterization of rutting and fatigue cracking resistance of asphalt binders. Additionally, under project 0-6881 (Karki et al. 2018), researchers identified that rheological properties obtained from frequency sweep tests and  $\Delta T_c$  value obtained from low temperature PG grade tests can discriminate asphalt binder properties based on the applied modification technique. These new tests are very critical to ensure that asphalt binders used in Texas have adequate field performance because suppliers continue to modify the techniques for producing asphalt binders.

To accomplish the objective of this particular task, TTI researchers first assembled several virgin asphalt binders obtained from major suppliers in Texas, extracted RAP and RAS binders, and aromatic extracts, bio-rejuvenators, fatty acids, PPA, and REOB (see Table 25). Aromatic extracts are conventional rejuvenators with higher intensity of polar aromatic rings (Zaumanis et al. 2014). Bio-rejuvenators are bio-based rejuvenators (Zhou et al. 2018). Rejuvenators are used in asphalt mixtures to restore the aged asphalt characteristics to a consistency level appropriate for construction purposes and for the end use of the mixture, restore the aged asphalt to its optimal chemical characteristics for durability, and provide sufficient additional binder to coat new aggregate and to satisfy mix design requirements (Epps et al. 1980). Research has shown rejuvenators enhance cracking resistance of asphalt binders and asphalt mixtures (Mogawer et al. 2013; Karki and Zhou 2016). Fatty acids are a common component of bio-rejuvenators. The total fatty acid directly impacts the performance of bio-rejuvenators, thereby the performance of asphalt binders and asphalt mixtures (Zhou et al. 2018). REOBs are upstream additives that are used to produce softer binders from stiffer binders (Karki and Zhou 2017; Karki et al. 2018; Karki and Zhou 2018). REOBs are primarily used to produce softer while PPAs are used to produce stiffer binders (Karki et al. 2018).

**Table 25. List of Materials Used to Produce Engineered Asphalt Binders.**

Material	CAS	Source	PG	ID
Asphalt binder	8052-42-4	1	64-22	A6422
		2	64-22	B6422
		3	64-34	C6434
			64-28	C6428
			64-22	C6422
		4	64-22	D6422
		5	64-22	E6422
		6	58-28	G5828
			64-22	G6422
			70-22	G7022
			64-22	J6422
		Aromatic Extract (0–20%)	64742-65-0	1
Bio-Rejuvenators (0–20%)	-	1	-	BR1
		2	-	BR2
		3	-	BR3
		4	-	BR4
		5	-	BR5
		6	-	BR6
		7	-	BR7
		8	-	BR8
		9	-	BR9
		10	-	BR10
		11	-	BR11
		12	-	BR12
Fatty Acid (0–12%)	60-33-3 112-80-1 57-10-3 Fatty Acid Blends*	1	-	LA
		2	-	OA
		3	-	PA
		4	-	FA1
		5	-	FA2
		6	-	FA3
		7	-	FA4
		8	-	FA5
Polyphosphoric Acids (0–2%)	8017-16-2	1	-	P1
Reclaimed Binders (0–30%)	8052-42-4	RAP	-	RAP1
			95.8-xx	RAP2
			-	RAP3 <sup>†</sup>
		RAS	-	RAS1
			-	RAS2
		RAP1 + RAS1	132.1-xx	RAS3 <sup>‡</sup>
		RAP3 + RAS3	110.8-xx	RAP/RAS
	98.7-xx	RAS/RAP		
Re-Refined Engine Oil Bottoms (0–25%)	-	1	-	R1
		2	-	R2
		3	-	R3
		4	-	R4
		5	-	R5
		6	-	R6

\* Prepared by blending LA, OA, PA at different percentages

<sup>†</sup> Prepared by blending RAP1 and RAP2

<sup>‡</sup> Prepared by blending RAS1 and RAS2

Secondly, researchers prepared engineered asphalt binders by blending these materials with each other at different proportions. Researchers first heated the asphalt binders at their mixing temperature and then doped them with selected dosages of one or more engineering agents by total weight of the blends. Researchers then thoroughly stirred the blends for about 2 minutes and reheated for about 5 minutes repeatedly for 3 times. Researchers then oxidized the blends, including the original asphalt binders, RTFO at 320°F (163°C) for 85 minutes for short-term aging (AASHTO T240 2013). Researchers again oxidized the RTFO-aged binders in a pressure aging vessel (PAV) at 100°C and 2.2 kPa for 20, 40, or 80 hours to simulate to long-term aging (AASHTO R28 2012).

Finally, researchers used four test methods to characterize these binders. They are the frequency sweep tests for characterizing rheological properties, bending beam tests for characterizing durability, MSCR tests for characterizing rutting resistance, and the original and modified versions of LAS test for characterizing fatigue cracking resistance of asphalt binders as detailed in the ensuing sections.

### **RHEOLOGICAL PROPERTIES: FREQUENCY SWEEP TESTS**

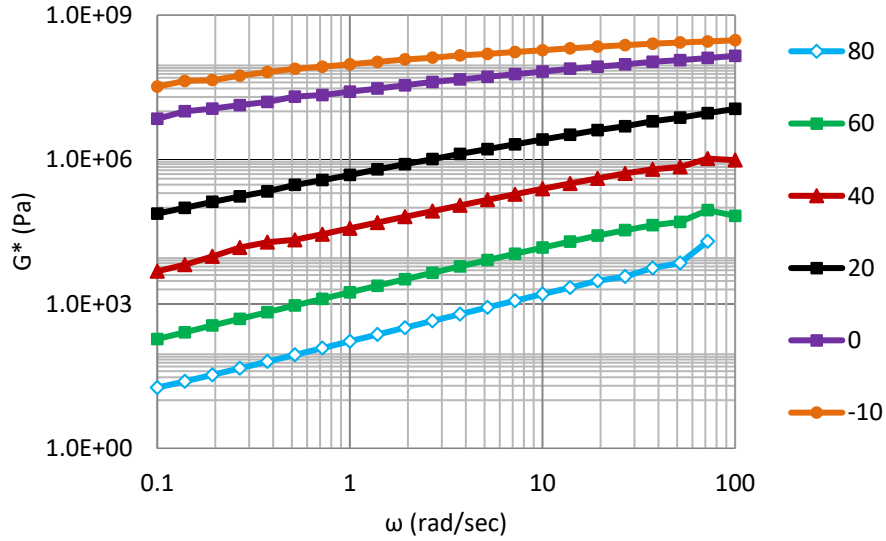
TTI researchers evaluated rheological properties of engineered asphalt binders in terms of the parameters extracted from their master curves. Researchers conducted frequency sweep tests of original and engineered asphalt binders from 0.1 rad/sec to 100 rad/sec at different loading and temperature conditions (80°C to -10°C) using a DSR (AASHTO T315 2012). For temperature of 20°C and less, researchers used sample diameter of 8 mm, sample thickness of 2 mm, and shear strain amplitude of 1 percent. Similarly, for temperatures above 20°C, researchers used a sample diameter of 25 mm, sample thickness of 1 mm, and shear strain amplitude of 0.1 percent. The measured shear modulus ( $G^*$ ) and input angular frequency( $\omega$ ) data from frequency sweep tests at each temperature (see Figure 16(a)) were then superimposed on each other to construct master curves at the reference temperature,  $T_r$  of 45°C, using the principle of time-temperature superposition of viscoelastic materials and the shift factors based on the Williams-Landel-Ferry (WLF) model (Ferry 1980; Williams et al. 1955). The curves were then fitted with the Christensen-Anderson model (Christensen and Anderson 1992):

$$G^*(\omega_r) = G_g \left[ 1 + \left( \frac{\omega_c}{\omega_r} \right)^{\frac{\log 2}{R}} \right]^{-\frac{R}{\log 2}} \quad (1)$$

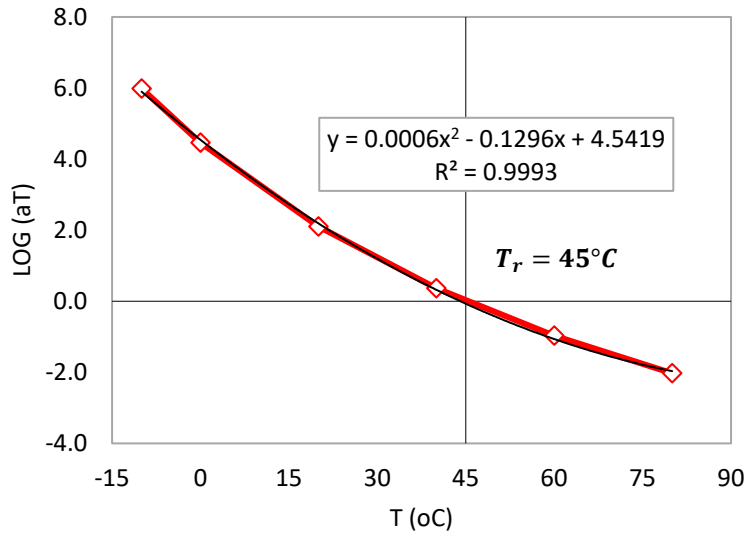
$$\log[a_T] = -C_1 \left[ \frac{T - T_r}{C_2 + T - T_r} \right] \quad (2)$$

The parameters  $\omega_r$ ,  $\omega_c$ ,  $R$ , and  $G_g$  in Equations 1 and 2 refer to reduced frequency, crossover frequency, rheological index, and glassy shear modulus (typically  $1.0 \times 10^9$  Pa), respectively. The parameter,  $a_T$ , refers to the WLF shift factor at temperature  $T$ , and the parameters  $C_1$  and  $C_2$

refer to WLF fitting constants. Figure 16(b) shows that shift factor is a function of temperature, 1 being its value for reference temperature in logarithmic scale. Figure 16(c) presents the master curve constructed by shifting the curves in Figure 16(a) using the relationship from Figure 16(b). From these curves, crossover frequency,  $\omega_c$ , and rheological index, R, were extracted and used to evaluate rheological properties of original and engineered asphalt binders.

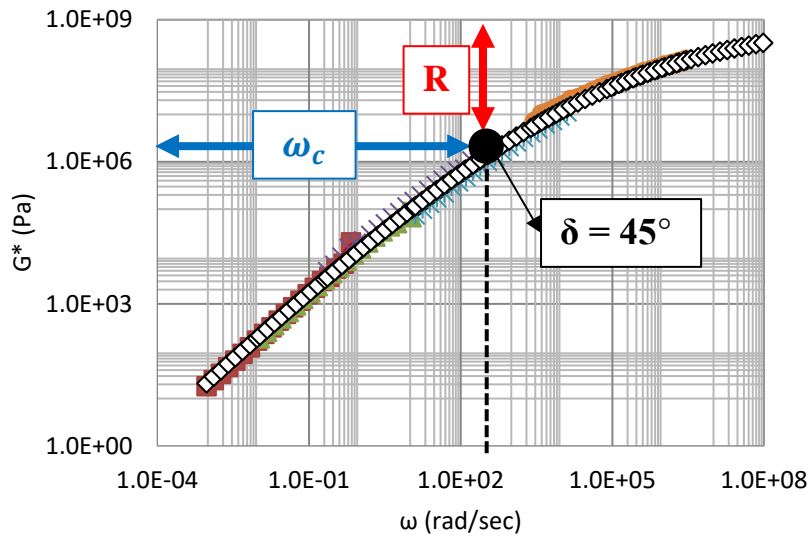


(a) Frequency Sweep Test Results



(b) Shift Factor Used to Construct the Master Curve





(c) Illustration of Rheological Parameters on a Master Curve

**Figure 16. Frequency Sweep Tests and Analyses: An Illustration.**

### Effect of Binder Sources and PGs

Figure 17 presents the black space diagram of crossover frequencies and rheological indices for original asphalt binders obtained from different sources (B, C, G, and J) with different PGs (PG58-28, PG64-22, and PG70-22). The figure shows that each of these binders shows different values for  $\omega_c$  (different stiffness) and  $R$  (different elastic-to-steady-state transition potential) as expected.

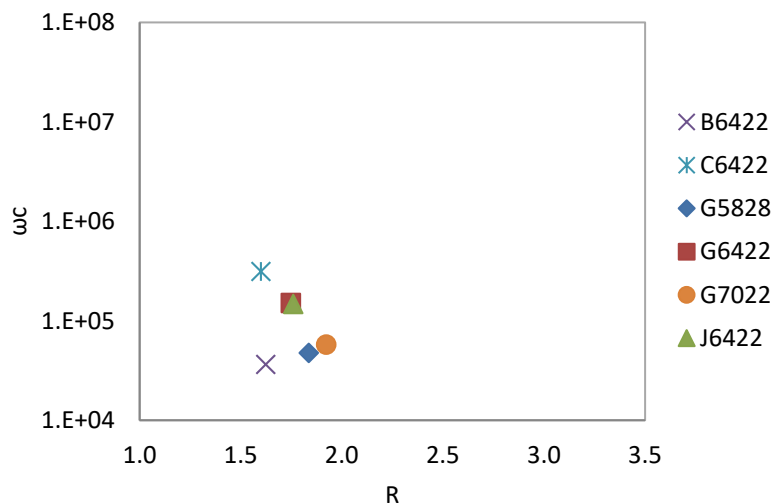


**Figure 17. Frequency Sweep Test Results: Original Binders.**

## Effect of Reclaimed Binders

Figure 18 presents the black space diagram of crossover frequencies and rheological indices for binders prepared with 0 percent (original) and 30 percent RAP or RAP/RAS-extracted binders by total weight of blends. The figure shows that binds prepared with aged (reclaimed) binders have lower values of  $\omega_c$  but higher  $R$ . This behavior is expected irrespective of separate or combined use of RAP and RAS extracted binders. These results suggest that the use of reclaimed binders make asphalt binders stiffer (more elastic or brittle) and less capable of relaxing microcracks, which can be directly attributed to the severely aged condition of the reclaimed binders.

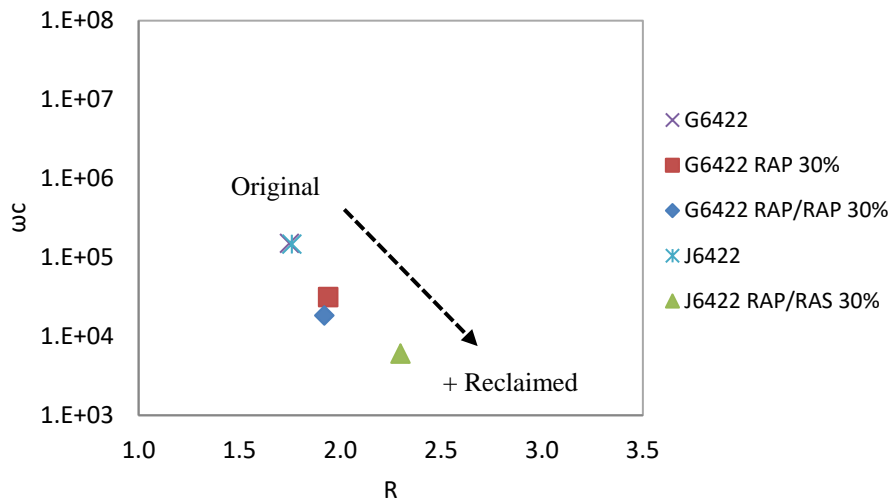
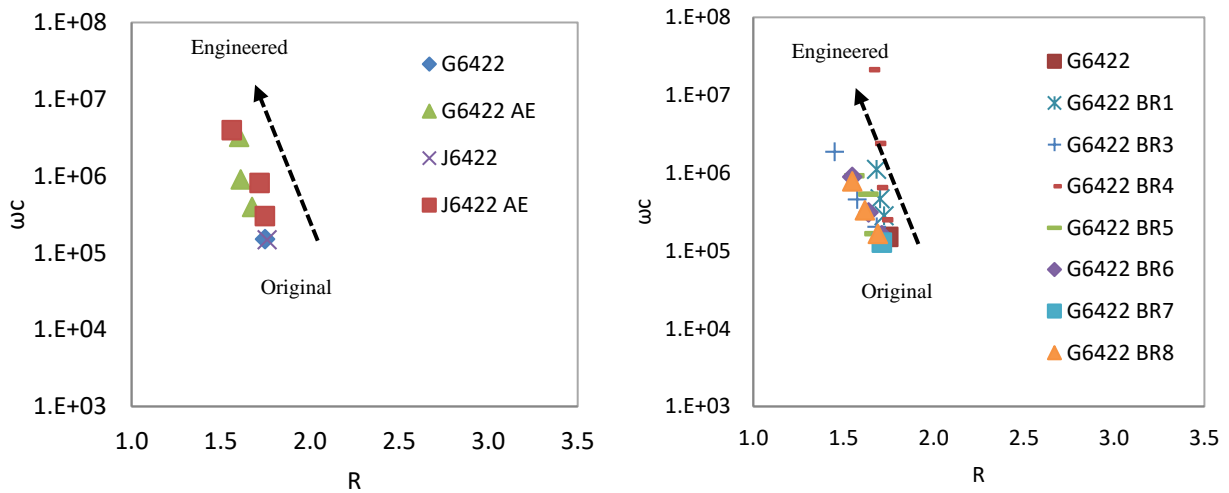


**Figure 18. Frequency Sweep Test Results: Effect of Reclaimed Binders.**

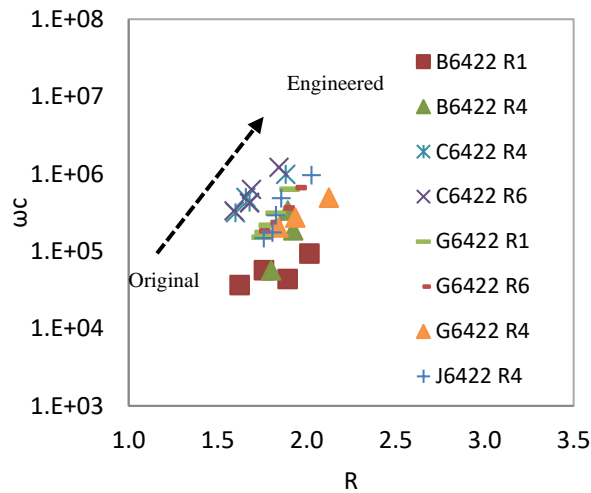
## Effect of Engineering Agents

Figure 19 presents the black space diagram of crossover frequencies and rheological indices for asphalt binders engineered with different engineering agents at different dosages. The figure shows that the  $\omega_c$  value increases with an increase aromatic extract, bio-rejuvenator, and re-refined engine bottom dosages, suggesting these engineering agents make original asphalt binders softer. Conversely, the figure shows that  $R$  value decreases with increased dosage of aromatic extract and bio-rejuvenator but increases with increased dosage of re-refined engine bottoms. These behaviors were observed consistently irrespective of any change in the source of binder (B, C, G, J), the source of engineering agents (AE, bio-rejuvenator from BR1 to BR6 versus REOBs from R1, R4, R6), and their applied dosages (0 percent to 20 percent), suggesting the opposite effect on elastic-to-steady state transition properties of asphalt binders. These results emphasize that not all softeners have similar effects on each rheological property of asphalt binders. Therefore, one must be cautious of unintended consequences of engineering a binder when only one parametric effect is considered.



(a) Aromatic Extract

(b) Bio-Rejuvenators

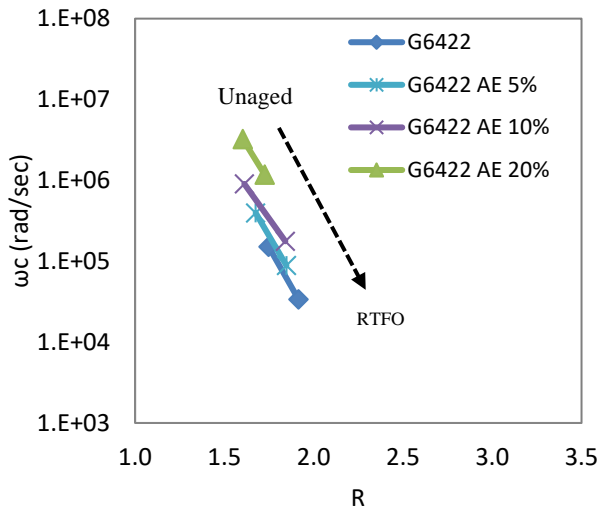


(c) REOB

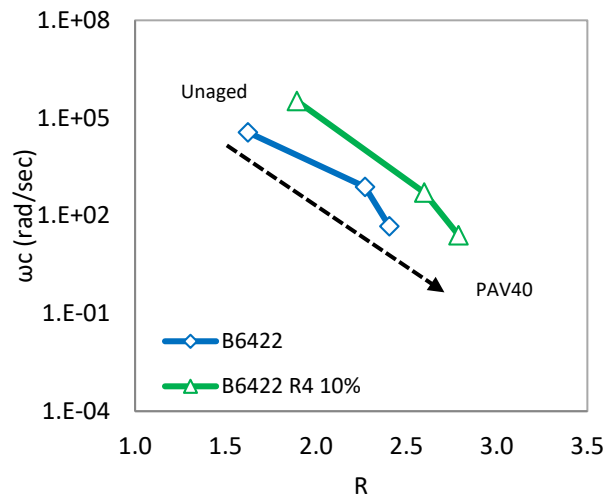
**Figure 19. Frequency Sweep Test Results: Effect of Engineering Agents.**

### Effect of Aging

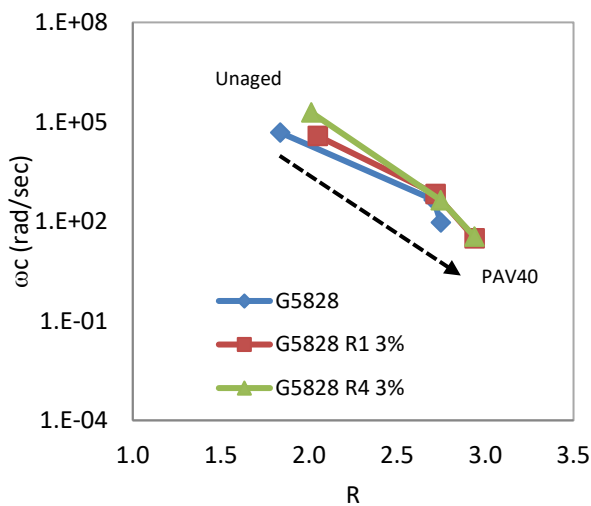
Figure 20 presents the black space diagram of crossover frequencies and rheological indices of original and engineered asphalt binders as a function of aging. The figure shows that the  $\omega_c$  value decreases while the  $R$  value increases with increased levels of aging. These behaviors were consistently observed irrespective of change in binder source (B, C, G, J), grade (PG58-28, PG64-22), modifier source (AE, R1, R4, P1), rejuvenator dosage (0 percent, 3 percent, and 10 percent), or REOB dosage (0 percent to 20 percent). These results strongly suggest that aging makes asphalt binders more brittle and reduces their ability to relax accumulated microstrains.



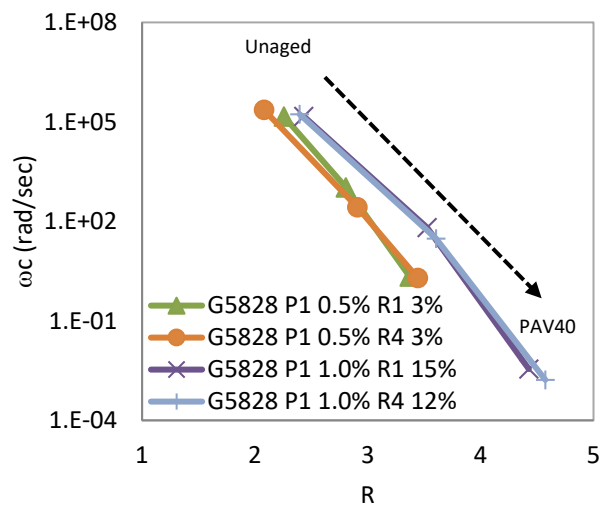
(a) Aromatic Extract



(a) PG64-22 + REOB



(a) PG58-28 + REOB



(a) PG58-28 + REOB + PPA

**Figure 20. Frequency Sweep Test Results: Effect of Chemical Aging.**

### RUTTING RESISTANCE: MSCR TESTS

TTI researchers evaluated rutting resistance of engineered asphalt binders in terms of non-recoverable creep compliance ( $J_{nr}$ ) and percent recovery (%*Rec.*) measured from the MSCR tests (AASHTO T350 2014). For these tests, asphalt binder samples were subjected to 10 cycles of creep and recovery steps at 0.1 kPa and 10 cycles of creep and recovery steps at 3.2 kPa in succession. Note that creep and recovery parts of each of these steps were 1.0 and 9.0 seconds long. The average value of unrecoverable compliance ( $J_{nr}$ ) and percent recovery (%*Rec.*) measured from the 10 creep and recovery steps involving the stress of 3.2 kPa were used to

discriminate rutting potential of asphalt binders (Zhou et al. 2014; Zhang et al. 2015). For consistent comparison, test temperature of 64°C was used for each of these original and engineered asphalt binders in this study

For this part of the study, materials from two field projects were used. From one of these projects, original PG64-22 asphalt binder from source G (G6422), RAP-extracted asphalt binder, and three bio-rejuvenators (BR3, BR5, and BR6) were obtained. The original asphalt binder was engineered by adding 0 (control sample), 2, 5, and 10 percent bio-rejuvenator and 30 percent RAP-extracted binder by total weight of blends. From the other project, PG64-22 asphalt binder from source J (J6422), RAP- and RAS-extracted asphalt binder, and three bio-rejuvenators (BR3, BR5, and BR7) were obtained. The original asphalt binder was engineered by adding 0 percent (control sample), 2, 5, and 10 percent bio-rejuvenator, 18 percent RAP-extracted, and 11 percent RAS-extracted asphalt binders by total weight of blends. A total of 20 blends were thereby prepared and tested for this part: 2 projects  $\times$  (1 control + 3 bio-rejuvenators  $\times$  3 dosages) = 20 samples.

### **Effect of Binder Sources and PGs**

Figure 21 presents %*Rec.* vs.  $J_{nr}$  plot for different sources and PGs of original binders. The figure shows that PG70-22 binder has higher %*Rec.* value and lower  $J_{nr}$  value than corresponding values of each of the two PG64-22 binders, suggesting even one degree increase in PG can significantly increase the capacity of binders to recover from permanent strain, thereby making binders less susceptible to rutting. The figure also suggests that the two PG64-22 binders have different %*Rec.* and  $J_{nr}$  values, suggesting the fact that the same PG binders obtained from different sources might have different capacity of binders to recover from permanent strain. These results highlight the importance of asphalt binder source and PG in rutting.

### **Effect of Reclaimed Binders**

Figure 22 shows that asphalt binders engineered with reclaimed binders have higher %*Rec.* and lower  $J_{nr}$  values than corresponding values of unmodified original binders, suggesting that binders blended with reclaimed binders (stiffer binders) accumulate less permanent strain and therefore provide more resistance to rutting than unmodified binders. The figure also shows that when the sources and ratios of reclaimed binders are different, their %*Rec.* and lower  $J_{nr}$  values are also different, suggesting that the source and the ratio of RAP and RAS affect rutting resistance too.

### **Effect of Engineering Agents**

Figure 23(a) presents  $J_{nr}$  and %*Rec.* values of asphalt binders engineered with different sources and dosages of engineering agents in the absence of reclaimed binders. Figure 23(b) shows that %*Rec.* value decreases while the  $J_{nr}$  value increases with the increased use of these agents.

These results clearly indicate that aromatic extract, bio-rejuvenators, and REOB negatively reduce the capacity of asphalt binders to recover from permanent strains, thereby making them more compliant to rutting. Additionally, Figure 23(a) also shows that the degree of influence of these bio-rejuvenators on rutting resistance also depend their individual sources.

The fact that strain recovery ( $\%Rec.$ ) decreases while permanent strain ( $J_{nr}$ ) increases with the use of reclaimed binders (as shown in Figure 22) but these trends reverse with the use of aromatic extract, bio-rejuvenators, and REOB (as shown in Figure 23[a]) suggest that asphalt binders engineered with one of these agents and asphalt binders engineered with aged binders possess drastically different rutting resistance as illustrated in Figure 23(b). Figure 23(b) strongly suggests that one must study the combined effect of aged binders and engineering agents when deciding the dosage of each of these components when engineering asphalt binders.

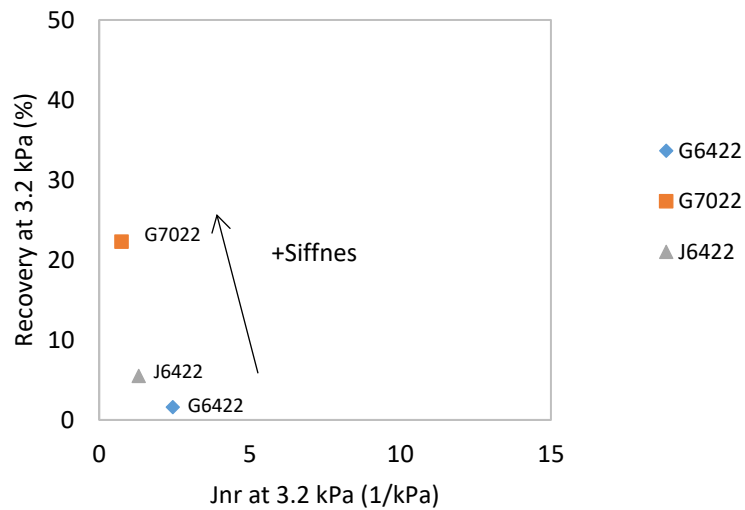


**Figure 21. MSCR Test Results: Original Binders.**

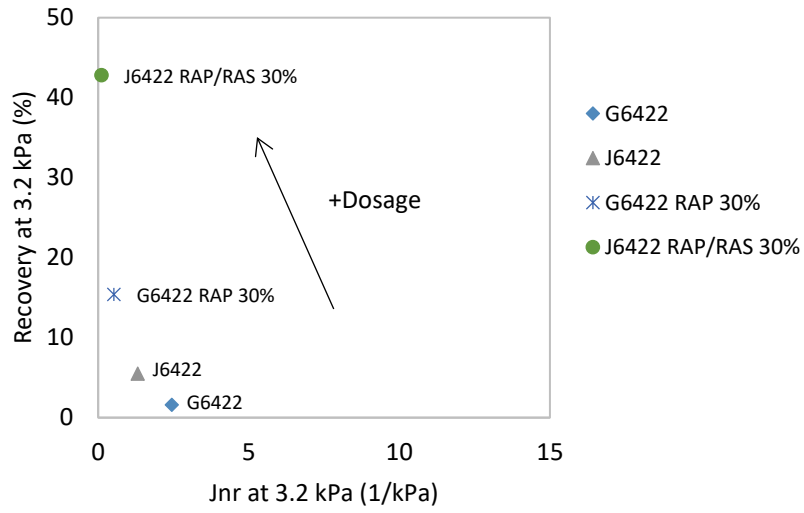
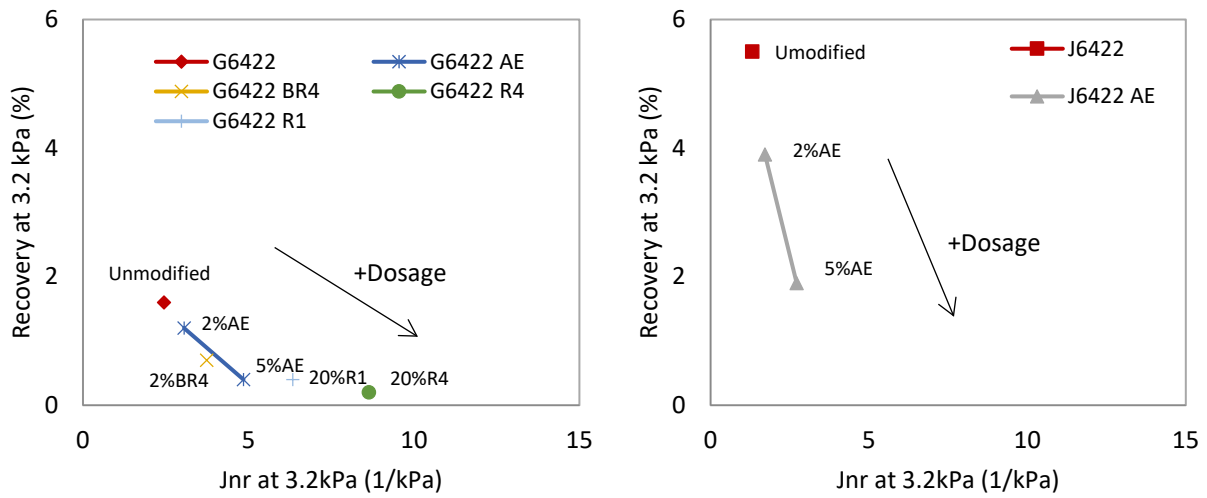
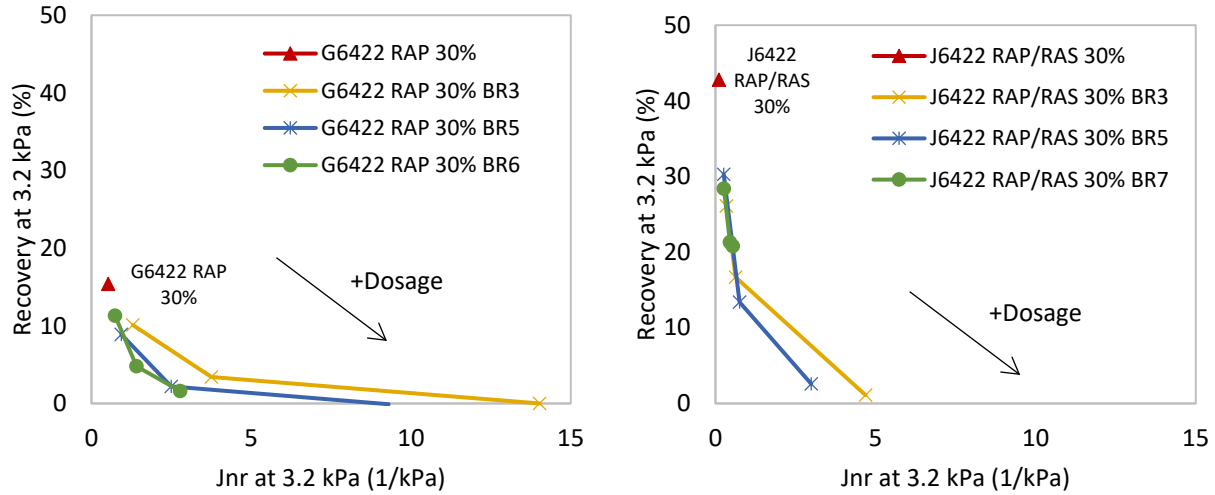


**Figure 22. MSCR Test Results: Effect of Reclaimed Binders.**



(a) Engineered Binders *without* Reclaimed Binders



(b) Engineered Binders *with* Reclaimed Binders

**Figure 23. MSCR Test Results: Effect of Engineering Agents.**

### DURABILITY: $\Delta T_c$ TESTS

Researchers evaluated durability of the original and the engineered asphalt binders in terms of the  $\Delta T_c$  values measured from low temperature PG (PGL) tests. To determine  $\Delta T_c$  values, 6.25 mm thick, 12.5 mm wide, and 127 mm long beams of PAV-aged asphalt binder samples were first conditioned at different test temperatures in a liquid bath for an hour and then subjected to constant load of 100 grams (980 mN) using a bending beam rheometer while the beams are supported at two ends that are 102 mm apart (AASHTO T315 2012). The temperatures for these tests are based on temperature recommended for determining the low temperature grade of binders, or PGL (AASHTO M320 2010):

$$T_{cs} = T_c (S = 300 \text{ kPa}) \quad (3)$$

$$T_{cm} = T_c (m = 0.300) \quad (4)$$

$$\Delta T_c = T_{cs} - T_{cm} \quad (5)$$

### Effect of Binder Source and PG

Researchers first tested PG58-28 asphalt binders obtained from two different sources and PG64-22 asphalt binders obtained from seven different sources for  $\Delta T_c$  values. Note that the four PG64-22 binders from sources G and the two PG64-22 binders from source J represent different dates of production or sampling.

Figure 24 presents  $\Delta T_c$  values of RTFO+PAV20 aged original binders. The figure demonstrates that  $\Delta T_c$  values of original asphalt binder are quite different for different sources and PGs. The figure also shows that  $\Delta T_c$  value binders from the same source are quite different for different



dates of production or sampling. The figure also shows that two of these binders had  $\Delta T_c > -5^\circ\text{C}$  even without aging and modification, which means that these binders are already poor in quality and are less durable if these binders are used without appropriate engineering. These results highlight the importance of determining the durability of base asphalt binders before engineering them with different agents.

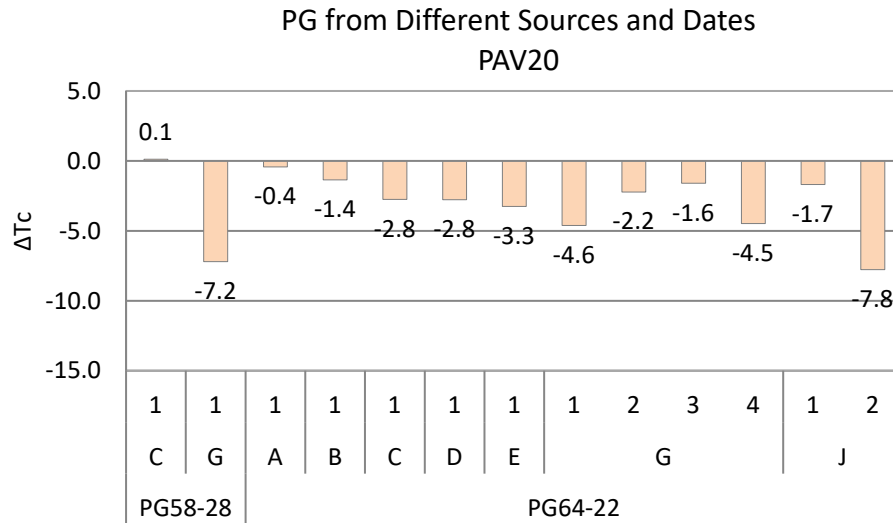


**Figure 24.  $\Delta T_c$  Results: Original Binders.**

### Effect of Reclaimed Binders

To study the effect of reclaimed or aged binders on asphalt binder durability, TTI researchers tested binders engineered by blending original unmodified PG58-28 and PG64-22 asphalt binders obtained from source G with different dosages of RAP- and RAS-extracted binders obtained from different sources in Texas.

Figure 25 presents  $\Delta T_c$  values of the 20 hr. PAV-aged binders with and without reclaimed binders. The figure shows that  $\Delta T_c$  value of each asphalt binder became more negative with an increase in the use of reclaimed binders. This result suggests that the use of severely aged asphalt binders (or aging of binder itself) degrades asphalt binder quality and makes them less durable. Figure 25 also shows the  $\Delta T_c$  of PG64-22 binder changed less with the use of RAP/RAS-extracted binder (PG 106-xx) than with the use of 30 percent RAP (PG 94-xx). Similarly, the figure also shows the  $\Delta T_c$  of PG58-22 binder changed only a little bit with the use of 8 to 11 percent RAP-extracted binder (PG 100-xx). Different amount of changes in  $\Delta T_c$  with extracted binders can be attributed to the different grades, sources, and dosages of recycled binders and different grades of original binders. More importantly, these results suggest that negative effect on durability of asphalt binders can be controlled by appropriately selecting the amount of recycled materials and asphalt binder grades.

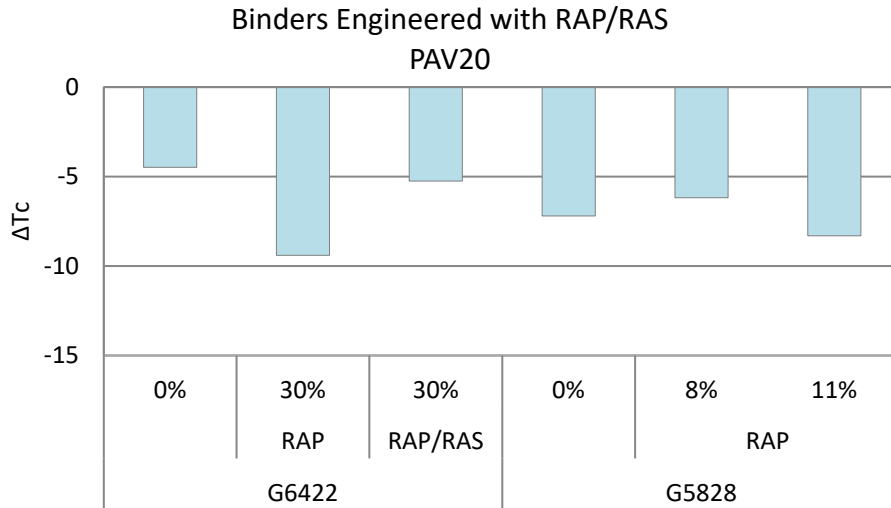


**Figure 25.  $\Delta T_c$  Results: Effect of Reclaimed Binders.**

### Effect of Engineering Agents

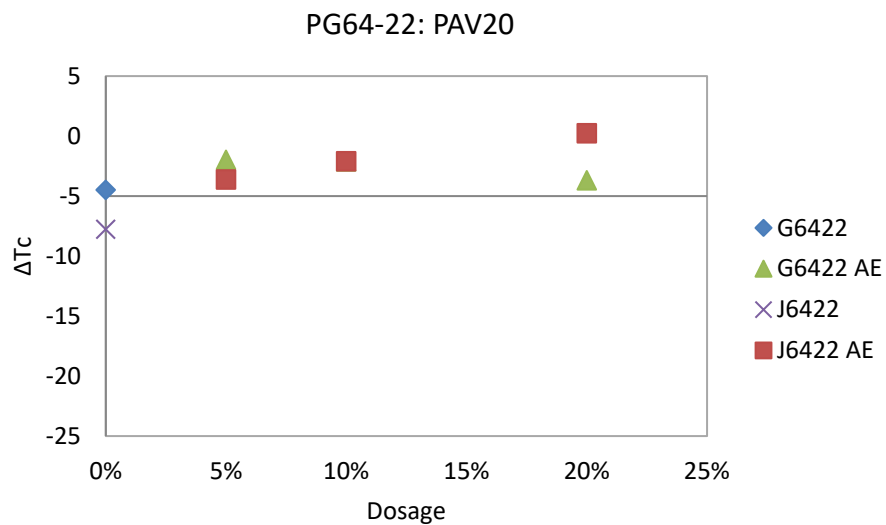
To study effect of engineering agents on asphalt binder durability, TTI researchers tested binders engineered by blending original PG58-28 and PG64-22 asphalt binders obtained from source G with different dosages of engineering agents obtained from various sources.

Figure 26(a) to Figure 26(d) present the  $\Delta T_c$  values of binders engineered by blending PG64-22 asphalt binder with aromatic extract, bio-rejuvenators, fatty acids, and REOBs. Figure 26(e) presents the  $\Delta T_c$  values of binders engineered by blending PG58-28 asphalt binder with PPA.

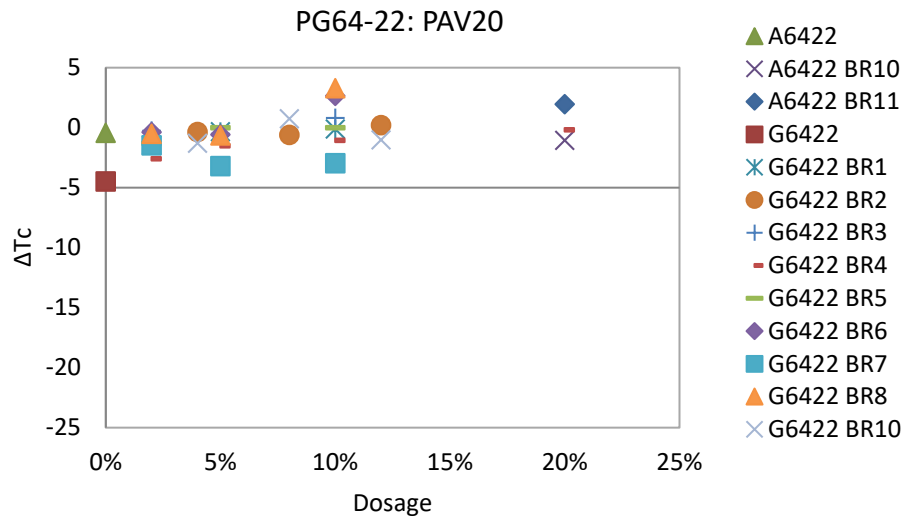
Figure 26(a) to Figure 26(c) show that  $\Delta T_c$  values became less negative (more durable) with the use of aromatic extract, bio-rejuvenators, and fatty acids than the  $\Delta T_c$  value of original binder. With an increase in their dosages, their  $\Delta T_c$  became even less negative than the  $\Delta T_c$  value of original binder. The fact that aromatic extract, bio-rejuvenators, and fatty acids made the  $\Delta T_c$  value less negative suggests that binders engineered with one or more of these engineering agents can enhance the quality of asphalt binders and make them more durable. The fact that increased use of fatty acids too increased the  $\Delta T_c$  value (made less negative) suggests that rejuvenators that contain a higher amount of fatty acids better enhance asphalt binder durability.

Conversely, Figure 26(d) and Figure 26(e) show that  $\Delta T_c$  values became more negative (less durable) with the use of REOB and PPA than the  $\Delta T_c$  value of original binder. With an increase in their dosages, their  $\Delta T_c$  became even more negative than the  $\Delta T_c$  value of original binder. The fact that the increased use of REOB and PPA makes the  $\Delta T_c$  value more negative suggests that asphalt binders engineered with one or both these engineering agents can degrade binder quality and make asphalt binders less durable.

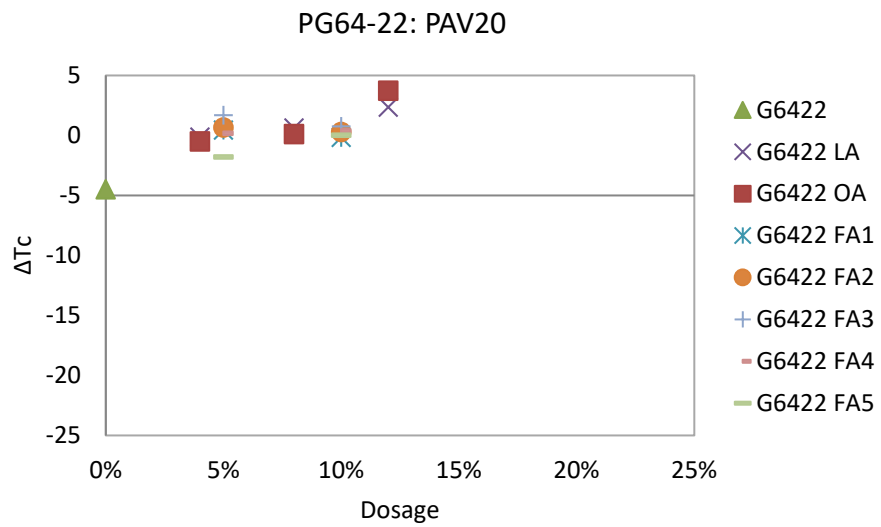
To synopsise,  $\Delta T_c$  results provide compelling evidence that aromatic extract, bio-rejuvenators, fatty acids have positive effects while REOB and PPA have negative effects on  $\Delta T_c$  or asphalt binder durability. The results also show that despite having the opposite (softening versus stiffening) effect on asphalt binder stiffness, REOB and PPA have similar (i.e., negative) effects on asphalt binder durability. The results also show that despite having similar (i.e., softening) effects on asphalt binder stiffness, REOBs and rejuvenating agents (aromatic extracts, bio-rejuvenators, and fatty acids) have opposite (i.e., negative versus positive) effects on asphalt binder durability. The results also suggest that the degree of these effects depends on the source of the engineering agent and the source and PG of the base asphalt binder. These observations strongly suggest that agents used for a completely different type of effect on binder stiffness can have a very similar type of effect on binder durability and vice versa. Therefore, one must study the type and the degree of effect an engineering agent has on both the durability and the stiffness of a given asphalt binder. Engineering an asphalt binder without considering effects on each of these parameters might lead to untoward consequences.



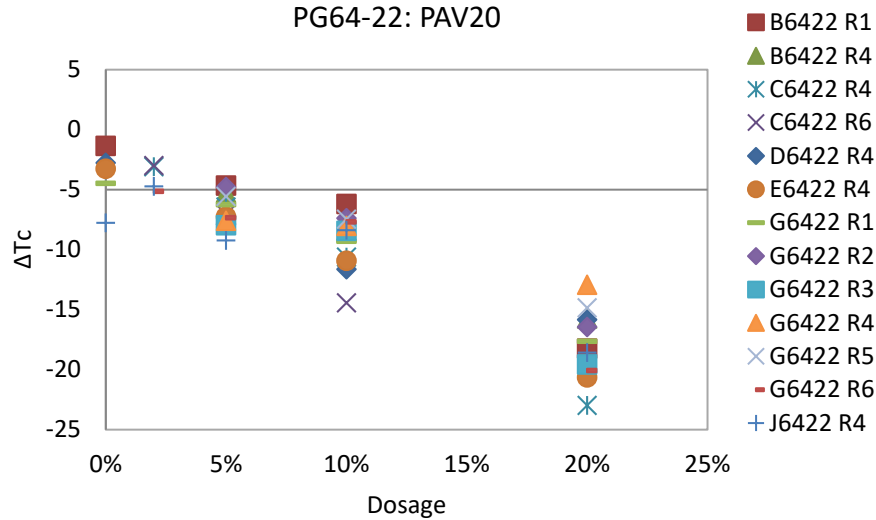
(a) Aromatic Extract



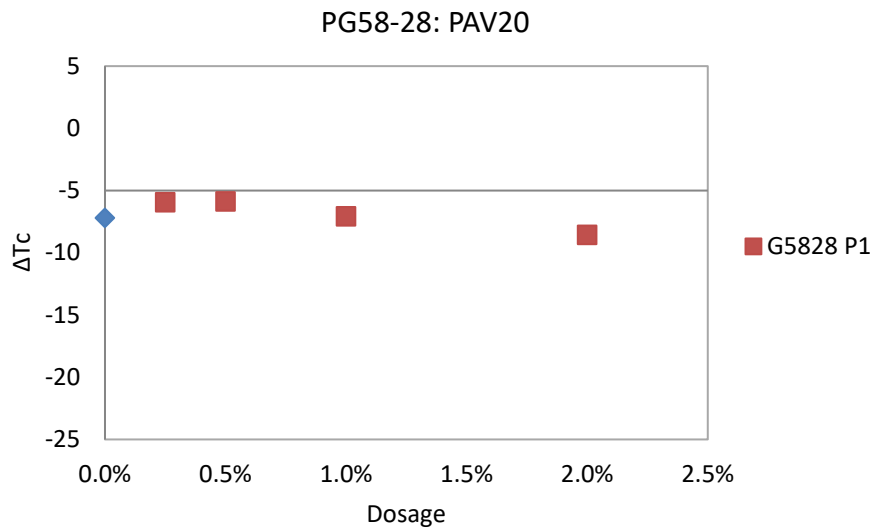
(b) Bio-Rejuvenators



(c) Fatty Acids



(d) REOBs



(e) Polyphosphoric Acid

**Figure 26.  $\Delta T_c$  Results: Effect of Engineering Agents.**

### Effect of Aging

To study the effect of aging on asphalt binder durability, TTI researchers used binders engineered by blending original PG64-22 asphalt binder obtained from source G with 30 percent severely aged binders reclaimed from RAP or RAS and 5 and 10 percent different engineering agents obtained from different sources (2 × bio-rejuvenators, 1 × aromatic extract, and 1 × REOB) by total weight of the blends. Researchers aged each of these engineered binders first in RTFO and later in PAV for 20 or 40 hours (PAV20 or PAV40) and determined their  $\Delta T_c$  values by conducting the bending beam rheometer tests.

Figure 27 presents the  $\Delta T_c$  values of 20 hr and 40 hr PAV-aged original and engineered asphalt binders. The figure shows that  $\Delta T_c$  values of original and engineered asphalt binders became more negative with increased level of aging, suggesting a negative impact of aging on asphalt binder durability. The figure also shows  $\Delta T_c$  values of aged and unaged engineered binders becomes less negative with an increase in bio-rejuvenator dosage but increases with an increase in reclaimed binder and REOB dosages, reconfirming a positive effect of bio-rejuvenates but a negative effect of recycled binders and REOBs on asphalt binder durability. These results strongly suggest that bio-rejuvenators are better engineering agents in terms of asphalt binder durability. These results also suggest aging degrades the durability of asphalt binders engineered with REOBs than binders engineered with bio-rejuvenators.

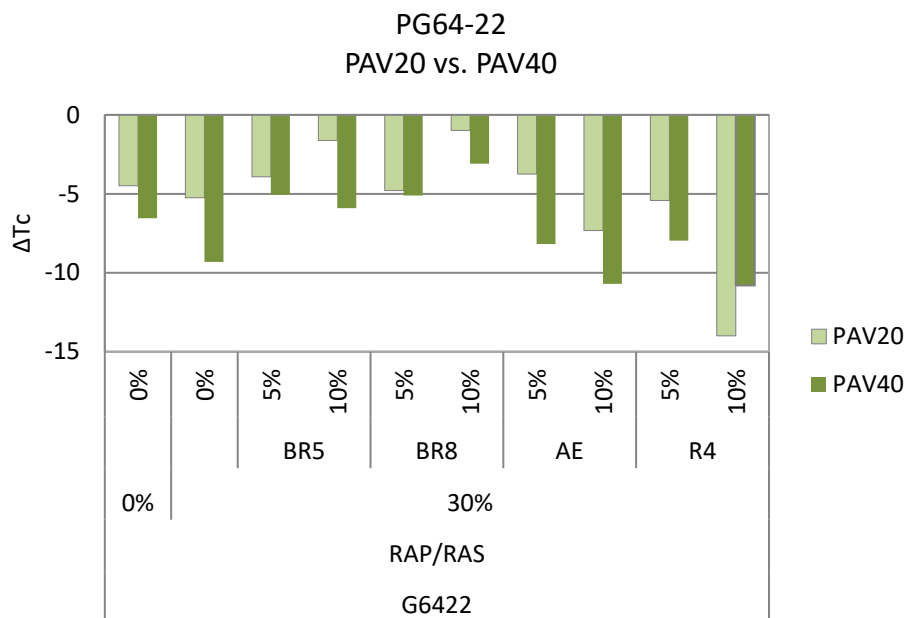


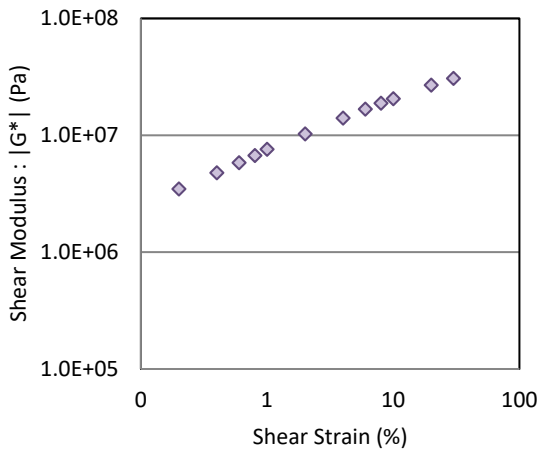
**Figure 27.  $\Delta T_c$  Results: Effect of Chemical Aging.**

## FATIGUE CRACKING RESISTANCE: LAS TESTS AND LIMITATIONS

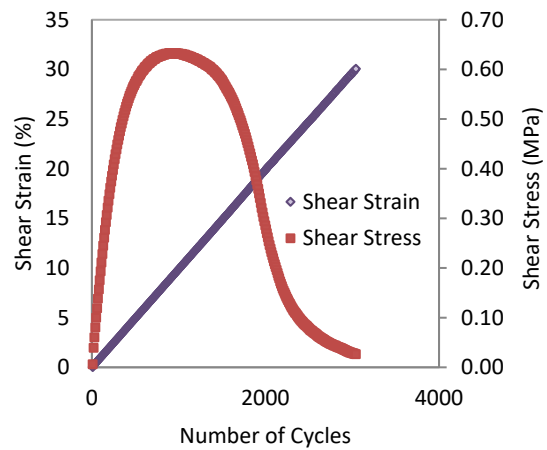
TTI researchers used the AASHTO TP 101 *Standard Method of Test for Estimating Fatigue Resistance of Asphalt binders Using the Linear Amplitude Sweep* to evaluate fatigue cracking resistance of engineered binders at intermediate temperature (2014). LAS tests are conducted using a DSR instrument. From these tests, characteristic stiffness versus damage evolution curves are obtained, which are then used to estimate the number of cycles required to fail asphalt binders at constant shear strains. There are two steps in this test.

In the first step, asphalt binder samples are first subjected to linear viscoelastic frequency sweep tests at constant shear strain, temperature, and frequency (see Figure 28[a]). The shear stress and shear strain history data recorded during the frequency sweep test (see Figure 28[a]) are then analyzed to obtain the linear viscoelastic properties of the asphalt binder –  $|G^*|_{LVE}$  and  $m$ . In the

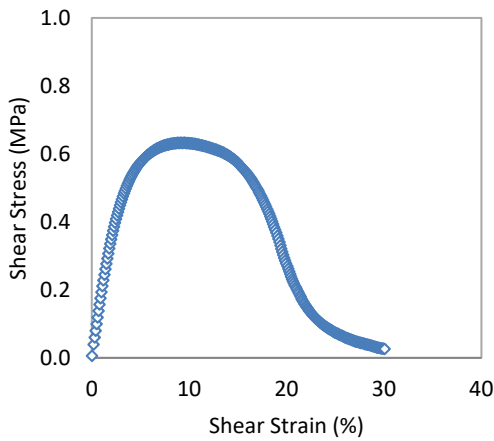
second step, the same samples are subjected to cyclic shear tests at the same temperature used in frequency sweep test (see Figure 28[b]). During this second step, shear strain is incrementally increased from 0 to 30 percent in every 100 cycles over the course of 3,100 cycles of loading. The shear stress versus shear strain history data recorded during the cyclic sweep test (see Figure 28[b] and Figure 28[c]) and the linear viscoelastic properties obtained from the first step are then used together to determine the characteristic damage behavior (i.e., C vs. D curves) of asphalt binder samples based on the viscoelastic continuum damage (VECD) mechanics model (see Figure 28[d]).



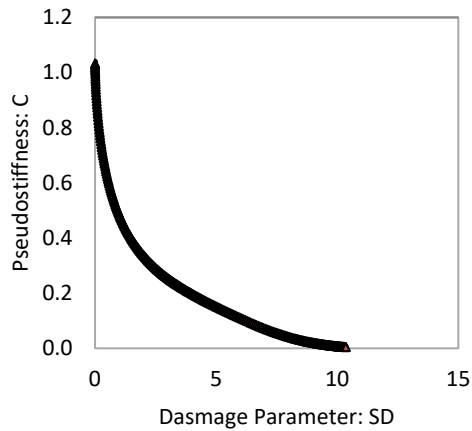
(a) Frequency Sweep Step



(b) Linear Amplitude Sweep Step



(c) Shear Stress  $\times$  Shear Strain Curve



(d) Characteristic Curve

**Figure 28. LAS Test and Analysis: An Illustration.**

## Effect of Binder Sources and PGs

For this part of the study, original PG64-34, PG64-28, PG64-22, and PG70-22 asphalt binders were RTFO-aged subjected to LAS tests following AASHTO TP101 (2014). Figure 29 presents the estimated fatigue lives of these binders at a controlled shear strain of 2.5 and 5.0 percent. The figure clearly shows that fatigue lives predicted from LAS-VECD analysis for these binders generally follow the relationship one would expect fatigue life would have with PG, except for PG70-22.

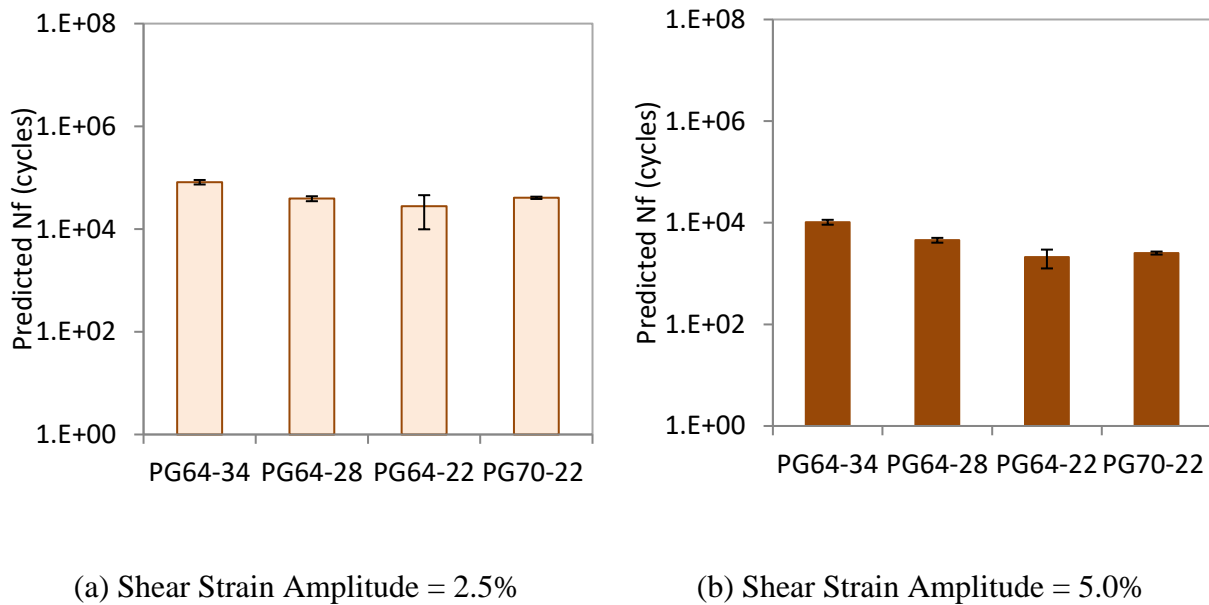


**Figure 29. LAS Test Results: Original Binders.**

## Effect of Aging

For this part of the study, original PG64-22 and PG70-22 binders were aged following the following different sequences: Unaged, RTFO + 0 hr PAV, RTFO + 20 hr PAV, RTFO + 40 hr PAV, and RTFO + 80 hr PAV (referred to as OB, RTFO, PAV20, PAV40, and PAV80, respectively). The aged and unaged samples of PG64-22 and PG70-22 binders were then subjected to LAS tests following AASHTO TP 101 (2014). Figure 30 presents the fatigue lives of these binders estimated at different aging and loading conditions. The figure clearly shows that fatigue lives predicted from LAS-VECD analysis for both binder grades do not follow the relationship one would expect fatigue life would have with aging. The inconsistency between estimated and expected trend might be due to using the VECD model to predict fatigue life even in severely aged asphalt binders. Using the VECD model in such estimations cannot be justified when the cracks are not homogeneously smeared in the continuum and the size of continuum is not significantly larger than the size of individual cracks. Since one cannot guarantee both these conditions are met when binders are severely aged, one cannot also justify the use of VECD in severely aged binders. As such, there is a need to develop a test method that can discriminate



asphalt binders based on their resistance to fatigue cracking at intermediate temperature even when the binders are severely aged conditions.

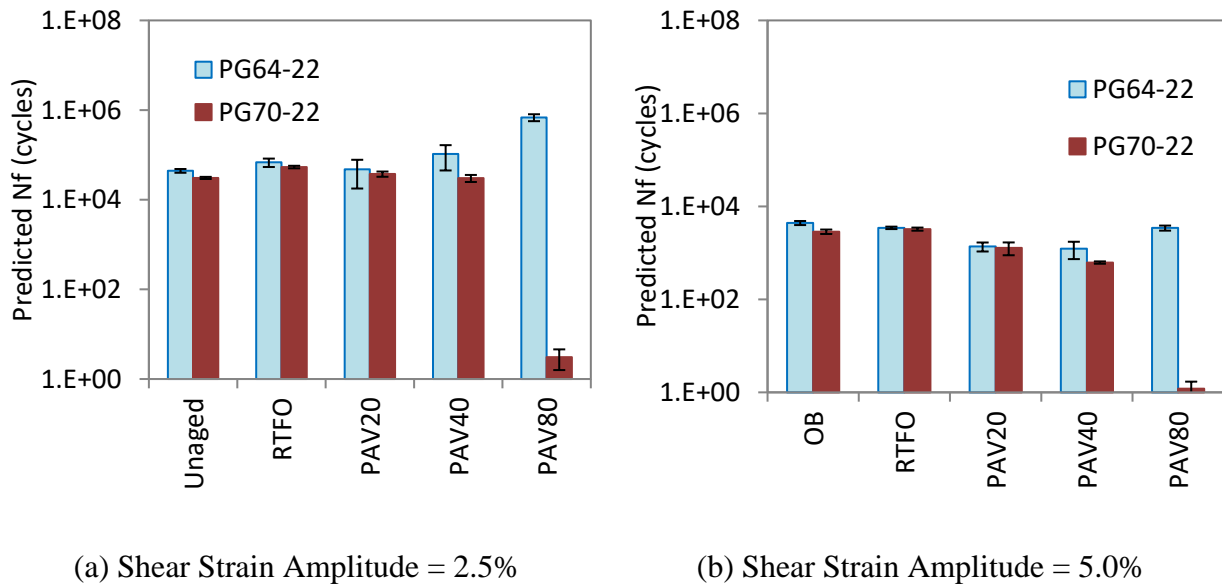
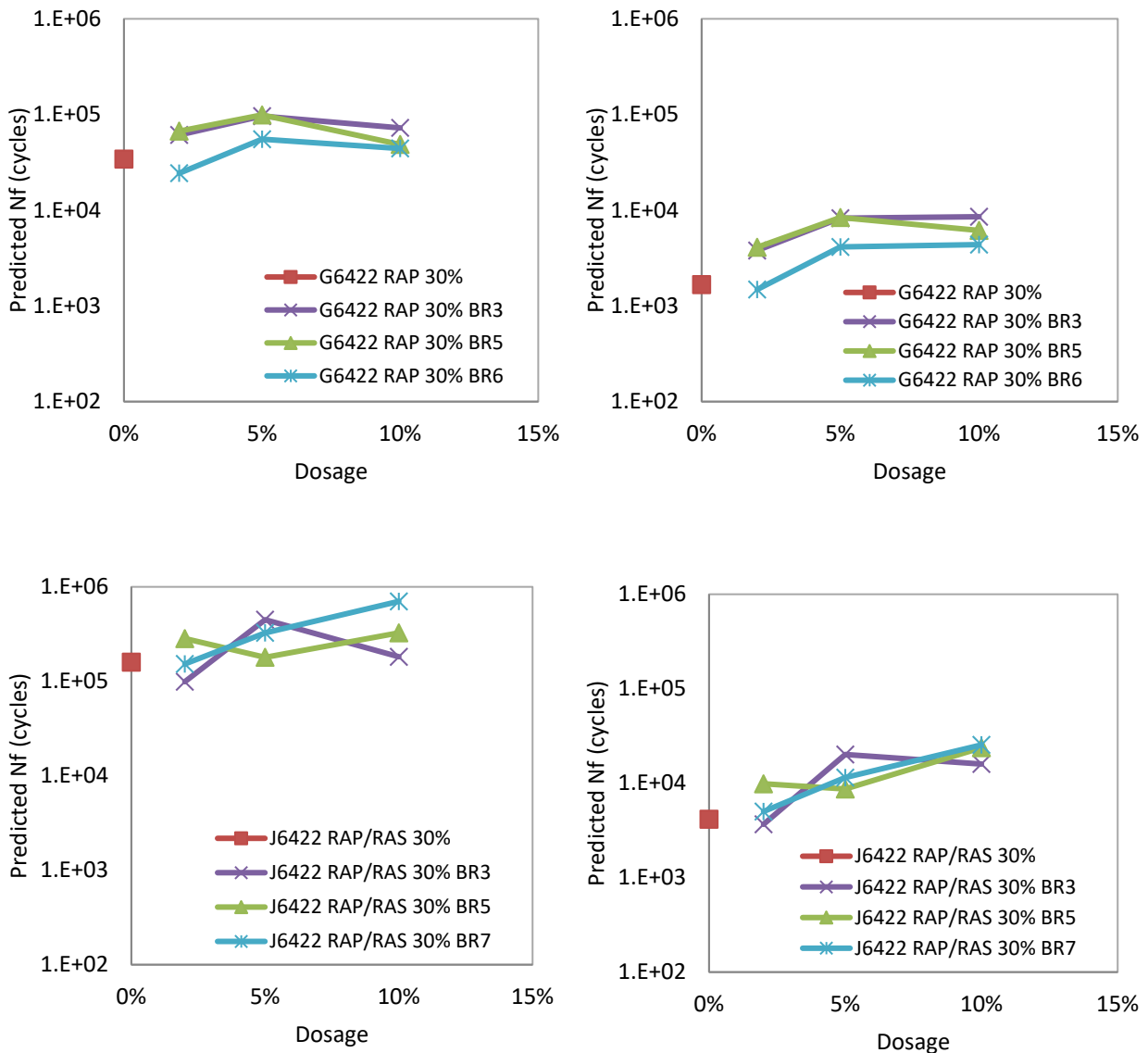


**Figure 30. LAS Test Results: Effect of Chemical Aging.**

### Effect of Engineering Agents

TTI researchers used materials obtained from two real field projects to evaluate the effect of engineering agents on fatigue cracking resistance of asphalt binders at intermediate temperature following LAS tests. From the materials obtained from one of these two field projects, PG64-22 asphalt binder from source G (G6422), 30 percent RAP-extracted asphalt binder, and 2, 5, and 10 percent bio-rejuvenators (BR3, BR5, and BR6) were used. From the materials obtained from the other field project, PG64-22 asphalt binder from source J (J6422); 18 percent RAP and 11 percent RAP- extracted asphalt binders; and 2, 5, and 10 percent bio-rejuvenators (BR3, BR5, and BR6) were used. The blends were tested at 15°C under the pure linear amplitude sweep (PLAS) test using two replicates per each blend. Figure 31 shows the predicted fatigue lives for binders engineered with bio-rejuvenators at different control strain rates. The results did not show consistent trends.



(a) Shear Strain Amplitude = 2.5%

(b) Shear Strain Amplitude = 5.0%

**Figure 31. LAS Test Results: Effect of Engineering Agents.**

### FATIGUE CRACKING RESISTANCE: PLAS TESTS

Hintz and Bahia (2013) discussed crack propagation of asphalt binders under the time sweep test in which a constant shear strain is applied to asphalt binder samples (8 mm in diameter and 2 mm in thickness) using a DSR. TTI researchers used a power law relationship between energy release rate,  $J$  and crack growth rate,  $\dot{c}$ , proposed previously by Schapery (1984), to describe asphalt binder propagation under DSR testing. Specifically, for DSR testing, Hintz and Bahia (2013) defined the energy release rate,  $J$  as:

$$J = \frac{|G^*|\gamma^2 h}{2r^2(r-c)} \left( r - c + z \left( 1 - e^{-\frac{c}{z}} \right) \right)^3 \left( 1 - e^{-\frac{c}{z}} \right) \quad (6)$$

Herein,  $|G^*|$  is shear modulus,  $\gamma$  is shear strain under the time sweep test,  $c$  is crack length,  $r$  is sample radius,  $h$  is sample height or thickness,  $z$  is a numerical factor equal to 0.1 for this case. When dealing with concrete fracture, Bazant and Prat (1988) proposed an alternative cracking growth rate equation:

$$\dot{c} = A \left( \frac{J}{J_f} \right)^n \quad (7)$$

Herein,  $\dot{c}$  is crack growth (or propagation) rate,  $J$  is the energy release rate,  $J_f$  is fracture energy determined from a monotonic test, and  $A$  and  $n$  are parameters determined by repetitive laboratory testing (such as the time sweep test). The foregoing equation shows that parameter  $\frac{J}{J_f}$  has significant influence on the crack growth rate, although it does not represent the whole cracking process. The larger is the  $\frac{J}{J_f}$  value, the faster is the crack growth. Thus, some characterizing parameter for asphalt binder fatigue resistance can potentially be derived from parameter  $\frac{J}{J_f}$  shown below:

$$\frac{J}{J_f} = \frac{|G^*|\gamma^2 h}{2r^2(r-c)J_f} \left( r - c + z \left( 1 - e^{-\frac{c}{z}} \right) \right)^3 \left( 1 - e^{-\frac{c}{z}} \right) \quad (8)$$

This equation shows that parameter  $\frac{J}{J_f}$  is directly proportional to  $\frac{|G^*|\gamma^2}{J_f}$  for a specific crack length,  $c$ . The parameters  $r$ ,  $h$ , and  $z$  are constants. Therefore, the cracking growth rate is highly related to parameter  $\frac{|G^*|\gamma^2}{J_f}$ . For a time sweep test, the smaller  $\frac{|G^*|\gamma^2}{J_f}$ , the slower crack growth, and accordingly the better fatigue crack resistance.

To recap, the new cracking parameter  $\frac{|G^*|\gamma^2}{J_f}$  is derived based on fracture mechanics and the time sweep test at a constant shear strain,  $\gamma$ .

The time sweep test is itself too long, and the LAS test was developed as an accelerated asphalt binder fatigue test. Thus, the new asphalt binder fatigue cracking test is proposed based on the latest LAS test. Since the characterizing parameter  $\frac{|G^*|\gamma^2}{J_f}$  is not a fundamental indicator but an index parameter, the shear modulus can be approximately calculated from the measured shear

stress versus shear strain curve of the LAS test. Thus, the initial frequency sweep test in the current LAS test becomes unnecessary. The new asphalt binder fatigue cracking test is a PLAS test running at a selected temperature using oscillatory shear in strain-control mode at a frequency of 10 Hz. The loading scheme consists of a continuous oscillatory strain sweep. Loading is increased linearly from 0 to 30 percent over the course of 3,000 cycles, as shown in Figure 28(a) and Figure 28(b).

Figure 32 shows peak shear strain and peak shear stress recorded every 10 load cycles (or every 1 sec).

The proposed PLAS test is different from the time sweep test in which the cyclic shear strain is constant. Thus the characterizing parameter  $\frac{|G^*|\gamma^2}{J_f}$  cannot be used for the PLAS test. An alternative fatigue resistant energy index (FREI) is proposed:

$$FREI = \frac{J_{f-\tau_{max}}}{G_{0.5\tau_{max}}} \cdot (\gamma_{0.5\tau_{max}})^2 \quad (9)$$

Where,  $J_{f-\tau_{max}}$  is the shear fracture energy calculated till maximum shear stress (see Figure 32),  $G_{0.5\tau_{max}}$  is the calculated shear modulus at the point of half of the maximum shear stress, and  $\gamma_{0.5\tau_{max}}$  is the shear strain at the point of half of the maximum shear stress.

FREI is a kind of reciprocal of parameter  $\frac{|G^*|\gamma^2}{J_f}$  but there are some differences. FREI characterizes the resistance of asphalt binder to fatigue cracking. The larger is the FREI; the better is fatigue cracking resistance. Other rationales for FREI definition are provided below:

- $J_{f-\tau_{max}}$ : It is well known that materials with larger fracture energy normally have better cracking resistance. Different from regular fracture energy calculation, only first half (till maximum shear stress) of the stress versus strain curve is used for calculating  $J_{f-\tau_{max}}$ . The reasons for that are 1) the stress/strain conditions asphalt binders experience in the real world asphalt binder pavements are far less severe than the maximum shear stress/strain, although it may be higher than the stress/strain conditions of asphalt binder concrete as a whole; and 2) the shear strain after the peak stress may not be the real strain asphalt binder experience due to potential macrocrack in the DSR asphalt binder specimen and consequently unknown true radius of asphalt binder specimen.
- $\gamma_{0.5\tau_{max}}$ : Different from the shear strain in the time sweep test, which is constant,  $\gamma_{0.5\tau_{max}}$  is the shear strain at the point of half of the maximum shear stress. For any two asphalt binders, larger  $\gamma_{0.5\tau_{max}}$  means better flexibility and relaxation capability of asphalt binder when both asphalt binders reach their half of maximum shear load bearing

capacities. That is the main reason for switching  $\gamma_{0.5\tau_{max}}$  to numerator from denominator (reciprocal of parameter  $\frac{|G^*|\gamma^2}{J_f}$  original derivation for the time sweep test).

- $G_{0.5\tau_{max}}$ : Larger shear modulus often leads asphalt binders to be more prone to cracking when all other factors are the same. The value of  $G_{0.5\tau_{max}}$  is not equal to asphalt binder shear modulus value measured at the small strain level. Instead, TTI researchers chose the shear modulus  $G_{0.5\tau_{max}}$  at the point of half of the maximum shear stress, because TTI researchers believe that the asphalt binders often experience higher shear strain than those used in frequency sweep test for determining shear modulus.

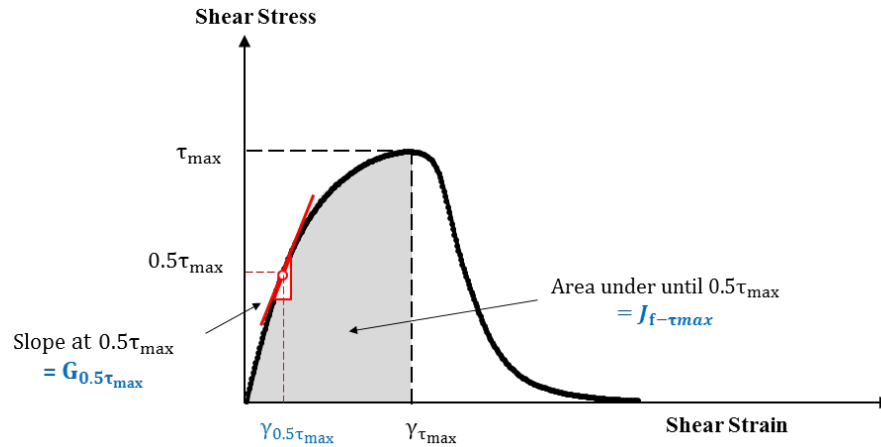


**Figure 32. PLAS Test and Analysis: An Illustration.**

Asphalt binder aging through oxidation makes asphalt binders more brittle and consequently less cracking resistant (Glover et al. 2005; Peterson 2009; Vallerga 1981). The more severe the aging, the worse is the asphalt binder fatigue resistance. Recently, bio-rejuvenators have been used with RAP materials to compensate aged asphalt binders in RAP or RAS. One of the main purposes of using bio-rejuvenators is to restore the lost chemical balance between asphaltenes and maltenes within aged asphalt binders so that the rejuvenated asphalt binders become more flexible and better fatigue resistant (Epps et al. 1980). The ensuing sections illustrate the success of the parameter FREI in discriminating effect of the source and PG of asphalt binders, the durations of chemical aging, and the sources and dosages of engineering agents.

### Effect of Binder Sources and PGs

For this part of the study, original PG64-34, PG64-28, PG64-22, and PG70-22 asphalt binders were first RTFO-aged and then subjected to LAS tests following AASHTO TP 101 (2014). For each original binder, two replicates were used. Figure 33 presents the estimated fatigue lives of RTFO-aged binders with different PGs at controlled shear strain of 2.5 and 5.0 percent. The figure clearly shows that fatigue lives predicted from LAS-VECD analysis for these binders generally follow the relationship one would expect fatigue life would have with PG.

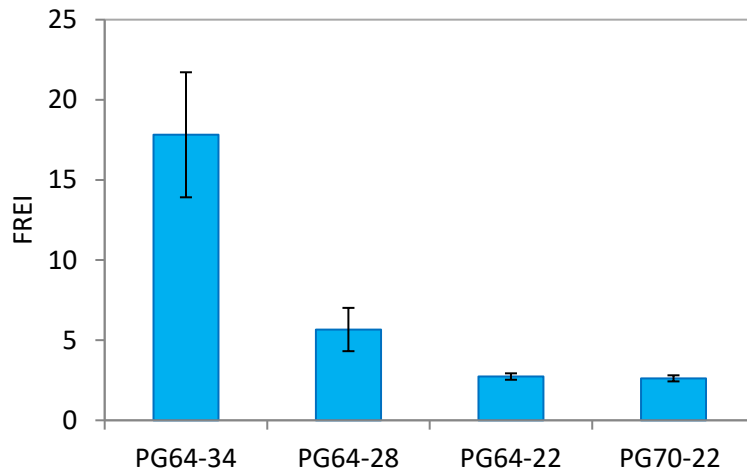


**Figure 33. PLAS Test Results: Original Binders.**

### Effect of Aging

The same two asphalt binders used to identify the deficiency of the LAS test (see Figure 30) were used for evaluate the effect of aging on fatigue cracking resistance of asphalt binders at intermediate temperature using the PLAS test. For each asphalt binder, the PLAS test was performed at 15°C for five asphalt binder aging conditions: original binder (OB), RTFO, PAV20, PAV40, and PAV80. For each aging condition, two replicates were used. Figure 34 shows the averaged FREI value for each asphalt binder at each specific aging condition. The figure clearly indicates that the FREI is a true indicator of asphalt binder fatigue resistance—the aged binders have lower values or FREI and thereby poorer fatigue resistance.

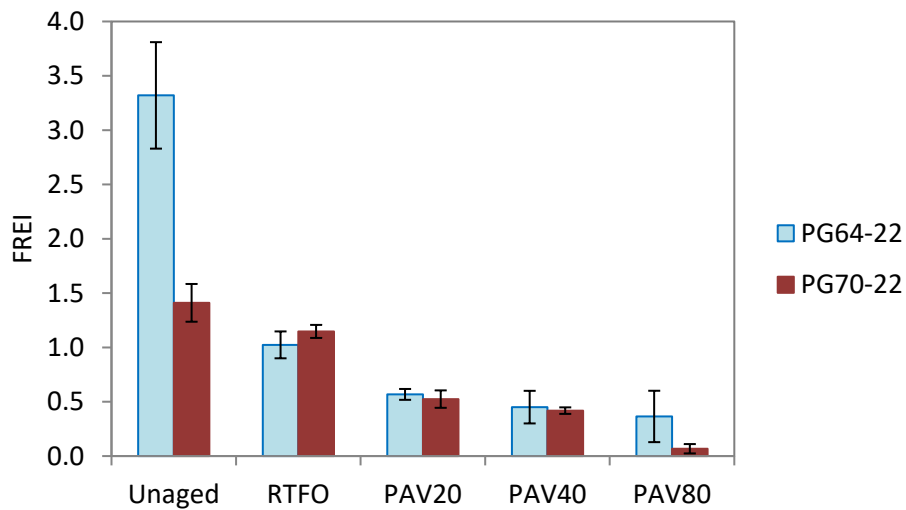


**Figure 34. PLAS Test Results: Effect of Chemical Aging.**

## Effect of Engineering Agents

Materials from the two real field projects as described before were used to evaluate the effect of engineering agents on FREI or fatigue cracking resistance of asphalt binders at intermediate temperature using PLAS test. Figure 35 shows the averaged FREI value for each bio-rejuvenator at each specific dosage rate. The figure clearly shows that FREI has a good correlation with dosage of bio-rejuvenator; the FREI value becomes higher with a higher dosage of bio-rejuvenator, suggesting an increase in bio-rejuvenator dosage makes asphalt binder more ductile and thereby more able to resist fatigue cracking at intermediate temperatures. The figure also shows FREI clearly discriminates the effectiveness of different sources of these agents.

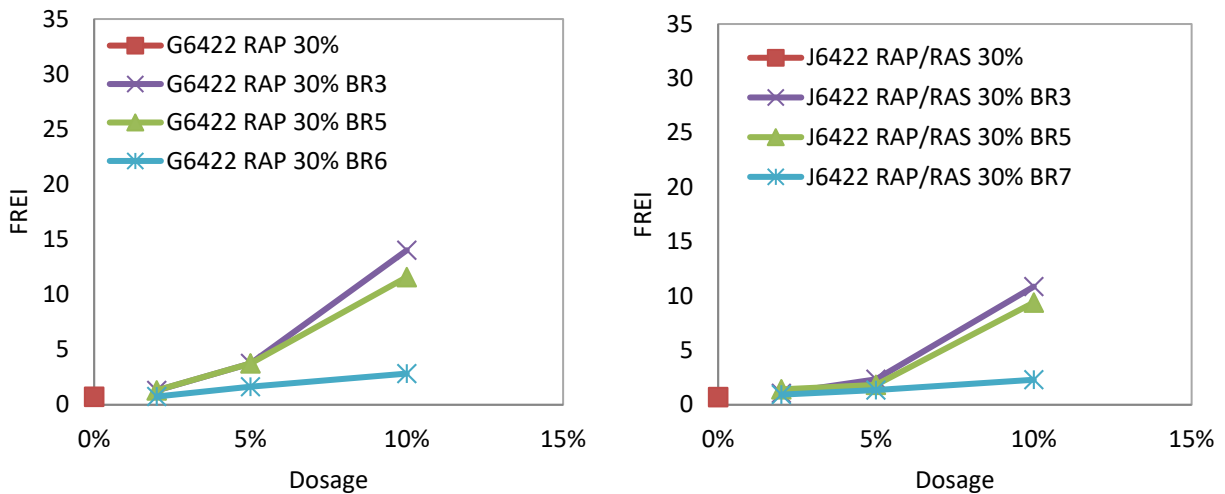


**Figure 35. PLAS Test Results: Effect of Engineered Binders.**

The juxtaposition of LAS and PLAS test reveals that PLAS is more effective than LAS test in discriminating the effect of the sources and PG of asphalt binder sources, the conditions of chemical aging, and the source and dosage of engineering agents.

## Correlation with Laboratory Mixture Cracking Tests

Many tests have been developed to evaluate cracking resistance of asphalt binder mixtures (Zhou et al. 2016b). Based on previous work (Zhou et al. 2016a), Texas OT (Tex-248-F 2014) and the Illinois Flexibility Index Test (Al-Qadi et al. 2015) were selected for this study. The Texas OT uses the number of cycles to fail (OT cycles) to discriminate cracking resistance of asphalt binder mixtures. The higher the number of OT cycles, the better the cracking resistance. The Illinois Flexibility Index Test (I-FIT) uses flexibility index (FI) to discriminate cracking resistance of asphalt binder mixtures. The larger the FI value, the better the cracking resistance.

The same limestone aggregates with the same gradation plus four different asphalt binders were used to produce a total of four different virgin asphalt binder mixtures. The nominal maximum

aggregate size for the mixtures was 9.5 mm and the same optimum asphalt binder content of 5.7 percent was used for all four mixtures. For each mixture, five replicates of OT and four replicates of I-FIT specimen at  $7.0 \pm 0.5$  percent air voids were prepared through the Superpave Gyratory Compactor (SGC) and then saw cutting. Before the compaction, each loose mix was conditioned in the oven for 4 hours at  $135^{\circ}\text{C}$ . Both tests were run at a room temperature of  $25^{\circ}\text{C}$  following the Tex-248-F (2014) and the procedure proposed by Al Qadi et al. (2015). Figure 36 shows the averaged OT cycles and FI values for four different mixtures used in this study. Both mixture cracking tests indicated that the asphalt binder PG64-34 had the best cracking resistance, followed by PG64-28, PG64-22, and PG70-22.

The same four asphalt binders were characterized under the PLAS test at  $15^{\circ}\text{C}$ . The calculated FREI for each asphalt binder is also presented in Figure 34. Comparing the calculated FREI values and those mixture cracking results, it is clearly seen that the rankings of cracking resistance between the PLAS test and mixture cracking tests on these four asphalt binders are exactly the same (from the best to the worst):

$$\text{PG64} - 34 > \text{PG64} - 28 > \text{PG64} - 22 > \text{PG70} - 22$$

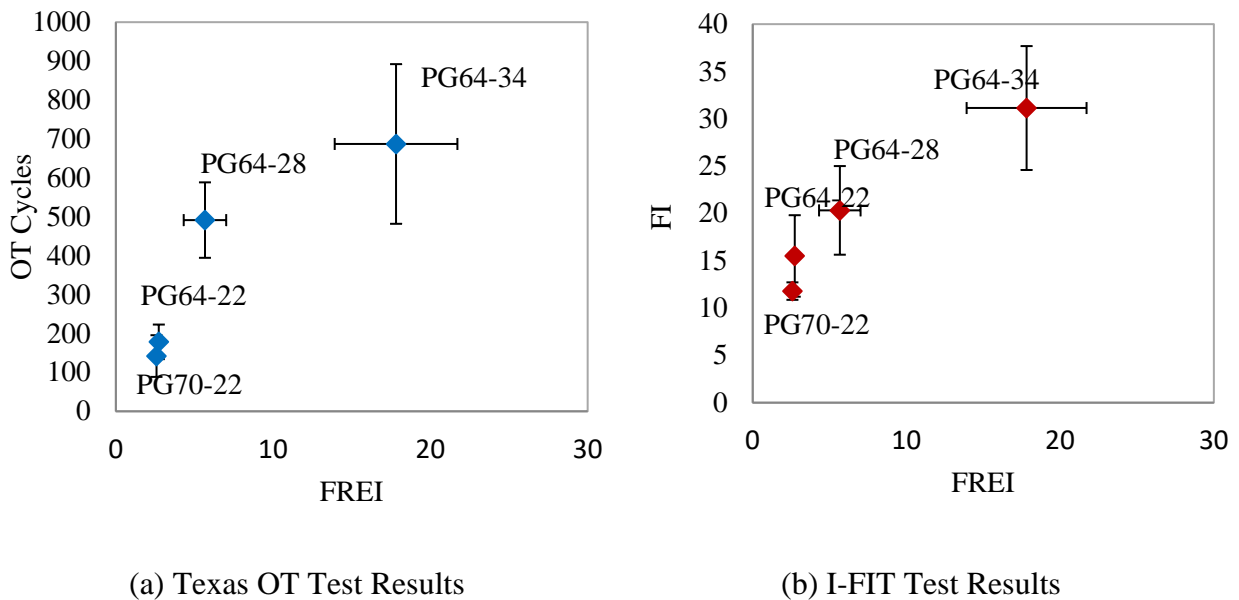


**Figure 36. PLAS Test Results: Correlation with Mixture Cracking Results.**

### Correlation with Full-Scale Accelerated Pavement Tests

To further validate the asphalt binder PLAS test, TTI researchers employed the fatigue data from the Federal Highway Administration accelerated loading facility (FHWA-ALF) testing on polymer modified asphalt binders (Gibson et al. 2012). Twelve full-scale lanes of pavement with various modified asphalt binders were constructed at FHWA-ALF under Pooled Fund Study TPF-5(019) in summer 2002. Figure 37 shows the layout of the 12 test lanes. All 12 lanes consist



of an asphalt binder layer and a granular base course over a uniformly prepared subgrade. The pavements were loaded with super single tire (74 kN or 16.6 kip and 827.4 kPa or 120 psi) at a temperature of 19°C (66°F). Lanes 2 to 6 had clear bottom-up fatigue cracking so that these five lanes were used for validating the asphalt binder PLAS test in this paper.

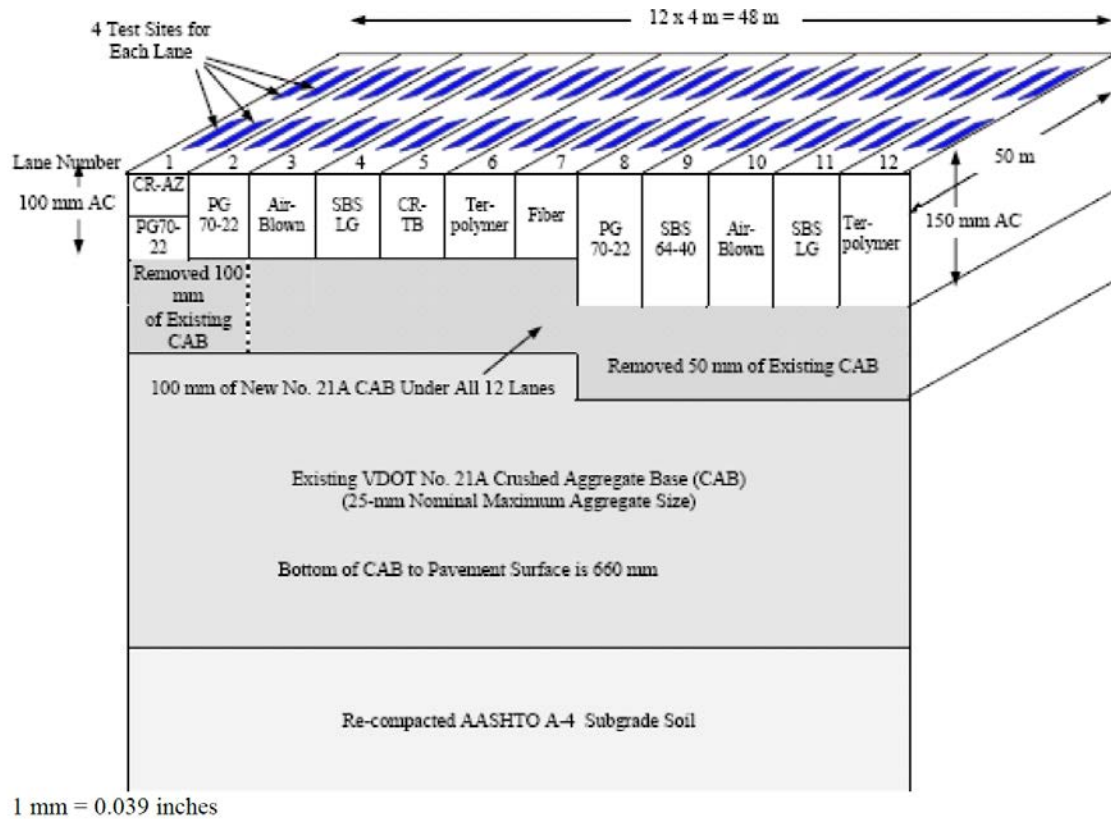


**Figure 37. Three-Dimensional Layout of the FHWA-ALF Test Section (Gibson et al. 2012).**

Although the FHWA-ALF testing was completed long time ago, original asphalt binders from Lanes 2, 3, 4, 5, and 6 were stored and available for this validation. To match the FHWA-ALF testing temperature, the PLAS tests on the RTFO aged original asphalt binders were run at 19°C as well. Figure 38 shows the comparison between the asphalt binder fracture index (FREI) and the load passes to 25 percent cracked area measured from FHWA-ALF. Clearly the PLAS test results match the overall trend of the FHWA-ALF fatigue data. Note that imperfect relationship shown in Figure 38 is expected because field fatigue performance is impacted by many factors in which asphalt binder is not the only one, as mentioned in the introduction section of this report. Thus, the results from full-scale field fatigue data also indicated that the PLAS test is an effective test for evaluating asphalt binder fatigue resistance.

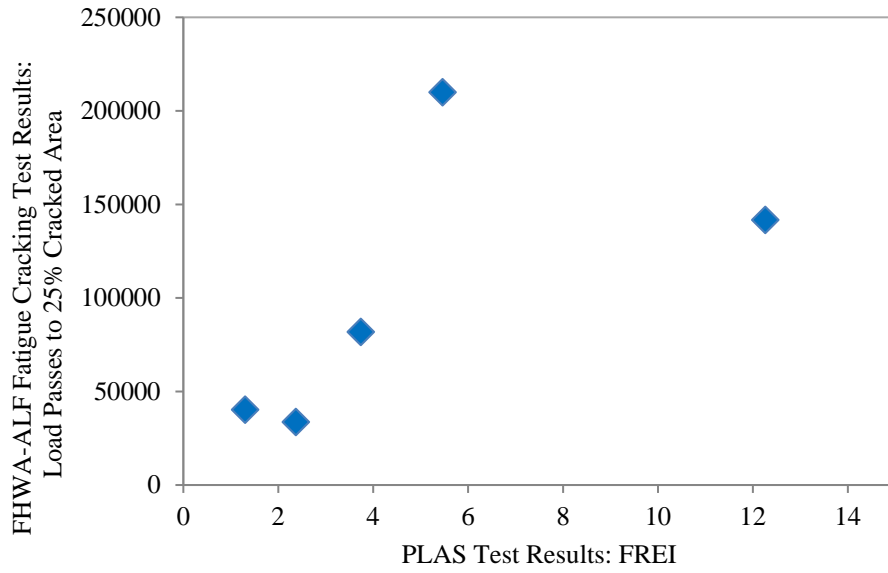


**Figure 38. PLAS Test Results: Correlation with FHWA-ALF Cracking Test Results.**

## **CHAPTER 5: UPDATED STATEWIDE ASPHALT BINDER SELECTION CATALOG**

### **INTRODUCTION**

This project updated TxDOT's statewide asphalt binder catalog based on the research findings of laboratory and field test results. To accomplish this objective, researchers first identified the difference between the catalog currently used in Texas and the catalog developed under project 0-6674 and then updated the existing catalog based on the latest research findings, as described below.

### **STATEWIDE PG BINDER SELECTION CATALOG CURRENTLY USED IN TEXAS**

TxDOT's current method for selecting asphalt binder PG grade for any pavement in Texas involves two major phases.

The *first phase* of this method involves selecting the high and low temperature PGs of asphalt binder based on the location of the project and the desired level of confidence (i.e., 95 or 98 percent confidence). Confidence level refers to the chances that the normal variations in temperature 20 mm below the surface of the pavement will never exceed the range of the selected binder grade. TxDOT provides color-coded location maps for a given confidence level to aid in this step. Figure 39 presents the color-coded location map with recommended starting binder PG.

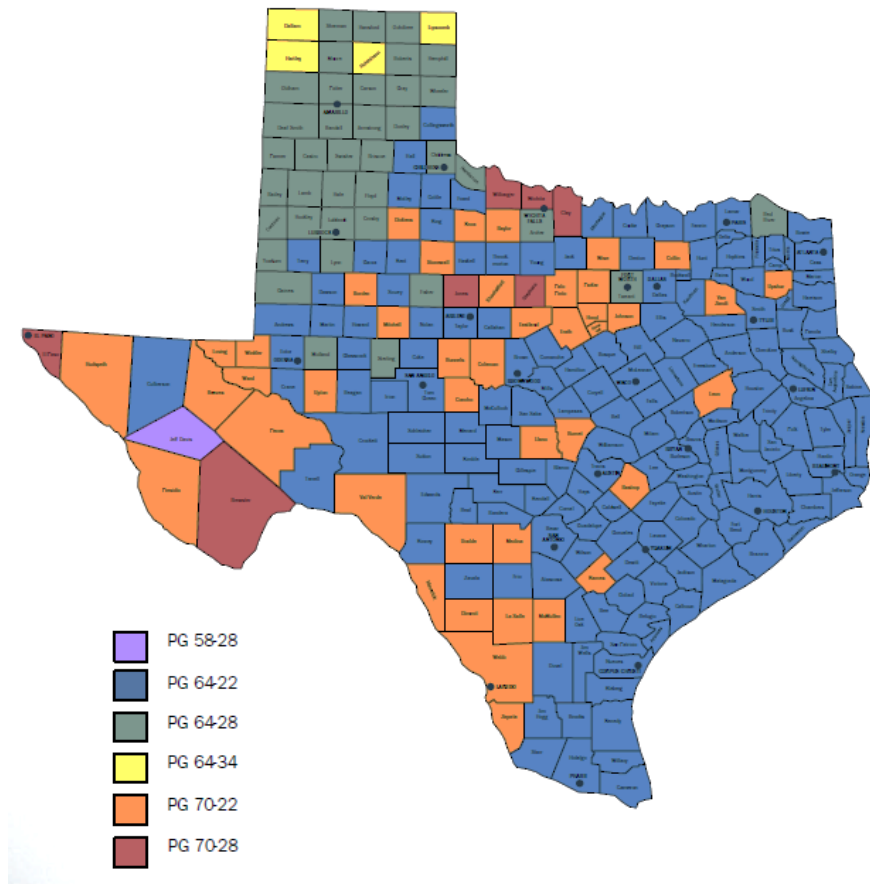


**Figure 39. Asphalt Binder Grade Recommendation: TxDOT Method.**

The *second phase* of TxDOT’s current method for asphalt binder PG selection involves four different steps for adjusting the starting binder PG. Each step deals with a different factor (traffic volume, traffic speed, pavement layer, and the use of recycled material) that influences the overall performance of asphalt pavement. Figure 40 presents these steps with corresponding impact each factor would have on the starting binder PG. In some cases, these factors change the starting binder PG up to two grades.

TxDOT’s current method recommends that the high temperature PG be 64 at the minimum and 76 at the maximum, and that the low temperature PG be –34 at the minimum and –22 at the maximum. However, in some special locations, the recommendations are a little bit different. The method recommends high temperature PG of 58 in select hot climates such as Jeff Davis County of the El Paso District, and low temperature PG of –34 in select cold climates such as counties north of the IH40, namely in Dallam, Hartley, Hutchinson, and Lipscomb Counties in the Amarillo District.

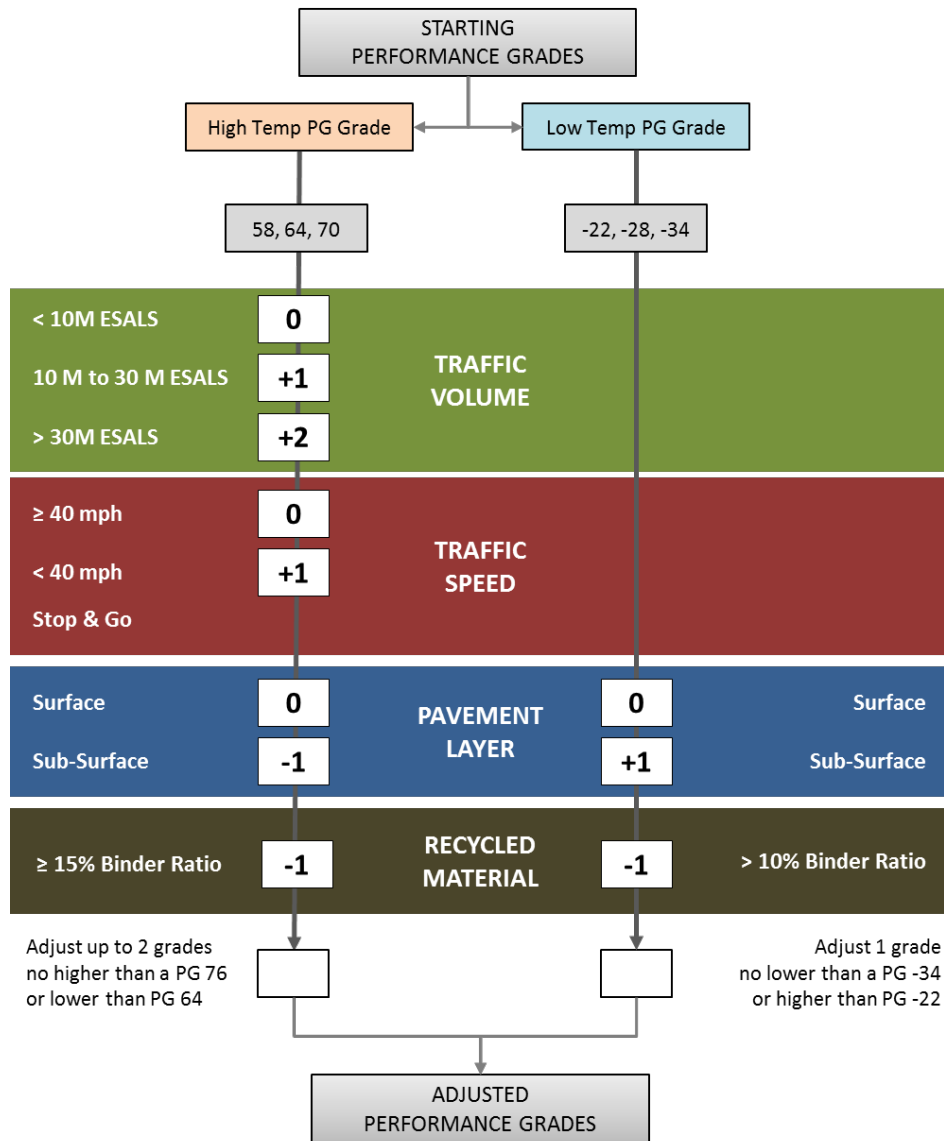


**Figure 40. Asphalt Binder Grade Adjustment: TxDOT Method.**

Despite these safe guards, the TxDOT’s current method does not consider whether the proposed project involves the construction of a new pavement or an asphalt overlay over an existing pavement when recommending binder PG.

**STATEWIDE ASPHALT BINDER SELECTION CATALOG DEVELOPED UNDER 0-6674**

To make TxDOT’s current binder grade selection method more robust, TTI researchers first established that the existing pavement layer, overlay thickness, traffic level, environmental zones (or climate), aggregate type, and asphalt binder PG influence the cracking performance of the overlays. For this purpose, researchers simulated cracking performance of 2700 different cases of overlays involving five different zones for climates, four different levels of traffic volume, three

different overlay thicknesses, three different types of existing pavement structures, three different types of aggregate types, and five different grades of asphalt binder (see Table 26). Researchers used the Texas Asphalt Concrete Overlay Design and Analysis System for these simulations. From the simulation results, researchers also determined the binder PG that would provide the best possible outcome in terms of cracking performance in each district in Texas.

Table 27 presents the recommended binder grades for each district in Texas based on these simulations. The table shows that each county in a given district is recommended the same binder PG. When recommended binders in Table 27 and Figure 39 are compared, one can notice that binder recommended by this new approach is usually softer than the binder recommended by the TxDOT's current method. This difference highlights the fact that binder recommendations for each county need to be updated when an overlay construction is considered.

## **NEW STATEWIDE ASPHALT BINDER SELECTION CATALOG**

Using TxDOT's current catalog, TTI researchers identified the counties in each district that have different recommended PGs and then updated them with newly recommended PGs. Table 28 presents the recommended high and low temperature PG for a brand new pavement construction and new overlay construction over existing pavement layers. Researchers second TxDOT's current protocol that the starting binder PG needs to be adjusted for traffic volume, traffic speed, pavement layer, and the use of recycled material whichever applicable. As such, researchers modified the two phases of TxDOT's current binder PG selection method as follows.

The *first phase* of the new approach involves selecting the high and low temperature PGs of asphalt binder based on the location of the project, the desired level of confidence, and the type of construction. The type of construction (new versus overlay) specifically plays a critical role in recommending low temperature PG for the project. Researchers developed color-coded location maps for 98 percent confidence level to aid in selecting the recommended PG for any given project in Texas:

- Figure 41 → PG for new pavement construction.
- Figure 42 → PG for asphalt overlay over existing asphalt concrete (AC).
- Figure 43 → PG for asphalt overlay over existing jointed concrete pavements (JPCP).

The *second phase* of the new approach involves adjusting the starting binder PG using four different steps. As in Texas's current approach, each of these steps deals with a different factor (traffic volume, traffic speed, pavement layer, and the use of recycled material) that might influence the overall performance of asphalt pavement. The adjustment for pavement layer might not be applicable for overlay design. Figure 44 illustrates each step included in Phase I and Phase II of the new approach.

**Table 26. Overlay Performance Simulation Factorial: 0-6674.**

<i>Factor</i>	<i>Details</i>		
Environmental Zones	Zone	Representative District	Case
	Dry-Cold	Amarillo	1
	Dry-Warm	Odessa	2
	Moderate	Austin	3
	Wet-Cold	Paris	4
	Wet-Warm	Beaumont	5
Existing Pavement Structure	Type		Case
	Conventional AC over granular base (GB)		1
	Existing JPCP over GB		2
	Thinner Existing AC over cement treated base (CTB)		3
Traffic Level	Equivalent single axle loads		Case
	3 million		1
	5 million		2
	10 million		3
	30 million		4
Overlay Thickness	Thickness		Case
	2 in.		1
	3 in.		2
	4 in.		3
Overlay Mixture	Aggregate	Binder	Case
	Limestone	PG 64-34	1
		PG 64-28	2
		PG 64-22	3
		PG 70-22	4
		PG 76-22	5
	Gravel	PG 64-34	1
		PG 64-28	2
		PG 64-22	3
		PG 70-22	4
		PG 76-22	5
	Granite	PG 64-34	1
		PG 64-28	2
		PG 64-22	3
		PG 70-22	4
PG 76-22		5	

**Table 27. Asphalt Binder Grade Recommendation: 0-6674.**

No.	District	Aggregate	Conventional Existing AC Pavement	Existing JPCP
1	Paris	Gravel	PG64-28	PG64-34
2	Fort Worth	Limestone	PG64-22 (Higher %AC) or PG64-28	PG64-34
3	Wichita Falls	Gravel	PG64-28	PG64-34
4	Amarillo	Gravel	PG64-28	PG64-34 (Higher %AC)
5	Lubbock	Gravel	PG64-28	PG64-34 (Higher %AC)
6	Odessa	Gravel	PG64-28	PG64-28
7	San Angelo	Gravel	PG64-28	PG64-28
8	Abilene	Gravel	PG64-28	PG64-34 (Higher %AC)
9	Waco	Limestone	PG64-22 (Higher %AC) or PG64-28	PG64-28
10	Tyler	Limestone	PG64-22 (Higher %AC) or PG64-28	PG64-34
11	Lufkin	Limestone	PG64-22 (Higher %AC) or PG64-28	PG64-28
12	Houston	Limestone	PG64-22 (Higher %AC) or PG64-28	PG64-28
13	Yoakum	Gravel	PG64-28	PG64-28
14	Austin	Limestone	PG64-22 (Higher %AC) or PG64-28	PG64-28
15	San Antonio	Limestone	PG64-22 (Higher %AC) or PG64-28	PG64-28
16	Corpus Christi	Gravel	PG64-22	PG64-22
17	Bryan	Limestone	PG64-22 (Higher %AC) or PG64-28	PG64-28
18	Dallas	Limestone	PG64-22 (Higher %AC) or PG64-28	PG64-28
19	Atlanta	Granite	PG70-22	PG64-28
20	Beaumont	Granite	PG70-22	PG64-28
21	Pharr	Gravel	PG64-22	PG64-22
22	Laredo	Gravel	PG64-22	PG64-22
23	Brownwood	Limestone	PG64-22 (Higher %AC) or PG64-28	PG64-28
24	El Paso	Limestone	PG64-22 (Higher %AC) or PG64-28	PG64-28
25	Childress	Gravel	PG64-28	PG64-34 (Higher %AC)



**Table 28. Asphalt Binder Grade Recommendation: New Catalog.**

No.	District	Counties	PGL:		PGL: Overlay	
			New & Overlay	New	Existing AC	Existing JPCP
1	Paris	Red River	64	-28	-28	-34
		Delta, Fannin, Franklin, Grayson, Hunt, Hopkins, Lamar, Rains	64	-22	-28	-34
		Tarrant	64	-28	-28	-34
2	Fort Worth	Jack	64	-22	-28	-34
		Erath, Hood, Johnson, Palo Pinto, Parker, Somervell, Wise	70	-22	-28	-34
		Archer	64	-28	-28	-34
3	Wichita Falls	Cooke, Montague, Throckmorton, Young	64	-22	-28	-34
		Baylor	70	-22	-28	-34
		Clay, Wichita, Wilbarger	70	-28	-28	-34
4	Amarillo	Armstrong, Carson, Deaf Smith, Gray, Hansford, Hemphill, Moore, Ochiltree, Oldham, Potter, Randall, Roberts, Sherman	64	-34	-34	-34
		Dallam, Hartley, Hutchinson, Lipscomb	64	-28	-28	-34
5	Lubbock	Bailey, Castro, Cochran, Crosby, Floyd, Garza, Hale, Hockley, Lamb, Lubbock, Lynn, Parmer, Swisher, Yoakum	64	-28	-28	-34
		Dawson, Gaines, Terry	64	-22	-28	-34
		Midland	64	-28	-28	-28
6	Odessa	Andrews, Crane, Ector, Martin, Terrell	64	-22	-28	-28
		Loving, Pecos, Reeves, Upton, Ward, Winkler	70	-22	-28	-28
		Sterling	64	-28	-28	-28
7	San Angelo	Coke, Crockett, Edwards, Glasscock, Itron, Kimble, Menard, Reagan, Real, Schleicher, Sutton, Tom Green	64	-22	-28	-28
		Concho, Runnels	70	-22	-28	-28
		Fisher	64	-28	-28	-34
8	Abilene	Callahan, Haskell, Howard, Kent, Nolan, Scurry, Taylor	64	-22	-28	-34
		Borden, Mitchell, Shackelford, Stonewall	70	-22	-28	-34
		Jones	70	-28	-28	-34
9	Waco	Bell, Bosque, Coryell, Falls, Hamilton, Hill, Limestone, McLennan	64	-22	-28	-28
		Anderson, Cherokee, Gregg, Henderson, Rusk, Smith, Wood	64	-22	-28	-34
10	Tyler	Van Zandt	70	-22	-28	-34
11	Lufkin	Angelina, Houston, Nacogdoches, Polk, Sabine, San Augustine, San Jacinto, Shelby, Trinity	64	-22	-28	-28
12	Houston	Brazoria, Fort Bend, Galveston, Harris, Montgomery, Waller	64	-22	-28	-28
13	Yoakum	Austin, Calhoun, Colorado, DeWitt, Fayette, Gonzales, Jackson, Lavaca, Matagorda, Victoria, Wharton	64	-22	-28	-28
14	Austin	Blanco, Caldwell, Gillespie, Hays, Lee, Mason, Travis, Williamson	64	-22	-28	-28
		Bastrop, Burnet, Llano	70	-22	-28	-28
15	San Antonio	Atascosa, Bandera, Bexar, Comal, Frio, Guadalupe, Kendall, Kerr, Wilson	64	-22	-28	-28
		McMullen, Medina, Uvalde	70	-22	-28	-28
16		Arañas, Bee, Goliad, Jim Wells, Kleberg, Live Oak, Nueces, Refugio, San Patricio	64	-22	-28	-22

No.	District	Counties	PGL: New & Overlay	PGL: New	PGL: Existing AC	PGL: Overlay Existing JPCP
	Corpus Christi	Karnes	70	-22	-22	-22
17	Bryan	Brazos, Burleson, Freestone, Grimes, Madison, Milam, Robertson, Walker, Washington Leon	64	-22	-28	-28
18	Dallas	Dallas, Denton, Ellis, Kaufman, Navarro, Rockwall Collins	64	-22	-28	-28
19	Atlanta	Bowie, Camp, Cass, Harrison, Marion, Morris, Panola, Titus Upshur	64	-22	-22	-28
20	Beaumont	Chambers, Hardin, Jasper, Jefferson, Liberty, Newton, Orange, Tyler	64	-22	-22	-28
21	Pharr	Brooks, Cameron, Hidalgo, Jim Hogg, Kenedy, Starr, Willacy Zapata	64	-22	-22	-22
22	Laredo	Duval, Kinney, Zavala Dimmit, La Salle, Maverick, Val Verde, Webb	64	-22	-22	-22
23	Brownwood	Brown, Comanche, Lampasas, McCulloch, Mills, San Saba Coleman, Eastland Stephens	64	-22	-28	-28
		Jeff Davis	70	-28	-28	-28
24	El Paso	Culberson Hudspeth, Presidio Brewster, El Paso	58	-28	-28	-28
			64	-22	-28	-28
			70	-22	-28	-28
			70	-28	-28	-28
25	Childress	Briscoe, Childress, Donley, Hardeman, Wheeler Collingsworth, Cottle, Foard, Hall, Motley, King Dickens, Knox	64	-28	-28	-34
			64	-22	-28	-34
			70	-22	-28	-34

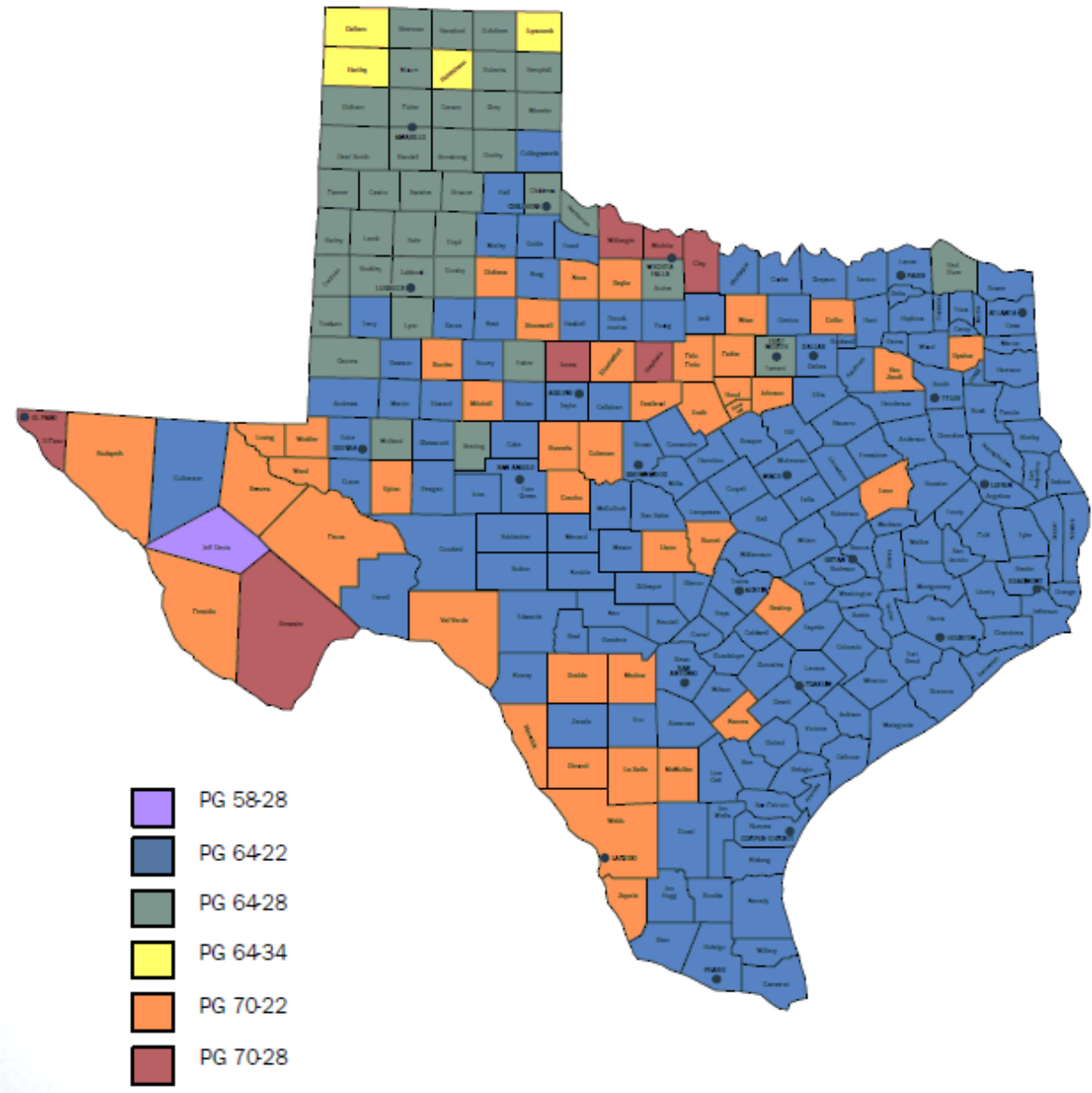


**Figure 41. PG Recommendation for New Construction.**

# PG GRADE RECOMMENDATION BASED ON CLIMATE - 98% CONFIDENCE

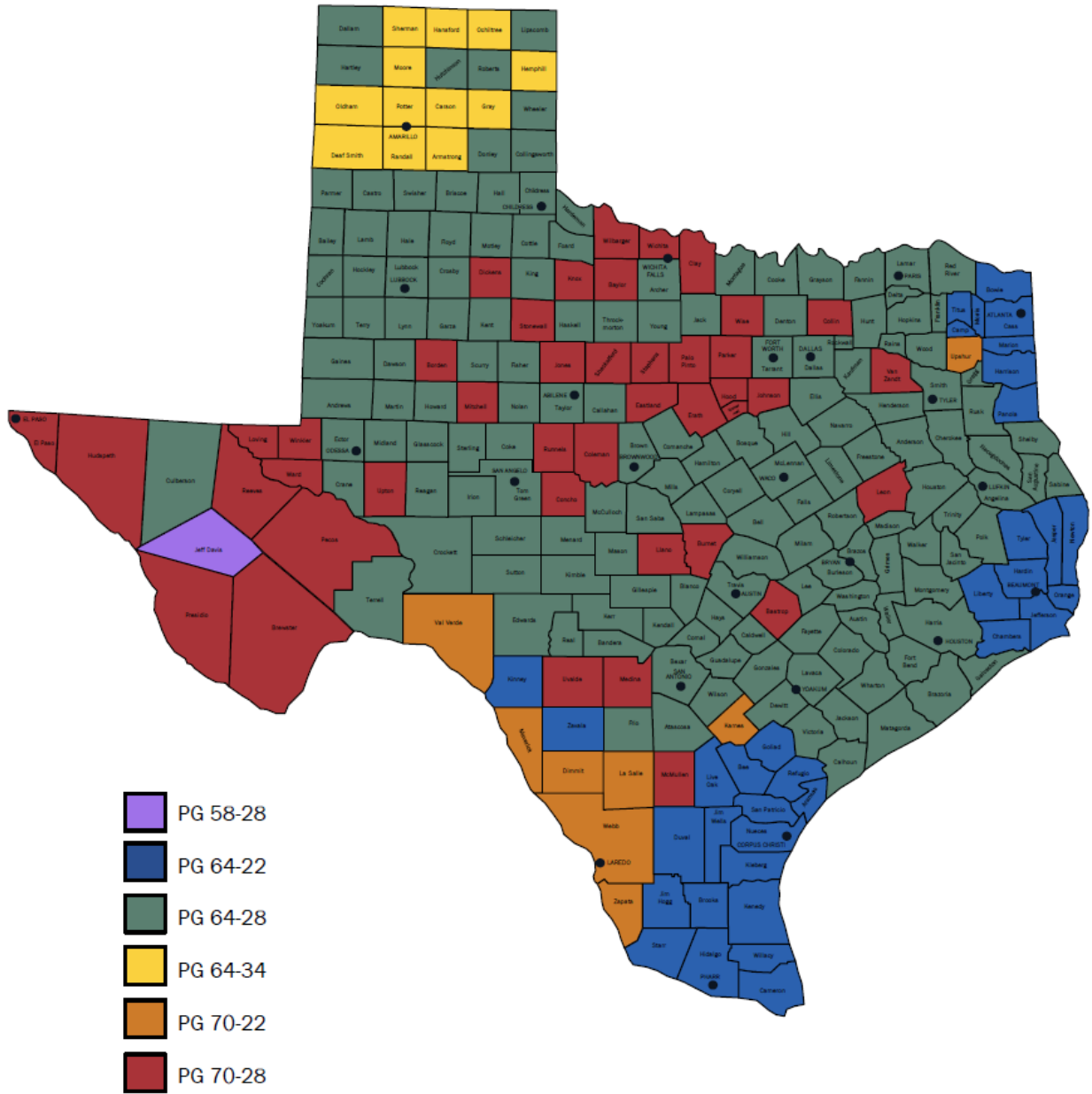


Figure 42. PG Recommendation for Asphalt Overlay over Existing AC.

# PG GRADE RECOMMENDATION BASED ON CLIMATE - 98% CONFIDENCE

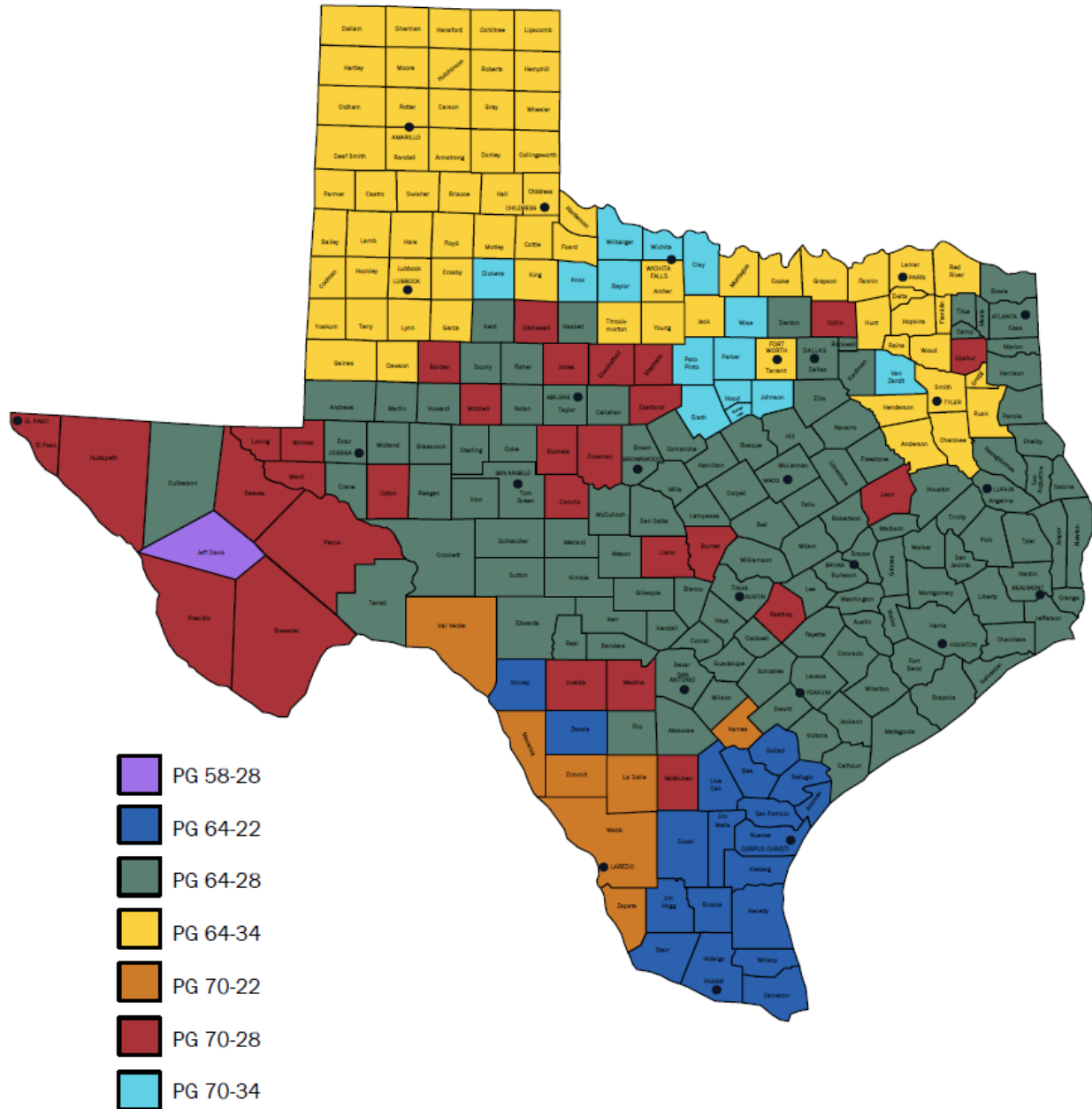
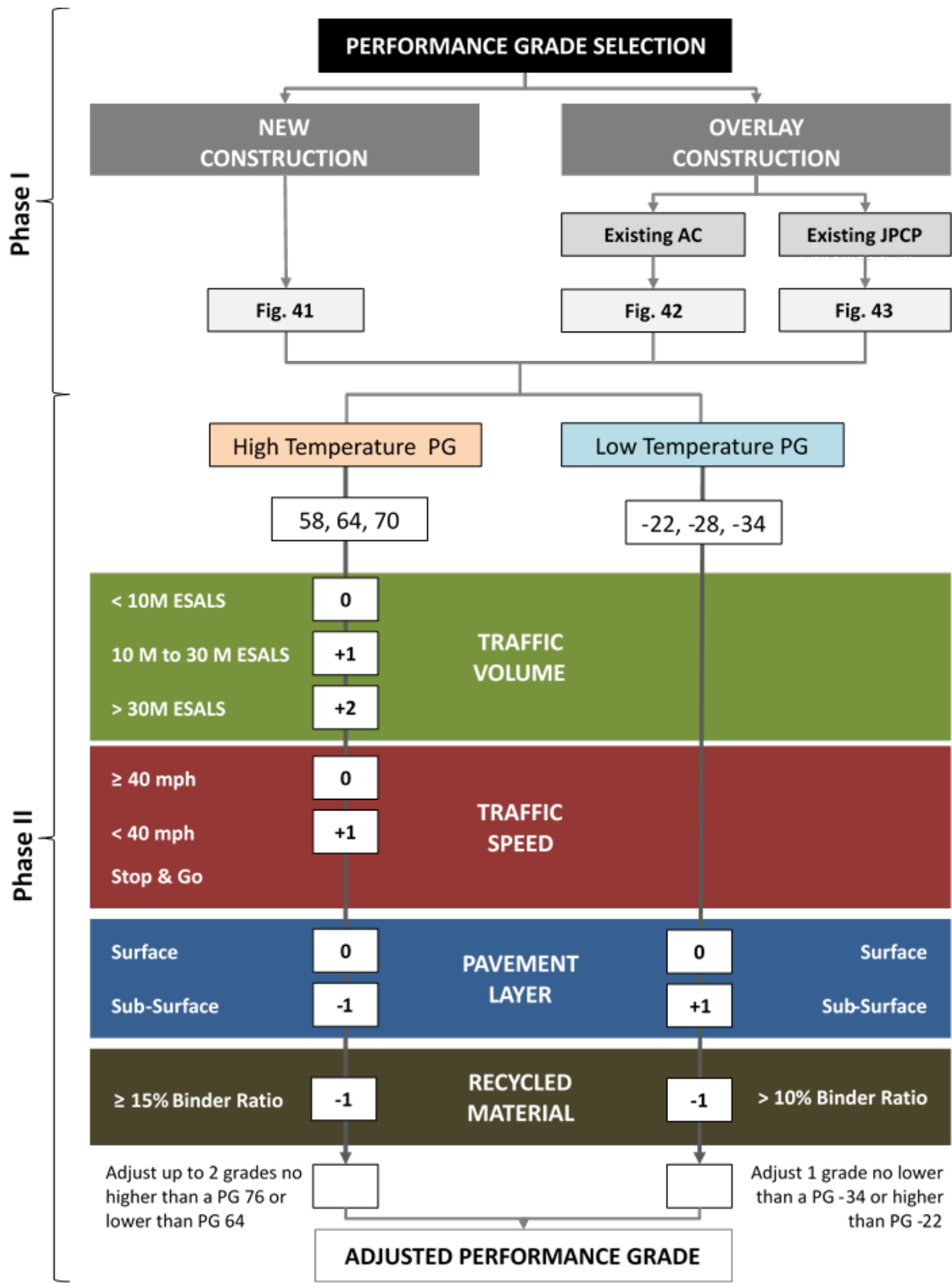


Figure 43. PG Recommendation for Asphalt Overlay over JPCP.



**Figure 44. Asphalt Binder PG Recommendation and Adjustment: New Method.**

## **CHAPTER 6: SUMMARY, CONCLUSIONS, AND RECOMMENDATIONS**

### **SUMMARY**

TxDOT became increasingly aware of cracking and durability issues of asphalt pavements. The advancement of newer techniques to engineer and manufacture asphalt binders has compromised the effectiveness of binder tests and parameters in capturing the prospective effect of engineering on asphalt binder, asphalt mixture, and asphalt pavement performances. It is especially true when soft, highly modified binders are used. The loss in effectiveness of binder tests in capturing properties directly impacts performance of the asphalt pavements.

TTI researchers identified several asphalt binder tests that can better capture the representative properties of asphalt binders. Researchers determined that pavements in Texas potentially need softer asphalt binders than currently recommended by TxDOT's binder PG selection catalog. Researchers also validated that softer binders yield better asphalt pavement performance by monitoring performance of 11 existing and 6 new field test sections around Texas. This project also updated the TxDOT binder selection catalog based on the laboratory and field performance data. Based on the data presented in this report, both conclusions and recommendations are offered below.

### **CONCLUSIONS**

#### **Previously Constructed Field Test Sections**

The existing field test sections constructed previously have mostly accumulated cracking over these years. The sections constructed with the softer binder have performed generally better than the ones constructed with the stiffer binders.

#### **Newly Constructed Field Test Sections**

The newly constructed field test sections have not accumulated significant cracking and rutting irrespective of PG 64-22 and 64-28 asphalt binders. This is mostly because these pavements were related new in age, slightly over 2 years.

#### **Statewide Asphalt Binder Selection Catalog Update**

A new approach has been developed to select asphalt binder PG for new pavement and overlay construction considering existing pavement layers. The starting high temperature PG is the same for new pavement and over construction irrespective of existing pavement later. However, starting low temperature PG differs between new pavement and overlay construction for each existing pavement layer. The low temperature PG recommended by the new approach is generally softer than the low temperature recommended by currently used approach. Instead of relying on one climate map for both high and low temperature asphalt binder PG selection, the new approach recommends using different maps for different applications (new construction,

overlay over existing AC or overlay over existing JPCP). For the overlays, the new approach provides a different map for each possible case of existing pavement layer.

### Characterization of Engineered Asphalt Binders

- **Durability:** The difference in critical low temperature obtained from creep stiffness and creep slope ( $\Delta T_c$ ) was effective indicator of asphalt binder quality or durability. Durability of asphalt binders increased with more use of bio-rejuvenators, aromatic extracts, and fatty increased (less negative  $\Delta T_c$ ) but decreased with more use of REOBs and aging (more negative  $\Delta T_c$ ).
- **Rutting Resistance:** The MSCR test was able to discriminate rutting resistance of asphalt binders engineered with different bio-rejuvenators in the presence of recycled binders. Rutting resistance of asphalt binders decreased with more use of REOBs, bio-rejuvenators, and aromatic extracts (higher  $J_{nr}$  and lower %Rec) but increased with more use of recycled or aged binders (lower  $J_{nr}$  and higher %Rec).
- **Overall Rheology:** Crossover frequency ( $\omega_c$ ) and rheological index ( $R$ ) obtained from time-temperature superposition of frequency sweep test data of asphalt binders were able to discriminate stiffness and inability of relaxing microstrains (or brittleness). Asphalt binders became stiffer increased with more aging (lower  $\omega_c$ ) but softer with more use of REOBs, bio-rejuvenators, and aromatic extracts (higher  $\omega_c$ ). Asphalt binders become less able to relax microcracks (more brittle) with more aging and increased use of REOBs (higher  $R$ ) but became more able to relax microcracks (more ductile) with more increased use of bio-rejuvenators and aromatic extracts (lower  $R$ ).
- **Cracking Resistance:** The LAS test could not always discriminate cracking resistance of asphalt binders engineered with different agents and unaged for different durations. Therefore, a new asphalt binder fatigue test called PLAS test was proposed. The FREI obtained from this test was more effective in discriminating cracking resistance of asphalt binders engineered with different agents and unaged for different durations. Asphalt binders become more resistant to cracking with more bio-rejuvenators (higher FREI) but less resistant to cracking with more aging (lower FREI).



## RECOMMENDATIONS

Researchers recommend the following:

- **Asphalt Binder PG Selection Catalog:** Implement the asphalt binder PG selection catalog and approach presented in this project in Texas.
- **Continuation of Monitoring Field Test Sections:** TxDOT should continue monitoring the new field test sections constructed under project 0-6674-01 so that the benefit of using softer asphalt binders could be further verified.
- **Asphalt Binder Characterization:** Use frequency sweep tests to evaluate overall rheological properties of these binders. Use  $\Delta T_c$ , MSCR, and PLAS tests to evaluate durability, rutting resistance, and cracking resistance of asphalt binders.



## REFERENCES

- AASHTO M320. (2010). “Standard Specification for Performance-Graded Asphalt Binder.”
- AASHTO R28. (2012). “Standard Practice for Accelerated Aging of Asphalt Binder Using a Pressurized Aging Vessel.”
- AASHTO T51. (2013). “Standard Method of Test for Ductility of Asphalt Materials.”
- AASHTO T240. (2013). “Standard Method of Test for Effect of Heat and Air on a Moving Film of Asphalt.”
- AASHTO T315. (2012). “Standard Method of Test for Determining the Rheological Properties of Asphalt Binder Using a Dynamic Shear Rheometer (DSR).”
- AASHTO T350. (2014). “Standard Method of Test for Multiple Stress Creep Recovery (MSCR) Test of Asphalt Binder Using a Dynamic Shear Rheometer (DSR).”
- AASHTO TP101. (2014). “Standard Method of Test for Estimating Fatigue Resistance of Asphalt Binders Using the Linear Amplitude Sweep.”
- Al-Qadi, I. L., Ozer, H., Lambros, J., El Khatib, A., Singhvi, P., Khan, T., Rivera-Perez, J., and Doll, B. (2015). *Testing Protocols to Ensure Performance of High Asphalt Binder Replacement Mixes Using RAP and RAS*. Illinois Center for Transportation, Urbana, IL.
- Anderson, D. (2002). “Zero Shear Viscosity of Asphalt Binders.” *Transportation Research Record: Journal of the Transportation Research Board*, 1810, 54–62.
- Anderson, D., Hir, Y., Marasteanu, M., Planche, J.-P., Martin, D., and Gauthier, G. (2001). “Evaluation of Fatigue Criteria for Asphalt Binders.” *Transportation Research Record: Journal of the Transportation Research Board*, 1766, 48–56.
- Anderson, R. M., Kriz, P., Hanson, D. I., and Planche, J.-P. (2011). “Evaluation of the Relationship between Asphalt Binder Properties and Non-Load Related Cracking.” *Journal of the Association of Asphalt Paving Technologists*, 80, 615–664.
- Andriescu, A., Hesp, S., and Youtcheff, J. (2004). “Essential and Plastic Works of Ductile Fracture in Asphalt Binders.” *Transportation Research Record: Journal of the Transportation Research Board*, 1875, 1–7.
- Bahia, H. U., Hanson, D. I., Zeng, M., Zhai, H., Khatri, M. A., and Anderson, R. M. (2001). *Characterization of Modified Asphalt Binders in Superpave Mix Design*. National Cooperative Highway Research Program, Washington, D.C.
- Bahia, H. U., Zhai, H., Zeng, M., Hu, Y., and Turner, P. (2002). “Development of Binder Specification Parameters Based on Characterization of Damage Behavior.” *Journal of the Association of Asphalt Paving Technologists*, 70, 442–470.
- Bazant, Z. P., and Prat, P. C. (1988). “Effect of Temperature and Humidity on Fracture Energy of Concrete.” *ACI Materials Journal*, 85(4), 262–271.
- Bennert, T., Ericson, C., Pezeshki, D., Haas, E., Shamborovskyy, R., and Corun, R. (2016). “Laboratory Performance of Re-refined Engine Oil Bottoms (REOB) Modified Asphalt.” *Proceedings of the Association of Asphalt Paving Technologists*, Indianapolis, IN.
- Bouldin, M., Dongre, R., and D’Angelo, J. A. (2001). “Proposed Refinement of Superpave High-Temperature Specification Parameter for Performance-Graded Binders.” *Transportation Research Record: Journal of the Transportation Research Board*, 1766, 40–47.
- Christensen, D. W., and Anderson, D. A. (1992). “Interpretation of dynamic mechanical test data for paving grade asphalt cements.” *Journal of the Association of Asphalt Paving Technologists*, 61, 67–116.

- D'Angelo, J. A., and Dongre, R. (2002). "Superpave Binder Specifications and their Performance Relationship to Modified Binders." 91–103.
- D'Angelo, J. A., Kluttz, R., Dongre, R., Stephens, K., and Zanzotto, L. (2007). "Revision of the Superpave High Temperature Binder Specification: The Multiple Stress Creep and Recovery Test." *Journal of the Association of Asphalt Paving Technologists*, 76, 123–162.
- Deacon, J. A., Harvey, J. T., Tayebali, A., and Monismith, C. L. (1997). "Influence of Binder Loss Modulus on the Fatigue Performance of Asphalt Concrete Pavements." *Journal of the Association of Asphalt Paving Technologists*, 66, 633–668.
- Desmazes, C., Lecomte, M., Lesueur, D., and Philipps, M. (2000). "A Protocol for Reliable Measurement of Zero-shear-viscosity in Order to Evaluate Antirutting Performance of Binders." Barcelona, Spain, 203–211.
- Dongre, R., and D'Angelo, J. A. (2003). "Refinement of Superpave High-Temperature Binder Specification Based on Pavement Performance in the Accelerated Loading Facility." *Transportation Research Record: Journal of the Transportation Research Board*, 1829, 39–46.
- Dongre, R., and D'Angelo, J. A. (2006). "Development of a high temperature performance-based specification in the United States." Quebec, Canada.
- Epps, J. A., Little, D. N., Holmgreen, R. J., and Terrel, R. L. (1980). *Guidelines for Recycling Pavement Materials*. NCHRP Report No. 224, Transportation Research Board, Washington, D.C.
- Ferry, J. D. (1980). *Viscoelastic Properties of Polymers*. Wiley.
- Gibson, N., Qi, X., Shenoy, A., Al-Khateeb, G., Kutay, M. E., Andriescu, A., Stuart, K., Youtcheff, J., and Harman, T. (2012). *Performance Testing for Superpave and Structural Validation*. Federal Highway Administration, McLean, VA.
- Glover, C., Davison, R., Domke, C., Ruan, Y., Juristyarini, P., Knorr, D., and Jung, S. (2005). *Development of a new method for assessing asphalt binder durability with field validation*. Texas A&M Transportation Institute, College Station, Texas.
- Hintz, C., and Bahia, H. U. (2013). "Understanding Mechanisms Leading to Asphalt Binder Fatigue in the Dynamic Shear Rheometer." *Journal of the Association of Asphalt Paving Technologists*, 82, 465–501.
- Hintz, C., Velasquez, R., Johnson, C., and Bahia, H. U. (2011a). "Modification and Validation of Linear Amplitude Sweep Test for Binder Fatigue Specification." *Transportation Research Record: Journal of the Transportation Research Board*, 2207, 99–106.
- Hintz, C., Velasquez, R., Li, Z., and Bahia, H. U. (2011b). "Effect of Oxidative Aging on Binder Fatigue Performance." *Journal of the Association of Asphalt Paving Technologists*, 80, 527–547.
- Hu, S., Zhou, F., and Scullion, T. (2014). *Texas Cracking Performance Prediction, Simulation, and Binder Recommendation*. Texas A&M Transportation Institute, College Station, Texas.
- Johnson, C. M. (2010). "Estimating Asphalt Binder Fatigue Resistance using an Accelerated Test Method." University of Wisconsin at Madison, Madison, WI.
- Karki, P., Meng, L., Im, S., Estakhri, C., and Zhou, F. (2018). *Re-refined engine oil bottom: Detection and upper limits in asphalt binders and seal coat binders*. Texas A&M Transportation Institute, College Station, Texas.

- Karki, P., and Zhou, F. (2016). "Effect of rejuvenators on rheological, chemical and aging properties of asphalt binders containing recycled binders." *Transportation Research Record: Journal of the Transportation Research Board*, 2574, 74–82.
- Karki, P., and Zhou, F. (2017). "Development of a systematic method for quantifying REOB content in asphalt binders with X-Ray fluorescence spectroscopy." *Transportation Research Record: Journal of the Transportation Research Board*, 2632, 52–59.
- Karki, P., and Zhou, F. (2018). "Determining re-refined engine oil bottom content in asphalt binders using a handheld X-ray fluorescence instrument." *Road Materials and Pavement Design*, 1–15.
- Li, X., Gibson, N., Andriescu, A., and Arnold, T. S. (2016). "Performance Evaluation of REOB Modified Asphalt Binders and Mixtures." Indianapolis, IN.
- Li, X., Gibson, N., Andriescu, A., and Arnold, T. S. (2017). "Performance Evaluation of REOB-Modified Asphalt Binders and Mixtures." *Road Materials and Pavement Design*, 18(Sup. 1), 128–153.
- Mogawer, W. S., Austerman, A. J., Al-Qadi, I., Buttlar, W. G., Ozer, H., and Hill, B. (2017). "Using binder and mixture space diagrams to evaluate the effect of re-refined engine oil bottoms on binders and mixtures after ageing." *Road Materials and Pavement Design*, 18(Supl. 1), 154–182.
- Mogawer, W. S., Booshehrian, A., Vahidi, S., and Austerman, A. J. (2013). "Evaluating the effect of rejuvenators on the degree of blending and performance of high RAP, RAS, and RAP/RAS mixtures." *Road Materials and Pavement Design*, 14(S2), 193–213.
- Peterson, J. C. (2009). "A Review of the Fundamentals of Asphalt Oxidation: Chemical, Physicalchemical, Physical Properties, and Durability Relationships." *TRB Transportation Research Circular*, (E-C140).
- Phillips, M. C., and Robertus, C. (1996). "Binder Rheology and Asphaltic Pavement Permanent Deformation; The Zero-shear Viscosity." Strasbourg, France, 134.
- Schapery, R. A. (1984). "Correspondence principles and a generalized J integral for large deformation and fracture analysis of viscoelastic media." *International Journal of Fracture*, 25(3), 195–223.
- Stuart, K., Mogawer, W. S., and Romero, P. (2000). *Validation of Asphalt Binder and Mixture Tests That Measure Rutting Susceptibility*. Interim Report, Federal Highway Administration, McLean, VA.
- Sybilski, D. (1996). "Zero-Shear Viscosity of Bituminous Binder and Its Relation to Bituminous Mixture's Rutting Resistance." *Transportation Research Record: Journal of the Transportation Research Board*, 1535, 15–21.
- Tex-248-F. (2014). "Overlay Test." Texas Department of Transportation.
- Tsai, B., and Monismith, C. L. (2005). "Influence of Asphalt Binder Properties on the Fatigue Performance of Asphalt Concrete Pavements." *Journal of Association of Asphalt Paving Technologists*, 74, 733–790.
- Vallerga, B. A. (1981). "Pavement Deficiencies Related to Asphalt Durability." *Journal of the Association of Asphalt Paving Technologists*, 50, 481–491.
- Williams, M. L., Landel, R. F., and Ferry, J. D. (1955). "The Temperature Dependence of Relaxation Mechanisms in Amorphous Polymers and Other Glass-forming Liquids." *Journal of American Chemical Society*, 77(14), 3701–3707.
- Zaumanis, M., Mallick, R. B., Poulikakos, L., and Frank, R. (2014). "Influence of six rejuvenators on the performance properties of Reclaimed Asphalt Pavement (RAP)

- binder and 100% recycled asphalt mixtures.” *Construction and Building Materials*, 71, 538–550.
- Zhang, J., Walubita, L. F., Faruk, A. N. M., Karki, P., and Simate, G. S. (2015). “Use of the MSCR test to characterize the asphalt binder properties relative to HMA rutting performance - A laboratory study.” *Construction and Building Materials*, 94, 218–227.
- Zhou, F., Im, S., Hu, S., Newcomb, D., and Scullion, T. (2016a). “Selection and Preliminary Evaluation of Laboratory Cracking Tests for Routine Asphalt Mix Designs.” *Journal of the Association of Asphalt Paving Technologists*, 85.
- Zhou, F., Karki, P., and Im, S. (2017). “Development of a simple fatigue cracking test for asphalt binders.” *Transportation Research Record: Journal of the Transportation Research Board*, 2632, 79–87.
- Zhou, F., Karki, P., Xie, S., Yuan, J. S., Sun, L., Lee, R., and Barborak, R. (2018). “Toward the development of performance-related specification for bio-rejuvenators.” *Construction and Building Materials*, 174, 443–455.
- Zhou, F., Li, H., Chen, P., and Scullion, T. (2014). *Laboratory Evaluation of Asphalt Binder Rutting, Fracture, and Adhesion Tests*. Texas A&M Transportation Institute, College Station, Texas.
- Zhou, F., Newcomb, D., and Gurganus, C. (2016b). *Experimental Design for Field Validation of Laboratory Tests to Assess Cracking Resistance of Asphalt Mixtures*. Texas A&M Transportation Institute, College Station, Texas.